

Reconstructing inflationary paradigm within Effective Field Theory framework

Sayantana Choudhury ^{1a}

^a*Department of Theoretical Physics, Tata Institute of Fundamental Research, Colaba, Mumbai - 400005, India*

E-mail: sayantana@theory.tifr.res.in

ABSTRACT: In this paper my prime objective is to analyze the constraints on a sub-Planckian excursion of a single inflaton field within Effective Field Theory framework in a model independent fashion. For a generic single field inflationary potential, using the various parameterization of the primordial power spectrum I have derived the most general expression for the field excursion in terms of various inflationary observables, applying the observational constraints obtained from recent Planck 2015 and Planck 2015 +BICEP2/Keck Array data. By explicit computation I have reconstructed the structural form of the inflationary potential by constraining the Taylor expansion co-efficients appearing in the generic expansion of the potential within the Effective Field Theory. Next I have explicitly derived, a set of higher order inflationary *consistency* relationships, which would help us to break the degeneracy between various class of inflationary models by differentiating them. I also provided two simple examples of Effective Theory of inflation- *inflection-point* model and *saddle-point* model to check the compatibility of the prescribed methodology in the light of Planck 2015 and Planck 2015 +BICEP2/Keck Array data. Finally, I have also checked the validity of the prescription by estimating the cosmological parameters and fitting the theoretical CMB TT, TE and EE angular power spectra with the observed data within the multipole range $2 < l < 2500$.

KEYWORDS: Inflation, Cosmological perturbations, Cosmology beyond the standard model, Effective Field Theory, Reconstruction of inflationary potential, CMB.

¹**Presently working as a Visiting (Post-Doctoral) fellow at DTP, TIFR, Mumbai, Alternative E-mail: sayanphysics@gmail.com.**

Contents

1	Introduction	1
2	Brief introduction to tensor to scalar ratio in inflation	8
3	Constraining the scale of effective field theory inflation via field excursion	14
4	Non-monotonic behaviour of slow-roll parameters within effective field theory	19
5	Reconstruction technique of the structure of inflationary effective potential	26
6	Higher order consistency relationships in effective theory	32
7	Example of Inflection point inflation within effective theory	34
8	Example of Saddle point inflation within effective theory	51
9	Multipole scanning of CMB spectra via reconstructed effective potential	55
10	Conclusion	63

1 Introduction

The primordial inflation [1–3] has two *key* predictions - creating the scalar density perturbations and the tensor perturbations during the accelerated phase of expansion [4], for a review, see [5]. One of the predictions, namely the temperature anisotropy due to the scalar density fluctuations has now been tested very accurately by the observations from the temperature anisotropy and polarization in the cosmic microwave background (CMB) radiation [6–8]. In the last year the detection of tensor modes has been initially confirmed by the ground based BICEP2 experiment [9], which according to the initial claim has detected for the first time a non-zero value of the tensor-to-scalar ratio at 7σ C.L. The value obtained by the BICEP2 team in conjunction with [Planck \(2014\)+WMAP-9+high L+BICEP2 \(dust\)](#)¹ to put a bound

¹Throughout the article we use [red](#) for the obsoleted [Planck \(2014\)+WMAP-9+high L+BICEP2 \(dust\)](#) data.

on the primordial gravitational waves, via tensor-to-scalar ratio, within a window:

$$0.15 \leq r(k_*) \equiv P_T(k_*)/P_S(k_*) \leq 0.27, \quad (1.1)$$

at the pivot scale, $k_* = 0.002\text{Mpc}^{-1}$ [9], where P_T and P_S denote the power spectrum for the tensor and scalar modes, respectively. But just after releasing this result BICEP2 analysis was put into question by several works [10–13] on its correctness in the physical ground. Most importantly it accounting for the contribution of foreground dust which will shift the value of tensor-to-scalar ratio r downward by an amount and further better constrained by the joint analysis performed by Planck and BICEP2/Keck Array team [14]. The final result is expressed as a likelihood curve for r , and yields an upper limit:

$$r(k_*) \equiv P_T(k_*)/P_S(k_*) \leq 0.12 \quad (1.2)$$

at the pivot scale, $k_* = 0.05\text{Mpc}^{-1}$ with 2σ confidence. Marginalizing over dust contribution and r , finally it is reported that the lensing B-modes are detected at 7σ significance. Very recently in ref. [15] the Planck team in 2015 data release also fixed the upper bound on the tensor-to-scalar ratio as:

$$r(k_*) \equiv P_T(k_*)/P_S(k_*) \leq 0.11 \quad (1.3)$$

at the pivot scale, $k_* = 0.002\text{Mpc}^{-1}$ with 2σ C.L. and perfectly consistent with the joint analysis performed by Planck and BICEP2/Keck Array team.

Note that large $r(k_*)$ is possible if the initial conditions for gravitational waves is quantum Bunch-Davis vacuum [16]², for a classical initial condition the amplitude of the gravitational waves would be very tiny and undetectable, therefore this can be treated as the first observable proof of quantum gravity. However, apart from the importance and applicability of quantum Bunch-Davis vacuum on its theoretical and observational ground it is still not at all clear from the previous works in this area that whether the quantum Bunch-Davies vacuum is the only source of generating large value of $r(k_*)$ during inflationary epoch or not. One of the prime possibilities comes from the deviation from quantum Bunch-Davies vacuum *aka* consideration of quantum non-Bunch-Davies or arbitrary vacuum in this picture which may also responsible for the generation of large $r(k_*)$ during inflation³.

In this paper, our aim will be to illustrate that it is possible to explain the current data sets within a sub-Planckian model of inflation, where:

- $\phi_0 \ll M_p$ - vev of the inflaton must be bounded by the cut-off of the particle theory, where $M_p = 2.4 \times 10^{18}$ GeV. We are assuming that 4 dimensions M_p puts a natural cut-off here for any physics beyond the Standard Model.

² Apart from the correctness of this argument, it is additionally important to mention here that, still it doesn't require the initial conditions for the quantum vacuum to be Bunch-Davis strictly.

³In this article I have not explored the possibility of non Bunch Davies vacuum.

- $|\Delta\phi| \approx |\phi_\star - \phi_e| \lesssim M_p$ - the inflaton potential has to be flat enough during which a successful inflation can occur. Here

$$\phi_\star \geq \phi_0 \geq \phi_e \quad (1.4)$$

represents the field VEV, and $\Delta\phi$ denotes the range of the field values around which all the relevant inflation occurs, ϕ_\star corresponds to the pivot scale and ϕ_e denotes the end of inflation. Note that the flatness of the potential has to be fine tuned and also there is no particle physics symmetry which can maintain the flatness. We will assume

$$V''(\phi_0) \approx 0, \quad (1.5)$$

where $V(\phi)$ denotes the inflaton potential, and prime denotes derivative w.r.t. the ϕ field. Naturally, the potential has to be flat enough within $\Delta\phi$ to support slow roll inflation.

The above requirements are important if the origin of the inflaton has to be embedded within a particle theory, where inflaton is part of a *visible sector* gauge group, i.e. Standard Model gauge group, instead of an arbitrary gauge singlet. If the inflaton is *gauged* under some gauge group, as in the case of a minimal supersymmetric Standard Model (MSSM), Ref. [17], then the inflaton VEV must be bounded by M_p , in order to keep the sanctity of an effective field theory description ⁴.

Our prescribed methodology will be very generic, with a Taylor expanded potential around VEV ϕ_0 is given by ⁵:

$$\begin{aligned} V(\phi) &= \sum_{n=0}^{\infty} \frac{(\phi - \phi_0)^n}{n!} \left(\frac{d^n V(\phi)}{d\phi^n} \right)_{\phi=\phi_0}, \\ &= V(\phi_0) + V'(\phi_0)(\phi - \phi_0) + \frac{V''(\phi_0)}{2}(\phi - \phi_0)^2 + \frac{V'''(\phi_0)}{6}(\phi - \phi_0)^3 \\ &\quad + \frac{V''''(\phi_0)}{24}(\phi - \phi_0)^4 + \dots, \end{aligned} \quad (1.6)$$

where the expansion co-efficients are characterized as follows:

- The first term:

$$V(\phi_0) \ll M_p^4 \quad (1.7)$$

denotes the height of the potential. Also this term will play the most significant role in fixing the scale of inflation within the present framework.

⁴ An arbitrary moduli or a gauge singlet inflaton can take large VEVs (super-Planckian) as in the case of a chaotic inflation [2]. Although, in the case of *assisted inflation* [18], see *chaotic assisted inflation* [19], the individual VEVs of the inflatons are sub-Planckian.

⁵For the sake of completeness I suggest the readers to see ref. [20], where I have explicitly studied the inflationary reconstruction technique within the framework of Randall Sundrum single brane set up, using the observational constraints obtained from Planck 2015 and BICEP2/Keck Array joint constraints.

- The Taylor expansion coefficients of the effective potential:

$$V'(\phi_0) \leq M_p^3, \quad (1.8)$$

$$V''(\phi_0) \leq M_p^2, \quad (1.9)$$

$$V'''(\phi_0) \leq M_p, \quad (1.10)$$

$$V''''(\phi_0) \leq \mathcal{O}(1), \quad (1.11)$$

determine the shape of the potential in terms of the model parameters.

- The *prime* denotes the derivative w.r.t. ϕ . In particular, some specific choices of the potential would be a *saddle point*, when

$$V'(\phi_0) = 0 = V''(\phi_0), \quad (1.12)$$

an *inflection point*, when

$$V''(\phi_0) = 0. \quad (1.13)$$

Previous studies regarding obtaining large $r(k_*)$ within sub-Planckian VEV models of inflation have been studied in Refs. [21–23]. In Ref. [21], the authors could match the amplitude of the power spectrum, P_S , at the pivot point, but not at the entire range of $\Delta\phi$ for the observable window of ΔN , where N is the number of e-foldings of inflation. In Ref. [24], the authors have looked into higher order slow roll corrections by expanding the potential around ϕ_0 . They pointed out that large

$$r \sim 0.05 \quad (1.14)$$

could be obtained in an *inflection-point* model of inflation where the slow roll parameter, ϵ_V , changes non-monotonically (for a definition of ϵ_V , see Eq. (2.8)). The ϵ_V parameter first increases within the observational window of ΔN and then decreases before increasing to exit the slow roll inflation by violating the slow roll condition, i.e. $\epsilon_V \approx 1$ ⁶. The value of r was still small in order to accommodate the WMAP

⁶The smallness of the observational window on ΔN also allows us to exploit another loophole in the derivation of the Lyth bound [25], namely the assumption that ϵ_V increases monotonically. This seems a natural assumption given that during inflation

$$\epsilon_V \ll 1 \quad (1.15)$$

and at the end of inflation

$$\epsilon_V \sim 1, \quad (1.16)$$

current observational constraints also strongly favour ϵ_V increasing during the $\Delta N \sim 17$ e-folds of the window achieved by the CMB distortion observation. However, outside this window the behaviour of ϵ_V is not constrained and the assumption of monotonicity is not strictly necessary. Relaxing this assumption makes it possible to construct a scalar potential for a single field that violates the Lyth bound. For more details see Ref. [24].

data, which had probed roughly $\Delta N \approx 8$ as compared to the Planck, which has now probed $\Delta N \approx 17$ e-foldings of inflation [23, 26–29] can be achieved by the CMB distortion observation. A generic bound on tensor-to-scalar ratio was explicitly derived in Ref. [23, 26, 27] for a generic type of *inflection-point* inflationary model, where I set $V''(\phi_0) = 0$ in the Taylor expanded form of the potential.

In this paper I will consider the full potential of Eq. (1.6), and our prime objective is to determine the values of the Taylor expansion co-efficients $V(\phi_0)$, $V'(\phi_0)$, $V''(\phi_0)$, $V'''(\phi_0)$ and $V''''(\phi_0)$ from the latest Planck 2015 and BICEP2/Keck Array+Planck 2015 joint data ⁷. In this respect I will be reconstructing the inflationary potential around ϕ_0 and at the pivot scale, $\phi_\star = \phi(k_\star)$, where I fix $k_\star = 0.002\text{Mpc}^{-1}$. We will also provide for the second order consistency relations for a sub-Planckian excursion of the inflaton field. This will be treated as an observational discriminator which could rule out various sub-Planckian models of inflation in future.

Within the region of $\Delta N \approx \mathcal{O}(8 - 17)$ e-foldings [23, 26–29], I will be able to constrain the power spectrum: P_S , spectral tilt: n_S , running of the spectral tilt: α_S , and running of running of the spectral tilt: κ_S , in the background of ΛCDM model for:

Planck (2013)+WMAP-9+high L data sets:[7, 8]

$$r(k_\star) \leq 0.12 \quad (\text{within } 2\sigma \text{ C.L.}), \quad (1.17)$$

$$\ln(10^{10}P_S) = 3.089_{-0.027}^{+0.024} \quad (\text{within } 2\sigma \text{ C.L.}), \quad (1.18)$$

$$n_S = 0.9600 \pm 0.0071 \quad (\text{within } 3\sigma \text{ C.L.}), \quad (1.19)$$

$$\alpha_S = dn_S/d\ln k = -0.013 \pm 0.009 \quad (\text{within } 1.5\sigma \text{ C.L.}), \quad (1.20)$$

$$\kappa_S = d^2n_S/d\ln k^2 = 0.020_{-0.015}^{+0.016} \quad (\text{within } 1.5\sigma \text{ C.L.}). \quad (1.21)$$

Planck (2014)+WMAP-9+high L+BICEP2 (dust) data sets:[9]

$$0.15 \leq r(k_\star) \leq 0.27 \quad (1.22)$$

$$\ln(10^{10}P_S) = 3.089_{-0.027}^{+0.024} \quad (\text{within } 2\sigma \text{ C.L.}), \quad (1.23)$$

$$n_S = 0.9600 \pm 0.0071 \quad (\text{within } 3\sigma \text{ C.L.}), \quad (1.24)$$

$$\alpha_S = dn_S/d\ln k = -0.022 \pm 0.010 \quad (\text{within } 1.5\sigma \text{ C.L.}), \quad (1.25)$$

$$\kappa_S = d^2n_S/d\ln k^2 = 0.020_{-0.015}^{+0.016} \quad (\text{within } 1.5\sigma \text{ C.L.}). \quad (1.26)$$

⁷ Additionally I have also mentioned the results using the obsoleted Planck+WAMP-9+high L+BICEP2(dust) data throughout the paper to explicitly show the validity of our prescribed methodology for any kind of observed data set.

Planck (2015)+WMAP-9+high L(TT) data sets:[15]

$$r(k_*) \leq 0.11 \quad (\text{within } 2\sigma \text{ C.L.}), \quad (1.27)$$

$$\ln(10^{10}P_S) = 3.089 \pm 0.036 \quad (\text{within } 2\sigma \text{ C.L.}), \quad (1.28)$$

$$n_S = 0.9569 \pm 0.0077 \quad (\text{within } 3\sigma \text{ C.L.}), \quad (1.29)$$

$$\alpha_S = dn_S/d\ln k = 0.011^{+0.014}_{-0.013} \quad (\text{within } 1.5\sigma \text{ C.L.}), \quad (1.30)$$

$$\kappa_S = d^2n_S/d\ln k^2 = 0.029^{+0.015}_{-0.016} \quad (\text{within } 1.5\sigma \text{ C.L.}). \quad (1.31)$$

Planck (2015)+BICEP2/Keck Array joint data sets:[14]

$$r(k_*) \leq 0.12 \quad (\text{within } 2\sigma \text{ C.L.}), \quad (1.32)$$

$$\ln(10^{10}P_S) = 3.089^{+0.024}_{-0.027} \quad (\text{within } 2\sigma \text{ C.L.}), \quad (1.33)$$

$$n_S = 0.9600 \pm 0.0071 \quad (\text{within } 3\sigma \text{ C.L.}), \quad (1.34)$$

$$\alpha_S = dn_S/d\ln k = -0.022 \pm 0.010 \quad (\text{within } 1.5\sigma \text{ C.L.}), \quad (1.35)$$

$$\kappa_S = d^2n_S/d\ln k^2 = 0.020^{+0.016}_{-0.015} \quad (\text{within } 1.5\sigma \text{ C.L.}). \quad (1.36)$$

In this paper-

- We will briefly recap the key equations for the inflationary tensor-to-scalar ratio in the most generalized case by taking into account of the effect of higher order slow-roll corrections. Throughout the analysis of the paper I assume:
 1. Inflaton field ϕ is minimally coupled to the Einstein gravity sector.
 2. Slow-roll prescription perfectly holds good after considering higher order slow-roll corrections.
 3. Convergence of the Taylor expanded potential.
 4. For the numerical estimations the generic form of Taylor expanded potential is truncated at the fourth power of inflaton field.
 5. We also assume that the major contribution for the generic version of inflationary potential comes from the first term $V(\phi_0)$ of the Taylor series for which convergence of the Taylor series holds good perfectly within the present framework. We will explicitly show in the next sections, within the slow-roll regime of inflation this assumption is compatible with the results obtained by applying the recent observational constraints.
 6. As the contribution from all the non-renormalizable effective field theory operators are highly suppressed by the various powers of the UV cut-off scale of the effective field theory Λ_{UV} , in the present context I neglect all such contribution due to its smallness.
 7. Initial condition for inflation is fixed via Bunch-Davies vacuum.

8. Sound speed is fixed at $c_S = 1$.
 9. UV cut-off of the effective theory is fixed at $\Lambda_{UV} = M_p$, where M_p is the reduced Planck mass. But in principle one can fix the scale between GUT scale and reduced Planck scale i.e. $\Lambda_{GUT} < \Lambda_{UV} \leq M_p$. But in such a situation Λ_{UV} acts as a regulating parameter in the effective field theory. To avoid all such complications I fix it at M_p .
- We will then derive the *most general* bound on $r(k_*)$ for a generic sub-Planckian VEV inflation by considering the effect of running and running of the running in primordial scalar and tensor power spectrum, and the corresponding values of H_* and $V(\phi_*)$ within the framework of effective field theory. For completeness of the presented analysis, in the Appendix of this paper I give also the expression for the bound obtained from the various parameterization in the primordial power spectrum.
 - We will then discuss the non-monotonic behaviour of slow-roll parameter and its effectiveness to evade the *Lyth bound* [25] in section 4.
 - Further I reconstruct the shape of the potential in section 5, by providing the observational constraints from Planck (2013)+WMAP-9+high-L [7, 8], Planck (2014)+WMAP-9+high-L+BICEP2 (dust) [9], Planck (2015)+WMAP-9+high-L(TT) [15] and Planck (2015)+BICEP2/Keck Array joint constraints [14] on the various Taylor expansion co-efficients $V'(\phi_0)$, $V''(\phi_0)$, $V'''(\phi_0)$ and $V''''(\phi_0)$ at VEV ϕ_0 , which are expressed in terms of the Taylor expansion co-efficients $V'(\phi_*)$, $V''(\phi_*)$, $V'''(\phi_*)$ and $V''''(\phi_*)$ at pivot/CMB scale ϕ_* .
 - In section 6, I will discuss the inflationary consistency relationships considering up to second order correction in slow-roll parameters.
 - In section 7, I will consider a specific case of inflection point inflation for the purpose of illustration.
 - In section 8, I will consider a specific case of saddle point inflation for the purpose of illustration.
 - Finally in section 9 I have discussed the multipole scanning of CMB TT, TE, EE and BB spectra via reconstructed potential by applying the constraints from Planck (2013)+WMAP-9+high-L, Planck (2014)+WMAP-9+high-L+BICEP2 (dust), Planck (2015)+WMAP-9+high-L(TT) and Planck (2015)+BICEP2/Keck Array data.
 - Additionally, in the Appendix of our paper for completeness I will provide all the key equations and detailed derivations of main results which are used frequently throughout the prescribed analysis of the paper.

2 Brief introduction to tensor to scalar ratio in inflation

The tensor to scalar ratio can be defined by taking into account of the higher order corrections, see Refs. [23, 30, 31]:

$$r = 16\epsilon_H \frac{[1 - (\mathcal{C}_E + 1)\epsilon_H]^2}{[1 - (2\mathcal{C}_E + 1)\epsilon_H + \mathcal{C}_E\eta_H]^2}, \quad (2.1)$$

where

$$\mathcal{C}_E = 4(\ln 2 + \gamma_E) - 5 \quad (2.2)$$

with $\gamma_E = 0.5772$ is the *Euler-Mascheroni constant* [30]. In Eq (2.1) the Hubble slow roll parameters (ϵ_H, η_H) are defined as:

$$\epsilon_H = -\frac{d \ln H}{d \ln a} = -\frac{\dot{H}}{H^2}, \quad (2.3)$$

$$\eta_H = -\frac{d \ln \dot{\phi}}{d \ln a} = -\frac{\ddot{\phi}}{H\dot{\phi}}, \quad (2.4)$$

where dot denotes time derivative with respect to the physical time. Now considering the effect from the leading order dominant contributions from the slow-roll parameters, the Hubble slow-roll parameters can be expressed in terms of the potential dependent slow-roll parameters, (ϵ_V, η_V) , as:

$$\epsilon_H \approx \epsilon_V + \dots, \quad (2.5)$$

$$\eta_H \approx \eta_V - \epsilon_V + \dots, \quad (2.6)$$

where \dots comes from the higher order contributions of (ϵ_V, η_V) .

The tensor to scalar ratio can be re-expressed in terms of inflationary potential as:

$$r \approx 16\epsilon_V \frac{[1 - (\mathcal{C}_E + 1)\epsilon_V]^2}{[1 - (3\mathcal{C}_E + 1)\epsilon_V + \mathcal{C}_E\eta_V]^2} \quad (2.7)$$

where slow-roll parameters (ϵ_V, η_V) are given by in terms of the inflationary potential $V(\phi)$, which can be expressed as:

$$\epsilon_V = \frac{M_p^2}{2} \left(\frac{V'}{V} \right)^2, \quad (2.8)$$

$$\eta_V = M_p^2 \left(\frac{V''}{V} \right). \quad (2.9)$$

We would also require two other slow-roll parameters, (ξ_V^2, σ_V^3) , in our analysis, which are given by:

$$\xi_V^2 = M_p^4 \left(\frac{V'V'''}{V^2} \right), \quad (2.10)$$

$$\sigma_V^3 = M_p^6 \left(\frac{V'^2V''''}{V^3} \right). \quad (2.11)$$

Note that I have neglected the contributions from the higher order slow-roll terms, as they are sub-dominant at the leading order. With the help of

$$\frac{d}{d \ln k} = -M_p \frac{\sqrt{2\epsilon_H}}{1 - \epsilon_H} \frac{d}{d\phi} \approx -M_p \frac{\sqrt{2\epsilon_V}}{1 - \epsilon_V} \frac{d}{d\phi}, \quad (2.12)$$

I can derive a simple expression for the tensor-to-scalar ratio, r , as:⁸

$$r = \frac{8}{M_p^2} \frac{(1 - \epsilon_V)^2 [1 - (\mathcal{C}_E + 1)\epsilon_V]^2}{[1 - (3\mathcal{C}_E + 1)\epsilon_V + \mathcal{C}_E\eta_V]^2} \left(\frac{d\phi}{d \ln k} \right)^2. \quad (2.13)$$

We can now derive a bound on $r(k)$ in terms of the momentum scale:

$$\begin{aligned} & \int_{k_e}^{k_\star} \frac{dk}{k} \sqrt{\frac{r(k)}{8}} \\ &= \frac{1}{M_p} \int_{\phi_e}^{\phi_\star} d\phi \frac{(1 - \epsilon_V) [1 - (\mathcal{C}_E + 1)\epsilon_V]}{[1 - (3\mathcal{C}_E + 1)\epsilon_V + \mathcal{C}_E\eta_V]}, \\ &\approx \frac{1}{M_p} \int_{\phi_e}^{\phi_\star} d\phi (1 - \epsilon_V) [1 + \mathcal{C}_E(2\epsilon_V - \eta_V) + \dots], \\ &\approx \frac{\Delta\phi}{M_p} \left\{ 1 + \frac{1}{\Delta\phi} \left[(2\mathcal{C}_E - 1) \int_{\phi_e}^{\phi_\star} d\phi \epsilon_V - \mathcal{C}_E \int_{\phi_e}^{\phi_\star} d\phi \eta_V \right] + \dots \right\}, \end{aligned} \quad (2.14)$$

where note that

$$\Delta\phi \approx \phi_\star - \phi_e > 0 \quad (2.15)$$

is positive in Eq. (2.14), and ϕ_e denotes the inflaton VEV at the end of inflation, and ϕ_\star denote the field VEV when the corresponding mode k_\star is leaving the Hubble patch during inflation. Here I have used the slow-roll approximation

$$\dot{\phi}/H \simeq \sqrt{2\epsilon_V}. \quad (2.16)$$

The physical significance of the Eq (2.14) are appended below:

- This gives the the analytical expression for the field excursion during inflation in terms of tensor-to-scalar ratio and other inflationary observables.
- This relation can be treated as a discriminator between sub-Planckian and super-Planckian inflationary models, depending on the value of field excursion.
- This relation also justifies the validity and correctness of Effective Field Theory framework, depending on the value of field excursion.
- Also this relation can be used to break the degeneracy between various class of inflationary models.

⁸ We have derived some of the key expressions in an Appendix, see for instance, Eq. (10.8), which I would require to derive the above expression, Eq. (2.13).

Note that $\Delta\phi > 0$ implies that the left hand side of the integration over momentum within an interval, $k_e < k < k_*$, is also positive, where k_e represents corresponding momentum scale at the end of inflation. Individual integrals involving ϵ_V and η_V are estimated in an Appendix, see Eqs. (10.12) and (10.13).

In order to perform the momentum integration in the left hand side of Eq (2.14), I have used the running of $r(k)$, which can be expressed as:

$$r(k) = r(k_*) \left(\frac{k}{k_*} \right)^{a + \frac{b}{2} \ln\left(\frac{k}{k_*}\right) + \frac{c}{6} \ln^2\left(\frac{k}{k_*}\right) + \dots}, \quad (2.17)$$

where

$$a = n_T - n_S + 1, \quad (2.18)$$

$$b = (\alpha_T - \alpha_S), \quad (2.19)$$

$$c = (\kappa_T - \kappa_S) \quad (2.20)$$

defined at the momentum pivot scale k_* . These parameterization characterizes the spectral indices, n_S , n_T , running of the spectral indices, α_S , α_T , and running of the running of the spectral indices, κ_S , κ_T . Here the subscripts, (S , T), represent the scalar and tensor modes. Now substituting the explicit form of the potential stated in Eq. (7.27), I can evaluate the crucial integrals of the first and second slow-roll parameters (ϵ_V , η_V) appearing in the right hand side of Eq. (2.14). For the details of the computation, see appendix.

It was earlier confirmed by the WMAP9+high- l +BAO+ H_0 combined constraints that [6]:

$$\alpha_S = -0.023 \pm 0.011, \quad (2.21)$$

$$\kappa_S = 0 \quad (2.22)$$

within less than 1σ C.L. . After the Planck release it is important to see the impact on $r(k_*)$ due to running, and running of the running of the spectral tilt by modifying the generic power law form of the parameterization of tensor-to-scalar ratio. The combined Planck (2013)+WMAP-9 constraint confirms that [8]:

$$\alpha_S = -0.0134 \pm 0.0090, \quad (2.23)$$

$$\kappa_S = 0.020^{+0.016}_{-0.015} \quad (2.24)$$

within 1.5σ statistical accuracy, which additionally includes

$$\kappa_S \neq 0 \quad (2.25)$$

possibility for the first time. Also the recent combined Planck (2015)+WMAP-9 constraint confirms that [15]:

$$\alpha_S = 0.011^{+0.014}_{-0.013}, \quad (2.26)$$

$$\kappa_S = 0.029^{+0.015}_{-0.016}, \quad (2.27)$$

within 1.5σ statistical accuracy, which first additionally includes

$$\alpha_S > 0 \tag{2.28}$$

possibility alongwith large running compared to the Planck (2013) data.

At the next to leading order, the simplest way to modify the power law parameterization is to incorporate the effects of higher order Logarithmic corrections in terms of the presence of non-negligible running, and running of the running of the spectral tilt as shown in Eq (2.17), which involves higher order slow-roll corrections ⁹.

After substituting Eq (2.17) in Eq (2.14), I will show that additional information can be gained from our analysis: first of all it provides more accurate and improved bound on tensor-to-scalar ratio in presence of non-negligible running and running of the running of the spectral tilt. In our analysis super-Planckian physics doesn't play any role as the effective theory puts naturally an upper cut-off set by the Planck scale. Consequently the prescription only holds good for:

1. sub-Planckian VEVs, $\phi_0 < M_p$,
2. field excursion, $\Delta\phi < M_p$ for inflation.

Both of these outcomes open a completely new insight into the particle physics motivated models of inflation, which are valid below the Planck scale.

Further note that the momentum integral has non-monotonous behaviour of the slow-roll parameters (ϵ_V, η_V) within the interval, $k_e < k < k_{cmb}$, which implies that ϵ_V and η_V initially increase within an observable window of e-foldings (which I will define in the next section, see Eq (3.1)), and then decrease at some point during the inflationary epoch when the observable scales had left the Hubble patch, and eventually increase again to end inflation [21, 24].

After substituting Eq (2.17) in the left hand side of I Eq (2.14), I obtain:

$$\begin{aligned} \int_{k_e}^{k_*} \frac{dk}{k} \sqrt{\frac{r(k)}{8}} &= \sqrt{\frac{r(k_*)}{8}} \int_{k_e}^{k_*} \frac{dk}{k} \sqrt{\left(\frac{k}{k_*}\right)^{a+\frac{b}{2}\ln\left(\frac{k}{k_*}\right)+\frac{c}{6}\ln^2\left(\frac{k}{k_*}\right)}}, \\ &= \sqrt{\frac{r(k_*)}{8}} \int_{k_e}^{k_*} \frac{dk}{k_* \left(\frac{k}{k_*}\right)} \left(\frac{k}{k_*}\right)^{A+B\ln\left(\frac{k}{k_*}\right)+C\ln^2\left(\frac{k}{k_*}\right)}, \end{aligned} \tag{2.29}$$

where

$$A = \frac{a}{2}, \quad B = \frac{b}{4}, \quad C = \frac{c}{12}.$$

Let us substitute,

$$k/k_* = \ln y, \tag{2.30}$$

⁹It is important to note that when Ref. [25] first derived a bound on large tensor-to-scalar ratio for super-Planckian inflationary models (with $\Delta\phi > M_p$), the above mentioned constraints on α_S, κ_S were not taken into account due to lack of observational constraints.

to simplify the mathematical form of the above Eq (2.29). Consequently, I get:

$$\int_{k_e}^{k_\star} \frac{dk}{k} \sqrt{\frac{r(k)}{8}} = \sqrt{\frac{r(k_\star)}{8}} \int_{e^{k_e/k_\star}}^{e^1} \frac{dy}{y \ln y} (\ln y)^{A+B \ln(\ln y)+C \ln^2(\ln y)}, \quad (2.31)$$

To evaluate the integral analytically, I apply the following technique. Let us consider:

$$(\ln y)^\alpha, \quad \text{where } \alpha \ll 1 \quad (2.32)$$

where the exponent α is defined as:

$$\alpha = A + B \ln(\ln y) + C \ln^2(\ln y) \quad (2.33)$$

where

$$|A|, |B|, |C| \ll 1 \quad (2.34)$$

with

$$|A| > |B| > |C|. \quad (2.35)$$

Now, for $\alpha \ll 1$, which is typically the case, one can expand the function mentioned in Eq (12) as ¹⁰:

$$(\ln y)^\alpha = 1 + \alpha \ln(\ln y) + \dots \quad (2.36)$$

Let us take first two terms in the right hand side of the series expansion. This finally results in:

$$\begin{aligned} \int_{k_e}^{k_\star} \frac{dk}{k} \sqrt{\frac{r(k)}{8}} &\approx \sqrt{\frac{r(k_\star)}{8}} \int_{e^{k_e/k_\star}}^{e^1} \frac{dy}{y \ln y} \left\{ 1 + [A + B \ln(\ln y) + C \ln^2(\ln y)] \ln(\ln y) \right\}, \\ &= \sqrt{\frac{r(k_\star)}{8}} \left[(1 - A + 2B - 6C) \ln y + (A - 2B + 6C) (\ln y) \ln(\ln y) \right. \\ &\quad \left. + (B - 3C) (\ln y) \ln^2(\ln y) + C (\ln y) (\ln(\ln y))^3 \right]_{e^{k_e/k_\star}}^{e^1}, \\ &= \sqrt{\frac{r(k_\star)}{8}} \left[(1 - A + 2B - 6C) \left[1 - \frac{k_e}{k_\star} \right] - (A - 2B + 6C) \frac{k_e}{k_\star} \ln \left(\frac{k_e}{k_\star} \right) \right. \\ &\quad \left. - (B - 3C) \frac{k_e}{k_\star} \ln^2 \left(\frac{k_e}{k_\star} \right) - C \frac{k_e}{k_\star} \ln^3 \left(\frac{k_e}{k_\star} \right) \right], \\ &= \sqrt{\frac{r(k_\star)}{8}} \left[\left(2 - \frac{a}{2} + \frac{b}{2} - \frac{c}{2} \right) \left[1 - \frac{k_e}{k_\star} \right] - \left(\frac{a}{2} - \frac{b}{2} + \frac{c}{2} - 1 \right) \frac{k_e}{k_\star} \ln \left(\frac{k_e}{k_\star} \right) \right. \\ &\quad \left. - \left(\frac{b}{4} - \frac{c}{4} \right) \frac{k_e}{k_\star} \ln^2 \left(\frac{k_e}{k_\star} \right) - \frac{c}{12} \frac{k_e}{k_\star} \ln^3 \left(\frac{k_e}{k_\star} \right) \right]. \end{aligned} \quad (2.37)$$

¹⁰One can verify the validity of $\alpha \ll 1$ for a generic single field slow roll inflation, within the interval $8.2 \times 10^{-11} \text{ Mpc}^{-1} \leq k \leq 0.056 \text{ Mpc}^{-1}$.

In any arbitrary momentum scale k spectral tilt, running of the tilt, and running of the running of the tilt for the scalar and tensor perturbations can be written as:

$$\begin{aligned} n_S(k) - 1 &\equiv \frac{d \ln P_S(k)}{d \ln k} \\ &= n_S(k_\star) - 1 + \alpha_S(k_\star) \ln \left(\frac{k}{k_\star} \right) + \frac{\kappa_S(k_\star)}{2} \ln^2 \left(\frac{k}{k_\star} \right) + \dots \end{aligned} \quad (2.38)$$

$$n_T(k) \equiv \frac{d \ln P_T(k)}{d \ln k} = n_T(k_\star) + \alpha_T(k_\star) \ln \left(\frac{k}{k_\star} \right) + \frac{\kappa_T(k_\star)}{2} \ln^2 \left(\frac{k}{k_\star} \right) + \dots \quad (2.39)$$

$$\alpha_{S,T}(k) \equiv \frac{dn_{S,T}(k)}{d \ln k} = \frac{d^2 \ln P_{S,T}(k)}{d \ln k^2} = \alpha_{S,T}(k_\star) + \kappa_{S,T}(k_\star) \ln \left(\frac{k}{k_\star} \right) + \dots \quad (2.40)$$

$$\kappa_{S,T}(k) \equiv \frac{d\alpha_{S,T}(k)}{d \ln k} = \frac{d^2 n_{S,T}(k)}{d \ln k^2} = \frac{d^3 \ln P_{S,T}(k)}{d \ln k^3} \approx \kappa_{S,T}(k_\star) + \dots \quad (2.41)$$

Also at scale k tilt, running and running of the running in tensor-to-scalar ratio can be expressed as:

$$n_r(k) \equiv \frac{dr(k)}{d \ln k} = r(k) \left[a + b \ln \left(\frac{k}{k_\star} \right) + \frac{c}{2} \ln^2 \left(\frac{k}{k_\star} \right) + \dots \right] \quad (2.42)$$

$$\begin{aligned} \alpha_r(k) &\equiv \frac{dn_r(k)}{d \ln k} = \frac{d^2 r(k)}{d \ln k^2} \\ &= [an_r(k) + br(k)] + [bn_r(k) + cr(k)] \ln \left(\frac{k}{k_\star} \right) + \frac{cn_r(k)}{2} \ln^2 \left(\frac{k}{k_\star} \right) + \dots \end{aligned} \quad (2.43)$$

$$\begin{aligned} \kappa_r(k) &\equiv \frac{d\alpha_r(k)}{d \ln k} = \frac{d^2 n_r(k)}{d \ln k^2} = \frac{d^3 r(k)}{d \ln k^3} \\ &= [a\alpha_r(k) + 2bn_r(k) + cr(k)] + [b\alpha_r(k) + 2cn_r(k)] \ln \left(\frac{k}{k_\star} \right) + \dots \end{aligned} \quad (2.44)$$

Here at an arbitrary scale k , the parameters a, b and c defined as:

$$a(k) \equiv \frac{d \ln r(k)}{d \ln k} = \left[a + b \ln \left(\frac{k}{k_\star} \right) + \frac{c}{2} \ln^2 \left(\frac{k}{k_\star} \right) + \dots \right] \quad (2.45)$$

$$b(k) \equiv \frac{da(k)}{d \ln k} = \frac{d^2 \ln r(k)}{d \ln k^2} = \left[b + c \ln \left(\frac{k}{k_\star} \right) + \dots \right] \quad (2.46)$$

$$c(k) \equiv \frac{d\alpha_r(k)}{d \ln k} = \frac{d^2 n_r(k)}{d \ln k^2} = \frac{d^3 \ln r(k)}{d \ln k^3} \approx [c + \dots] \quad (2.47)$$

In the present context the potential dependent slow-roll parameters: $(\epsilon_V, \eta_V, \dots)$, satisfy the joint Planck (2013)+WMAP-9 constraints, which imply that [8]:

$$\epsilon_V < 10^{-2} \quad (\text{within } 1.5\sigma \text{ C.L.}), \quad (2.48)$$

$$5 \times 10^{-3} < |\eta_V| < 0.021 \quad (\text{within } 1.5\sigma \text{ C.L.}), \quad (2.49)$$

and also satisfy the joint Planck (2015)+WMAP-9+high-L (TT) constraints, which imply that [15]:

$$\epsilon_V < 0.011 \quad (\text{within } 2\sigma \text{ C.L.}), \quad (2.50)$$

$$8 \times 10^{-3} < |\eta_V| < 0.021 \quad (\text{within } 1.5\sigma \text{ C.L.}), \quad (2.51)$$

$$8 \times 10^{-3} < |\xi_V^2| < 0.021 \quad (\text{within } 1.5\sigma \text{ C.L.}), \quad (2.52)$$

for which the inflationary potential is concave in nature for both the cases. In the next section, I will discuss model independent bounds on the coefficients $(V(\phi_\star), V'(\phi_\star), \dots)$ for a generic sub-Planckian VEV inflationary setup, for which I will satisfy the joint constraints from: Planck(2013 & 2015)+WMAP-9+high-L, Planck (2015)+BICEP2/Keck Array and Planck (2014)+WMAP-9+high L+BICEP2 (dust) data sets.

3 Constraining the scale of effective field theory inflation via field excursion

The number of e-foldings, $N(k)$, can be expressed as [32]:

$$N(k) \approx 71.21 - \ln\left(\frac{k}{k_\star}\right) + \frac{1}{4} \ln\left(\frac{V_\star}{M_p^4}\right) + \frac{1}{4} \ln\left(\frac{V_\star}{\rho_e}\right) + \frac{1 - 3w_{int}}{12(1 + w_{int})} \ln\left(\frac{\rho_{rh}}{\rho_e}\right), \quad (3.1)$$

where ρ_e is the energy density at the end of inflation, ρ_{rh} is an energy scale during reheating, $k_\star = a_\star H_\star$ is the present Hubble scale, V_\star corresponds to the potential energy when the relevant modes left the Hubble patch during inflation corresponding to the momentum scale k_\star , and w_{int} characterises the effective equation of state parameter between the end of inflation, and the energy scale during reheating.

Within the momentum interval, $k_e < k < k_\star$, the corresponding number of e-foldings is given by, ΔN , as:

$$\Delta N = N_\star - N_e \approx \ln\left(\frac{k_\star}{k_e}\right) = \ln\left(\frac{a_\star}{a_e}\right) + \ln\left(\frac{H_\star}{H_e}\right) \approx \ln\left(\frac{a_\star}{a_e}\right) + \frac{1}{2} \ln\left(\frac{V_\star}{V_e}\right) \quad (3.2)$$

where (a_\star, H_\star) and $(a_e H_e)$ represent the scale factor and the Hubble parameter at the pivot scale and end of inflation, and I have used the fact that

$$H^2 = \frac{V(\phi)}{3M_p^2} \quad (3.3)$$

which is true within the framework of Einstein's General Relativity. We can estimate

the contribution of the last term of the right hand side by using Eq (7.27) as follows:

$$\begin{aligned}
\ln\left(\frac{V_\star}{V_e}\right) &= \ln\left(\frac{\alpha + \beta(\phi_\star - \phi_0) + \gamma(\phi_\star - \phi_0)^3 + \kappa(\phi_\star - \phi_0)^4 + \dots}{\alpha + \beta(\phi_e - \phi_0) + \gamma(\phi_e - \phi_0)^3 + \kappa(\phi_e - \phi_0)^4 + \dots}\right), \\
&\approx \ln\left(1 + \underbrace{M_p \frac{\beta}{\alpha} \left(\frac{\Delta\phi}{M_p}\right)}_{\ll 1} \left[1 + \underbrace{\dots}_{\ll 1}\right]\right), \\
&\approx \ln(1 + \underbrace{\dots}_{\ll 1}),
\end{aligned} \tag{3.4}$$

where

$$(\Delta\phi/M_p) \ll 1, \tag{3.5}$$

and additionally I assume that

$$(\beta M_p/\alpha) \ll 1. \tag{3.6}$$

Consequently, Eq (3.2) reduces to the following simplified expression:

$$\Delta N \approx \ln\left(\frac{k_\star}{k_e}\right) \approx \ln\left(\frac{a_\star}{a_e}\right) \approx \mathcal{O}(8 - 17) \text{ e-folds}. \tag{3.7}$$

Within the observed limit of CMB distortion, i.e. $\Delta N \approx 17$, the slow-roll parameters, see Eqs. (10.12, 10.13) of Appendix, show non-monotonic behaviour, where the corresponding scalar and tensor amplitude of the power spectrum remains almost unchanged¹¹. Substituting the results obtained from Eq. (10.12) and Eq. (10.13) (see Appendix), and with the help of Eq. (3.2), up to the leading order, I obtain:

$$\sum_{n=0}^{\infty} \mathbf{G}_n \left(\frac{|\Delta\phi|}{M_p}\right)^n \approx \sqrt{\frac{r(k_\star)}{8}} \times \left|\frac{a}{2} - \frac{b}{2} + \frac{c}{2} - 2\right| + \dots \tag{3.8}$$

where for $\Delta N = 17$ and $\Delta N = 8$ I have used

$$(k_e/k_\star) \approx \exp(-\Delta N) = \exp(-17) \approx 4.13 \times 10^{-8}, \tag{3.9}$$

$$(k_e/k_\star) \approx \exp(-\Delta N) = \exp(-8) \approx 3.35 \times 10^{-4}. \tag{3.10}$$

Here I will concentrate on

$$a, b, c \neq 0 \tag{3.11}$$

¹¹In this paper I fix $\Delta\mathcal{N} \approx \mathcal{O}(8 - 17)$ e-foldings as within this interval the combined constraints from Planck (2013 & 2015)+WMAP-9+high-L and Planck (2015)+BICEP2/Keck Array are satisfied. Additionally I have also mentioned the results by applying the constraints from [Planck \(2014\)+WMAP-9+high L+BICEP2 \(dust\)](#) data to explicitly show that our prescribed methodology also holds good for $r(k_\star) > 0.12$.

where additionally

$$a \gg b \gg c \quad (3.12)$$

case is satisfied (for the details, see [23, 26, 27, 33]). In Eq (3.8) the series appearing in the left side of the above expression is convergent, since the expansion coefficients can be expressed as:

$$\mathbf{G}_n = \begin{cases} \left(1 + \underbrace{\sum_{m=0}^{\infty} \mathbf{A}_m \left(\frac{\phi_e - \phi_0}{M_p} \right)^m}_{\ll 1} \right) \sim 1 & \text{for } n = 1 \\ \ll 1 & \text{for } n \geq 2, \end{cases} \quad (3.13)$$

and I have defined a new dimensionless binomial expansion co-efficient (\mathbf{A}_m), defined as:

$$\mathbf{A}_m = M_p^{m+2} \left[\left(\mathcal{C}_E - \frac{1}{2} \right) \mathbf{C}_m - \mathcal{C}_E \mathbf{D}_m \right] \quad (\forall m = 0, 1, 2, \dots), \quad (3.14)$$

which is obtained from the binomial series expansion from the leading order results of the slow-roll integrals stated in the Appendix ¹².

Note that the expansion co-efficient $\mathbf{A}_m (\forall m)$ are suppressed by, $V(\phi_0)$, which is the leading order term in a generic expansion of the inflationary potential as shown in Eq (1.6) and Eq (7.27)(see also Eq (10.14) in the Appendix). We can expand the left side of Eq. (3.8) in the powers of $\Delta\phi/M_p$, using the additional constraint

$$\Delta\phi < (\phi_e - \phi_0) < M_p, \quad (3.15)$$

and I keep the leading order terms in $\Delta\phi/M_p$.

To the first order approximation - I can neglect all the higher powers of $k_e/k_\star \approx \mathcal{O}(10^{-4} - 10^{-8})$ from the left hand side of Eq (3.8), within $\mathcal{O}(8 - 17)$ e-foldings of inflation [23, 28, 29]. Consequently, Eq. (3.8) reduces to the following compact form for $r(k_\star)$:

$$\frac{9}{25} \sqrt{\frac{r(k_\star)}{0.27}} \left| \frac{27}{1600} \left(\frac{r(k_\star)}{0.27} \right) - \frac{\eta_V(k_\star)}{2} - 1 + \dots \right| \approx \frac{|\Delta\phi|}{M_p} \leq 1, \quad (3.16)$$

provided at the pivot scale, $k = k_\star \gg k_e$, in this regime

$$|\eta_V| \gg \{ \epsilon_V^2, \eta_V^2, \xi_V^2, \sigma_V^3, \dots \} \quad (3.17)$$

¹²In Eq. (3.14), and Eqs. (10.12, 10.13) (see Appendix), \mathbf{C}_p and \mathbf{D}_q are Planck suppressed dimensional (mass dimension $[M_p^{-(m+2)}]$) binomial series expansion coefficients, which are expressed in terms of the generic model parameters ($V(\phi_\star), V'(\phi_\star), \dots$) as presented in Eq (7.27).

approximation is valid. Our expression, Eq. (3.16), shows that large value of $r(k_*)$ can be obtained for models of inflation where inflation occurs below the Planck cut-off. Once the field excursion, $|\Delta\phi|/M_p$, and η_V , are known from any type of sub-Planckian inflationary setup, one can easily compute the tensor-to-scalar ratio by finding the roots.

The expression, as stated in Eq (3.16), is in the form of a simple algebraic (cubic) equation. In order to find the roots of tensor-to-scalar ratio r in terms of the field excursion $|\Delta\phi|/M_p$, one has to solve a cubic equation:

$$x^3 + Ux - W = 0, \quad (3.18)$$

where

$$x := \sqrt{\frac{r(k_*)}{0.27}}, \quad (3.19)$$

$$U := \frac{800}{27} (\eta_V + 2), \quad (3.20)$$

$$W := \frac{40000}{243} \frac{|\Delta\phi|}{M_p}. \quad (3.21)$$

The three roots x_1, x_2, x_3 are explicitly given by:

$$x_1 = -\frac{\left(\frac{2}{3}\right)^{1/3} U}{Y} + \frac{Y}{2^{1/3} 3^{2/3}}, \quad (3.22)$$

$$x_2 = \frac{(1 + i\sqrt{3}) U}{2^{2/3} 3^{1/3} Y} - \frac{(1 - i\sqrt{3}) Y}{2^{4/3} 3^{2/3}}, \quad (3.23)$$

$$x_3 = \frac{(1 - i\sqrt{3}) U}{2^{2/3} 3^{1/3} Y} - \frac{(1 + i\sqrt{3}) Y}{2^{4/3} 3^{2/3}}. \quad (3.24)$$

where the symbol,

$$Y = \left(9W + \sqrt{3}\sqrt{4U^3 + 27W^2}\right)^{1/3}. \quad (3.25)$$

Here the complex roots x_2 and x_3 are physically redundant. The only acceptable root is the real one, i.e. x_1 which will finally contribute for the estimation of field excursion for a specified value of tensor-to-scalar ratio $r(k_*)$.

Further note that our formulation will also hold true if inflation were to start at the hill-top, such as

$$\phi = 0. \quad (3.26)$$

However in this case one would have to proceed similarly by expanding the potential around

$$\phi_0 = 0, \quad (3.27)$$

and then follow the algorithm I have provided here.

Now, it is also possible to recast $a(k)$, $b(k)$, $c(k)$, in terms of $r(k)$, and the slow roll parameters by using the relation, Eq. (10.8) (see Appendix):

$$\begin{aligned} a(k_*) &\approx \left[\frac{r(k_*)}{4} - 2\eta_V(k_*) + \dots \right], \\ b(k_*) &\approx [16\epsilon_V^2(k_*) - 12\epsilon_V(k_*)\eta_V(k_*) + 2\xi_V^2(k_*) + \dots], \\ c(k_*) &\approx [-2\sigma_V^3 + \dots], \end{aligned} \quad (3.28)$$

where “...” involve the higher order slow roll contributions, which are negligibly small in the leading order approximation.

Now at the pivot scale, $k_* = 0.002 \text{ Mpc}^{-1}$, the scale of inflation $V^{1/4}(\phi_*)$ can be expressed as:

$$V^{1/4}(\phi_*) = \left(\frac{3}{2} P_S(k_*) r(k_*) \right)^{1/4} \times \sqrt{\pi} M_p \leq (2.40 \times 10^{16} \text{ GeV}) \times \left(\frac{r(k_*)}{0.27} \right)^{1/4}. \quad (3.29)$$

The equivalent statement can be made in terms of the upper bound on the numerical value of the Hubble parameter at the exit of the relevant modes:

$$H_* \leq 1.38 \times 10^{14} \times \sqrt{\frac{r(k_*)}{0.27}} \text{ GeV}. \quad (3.30)$$

Combining Eqs. (3.16), (3.30) and (3.29), I can now obtain a closed relationships:

$$\frac{|\Delta\phi|}{M_p} \leq \frac{\sqrt{V_*}}{(1.55 \times 10^{-2} M_p)^2} \left| \frac{V_*}{(2.78 \times 10^{-2} M_p)^4} - \frac{\eta_V(k_*)}{2} - 1 \right|. \quad (3.31)$$

$$\frac{|\Delta\phi|}{M_p} \leq \frac{H_*}{(1.39 \times 10^{-4} M_p)} \left| \frac{H_*^2}{(1.99 \times 10^{-7} M_p^2)} - \frac{\eta_V(k_*)}{2} - 1 \right|. \quad (3.32)$$

where additionally

$$|\eta_V| \gg \{ \epsilon_V^2, \eta_V^2, \xi_V^2, \sigma_V^3, \dots \} \quad (3.33)$$

are satisfied. Similar expressions were derived in Ref. [23] for *inflection-point* model of inflation, where an additional constraint

$$V''(\phi_0) = 0 \quad (3.34)$$

is considered for the computation. The above Eqs. (3.31, 3.32) characterize the bounds on $\Delta\phi$ for:

$$\phi_0 < M_p, \quad (3.35)$$

$$\Delta\phi \lesssim M_p. \quad (3.36)$$

Our conditions, Eqs. (3.16, 3.31), provide new constraints on model building for inflation within particle theory, where the inflaton potential is always constructed within an effective field theory with a cut-off. Note that

$$|\eta_V(k_*)| > 0 \quad (3.37)$$

can provide the largest contribution, in order to satisfy the latest bound on the tensor-to-scalar ratio, the shape of the potential has to be *concave* in nature. Further applying this input in Eq (3.29), one can get a preferred bound on the scale of sub-Planckian VEV inflation as:

Planck (2013)+WMAP-9+high L:

$$\sqrt[4]{V_*} \leq 1.96 \times 10^{16} \text{ GeV} \quad \text{for} \quad r_* \leq 0.12, \quad (3.38)$$

$$H_* \leq 9.20 \times 10^{13} \text{ GeV} \quad \text{for} \quad r_* \leq 0.12, \quad (3.39)$$

Planck (2014)+WMAP-9+high L+BICEP2 (dust):

$$2.07 \times 10^{16} \text{ GeV} \leq \sqrt[4]{V_*} \leq 2.40 \times 10^{16} \text{ GeV} \quad \text{for} \quad 0.15 \leq r_* \leq 0.27, \quad (3.40)$$

$$1.03 \times 10^{14} \text{ GeV} \leq H_* \leq 1.38 \times 10^{14} \text{ GeV} \quad \text{for} \quad 0.15 \leq r_* \leq 0.27. \quad (3.41)$$

Planck (2015)+WMAP-9+high L(TT):

$$\sqrt[4]{V_*} \leq 1.92 \times 10^{16} \text{ GeV} \quad \text{for} \quad r_* \leq 0.11, \quad (3.42)$$

$$H_* \leq 8.80 \times 10^{13} \text{ GeV} \quad \text{for} \quad r_* \leq 0.11, \quad (3.43)$$

Planck (2015)+BICEP2/Keck Array :

$$\sqrt[4]{V_*} \leq 1.96 \times 10^{16} \text{ GeV} \quad \text{for} \quad r_* \leq 0.12, \quad (3.44)$$

$$H_* \leq 9.20 \times 10^{13} \text{ GeV} \quad \text{for} \quad r_* \leq 0.12. \quad (3.45)$$

4 Non-monotonic behaviour of slow-roll parameters within effective field theory

Let us now discuss the non-monotonous features of slow-roll parameters $\epsilon_V, \eta_V, \xi_V^2, \sigma_V^3$ appearing in the present context of the paper:-

- To violate the Lyth bound mainly ϵ_V and also the other slow-roll parameters $\eta_V, \xi_V^2, \sigma_V^3$ must decrease at some point during the inflationary epoch. This is evident from the definition of no. of e-foldings,

$$\begin{aligned} N &= \frac{1}{M_p} \int_{\phi_{emb}}^{\phi_e} \frac{d\phi}{\sqrt{2\epsilon_V}} \\ &\approx \frac{1}{M_p} \int_{\phi_{emb}}^{\phi_e} \sqrt{\frac{8}{r}} d\phi, \end{aligned} \quad (4.1)$$

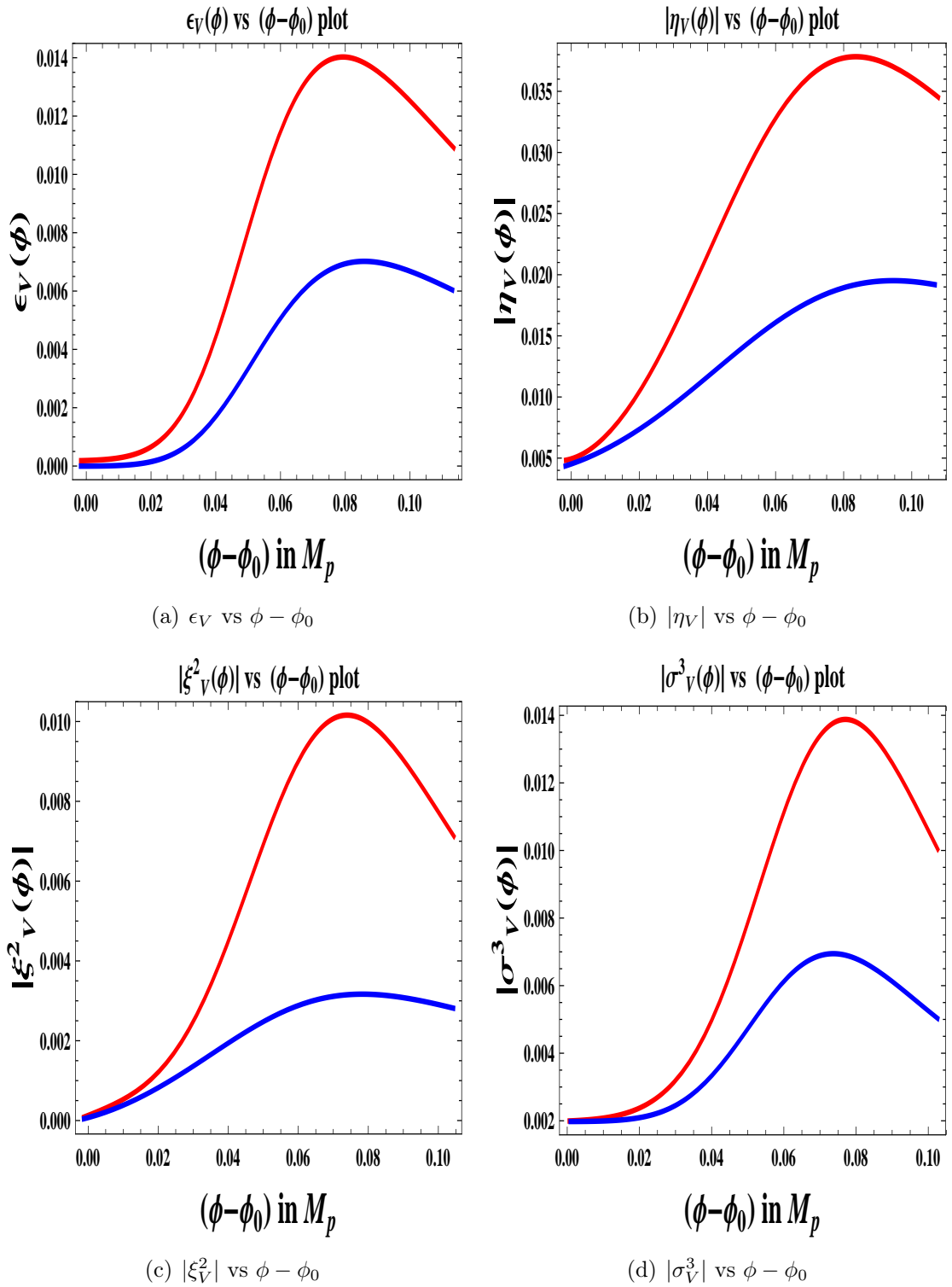


Figure 1. Non-monotonous evolution of the slow roll parameters are shown with respect to $\phi - \phi_0$. The upper and lower bounds are set by Eqs. (5.11-5.15).

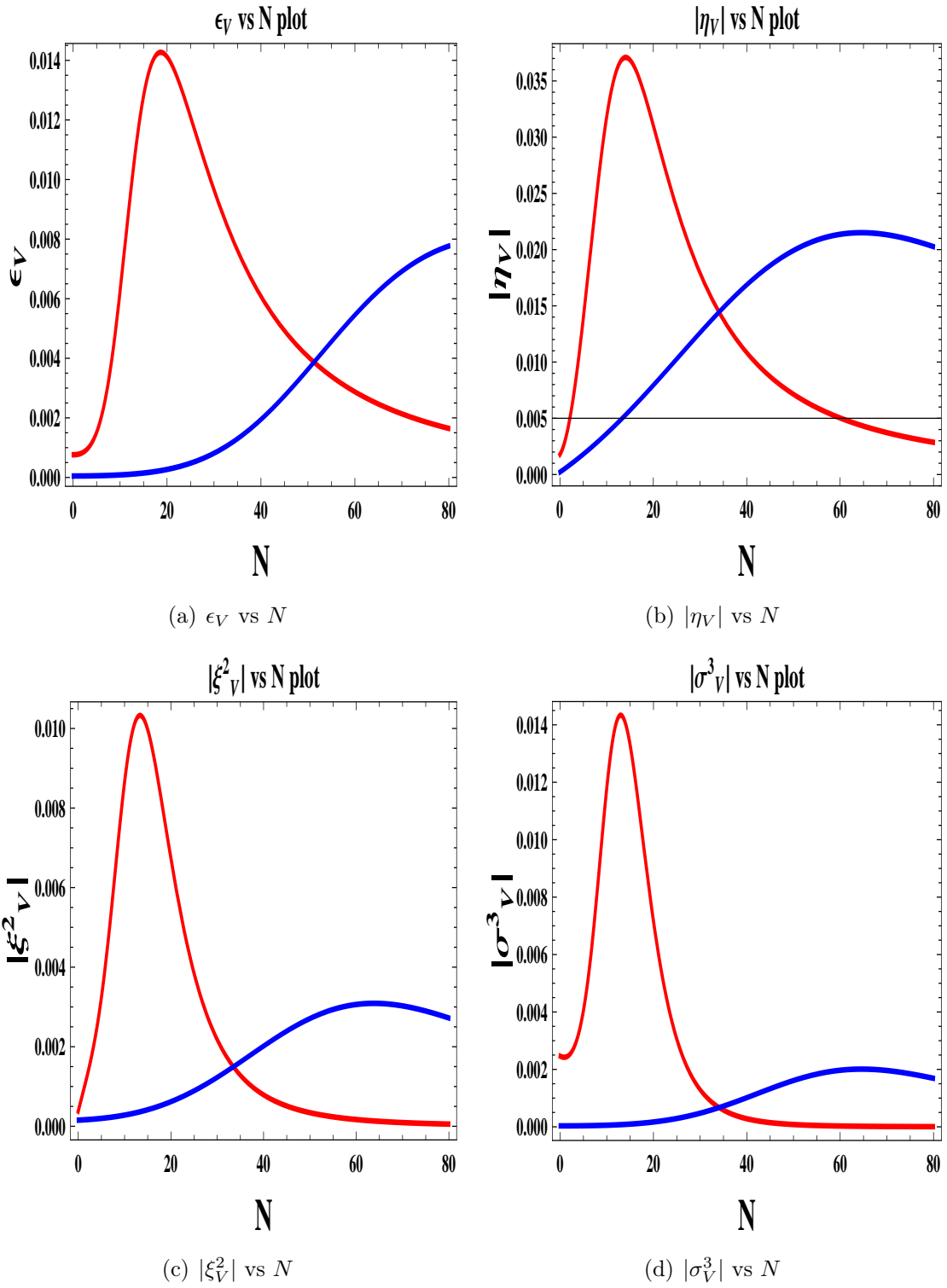


Figure 2. Non-monotonous evolution of the slow roll parameters are shown with respect to number of e-foldings N . The upper and lower bounds are set by Eqs. (5.11-5.15).

where, if ϵ_V decreases, ΔN will increase for the same field excursion, $\Delta\phi$. Unfortunately this alone is not sufficient enough to successfully evade the Lyth bound and match all observations.

- At CMB scale,

$$k = k_{cmb}(= aH), \quad (4.2)$$

at least ϵ_V must be large enough to generate an observable value of tensor-to-scalar ratio r . In our methodology I have considered that the other slow-roll parameters $\eta_V, \xi_V^2, \sigma_V^3$ also be sufficiently large to confront observation at CMB scale.

- Also ϵ_V and the other slow-roll parameters must increase over the $\Delta N \approx 17$ e-fold observational window [23, 28, 29]. This is dictated by a combination of the spectral index constraint and the observed value of σ_8 from large-scale structure (LSS) [34], which means the spectrum must decrease over the observational window. When running of the spectral index is allowed, the best fit value for the spectral index is indeed

$$n_S > 1, \quad (4.3)$$

but the running is

$$\alpha_S < 0, \quad (4.4)$$

therefore ϵ_V must increase eventually. Also, the value of σ_8 measured independently from LSS strongly favours a primordial spectrum that decreases amplitude between Planck and LSS scales.

- After observable scales have left the horizon ($k > aH$), ϵ_V and the other slow-roll parameters must quickly decrease. The quick decrease of ϵ_V and as well as other slow-roll parameters are necessary to generate enough e-folds required for inflation. If instead ϵ_V decreases gradually within the present context, then it will need to eventually decrease to a much smaller value because in such a situation

$$\epsilon_V \propto (\Delta\phi/2M_p\Delta N)^2, \quad (4.5)$$

$$\eta_V \propto 2\epsilon_V + (1/\sqrt{2}\Delta N), \quad (4.6)$$

$$\xi_V^2 \propto 2\epsilon_V \left[1 + 2\epsilon_V + (\sqrt{2}/\Delta N) \right] + (1/\sqrt{2}\Delta N)^2, \quad (4.7)$$

$$\sigma_V^3 \propto 2\epsilon_V \left\{ 4\epsilon_V \left[1 + \epsilon_V + (\sqrt{2}/\Delta N) \right] + (1/\sqrt{2}\Delta N) \left[\sqrt{2} + (1/2\epsilon_V\Delta N)^2 \right] + 3(1/\sqrt{2}\Delta N)^2 \right\}, \quad (4.8)$$

and I finally require

$$\Delta\phi \leq M_p \quad (4.9)$$

to violate the Lyth bound in the present context. Consequently, the slope of $\epsilon_V, \eta_V, \xi_V^2, \sigma_V^3$ in fig (1) and fig (2) can be computed as:

$$\Delta\epsilon_V/\Delta\phi \propto (\sqrt{\epsilon_V}/M_p\Delta N), \quad (4.10)$$

$$\Delta\eta_V/\Delta\phi \propto 2(\sqrt{\epsilon_V}/M_p\Delta N) + (1/2M_p\sqrt{2\epsilon_V}(\Delta N)^2), \quad (4.11)$$

$$\begin{aligned} \Delta\xi_V^2/\Delta\phi \propto 2(\sqrt{\epsilon_V}/M_p\Delta N) \left[1 + 4\epsilon_V + (\sqrt{2}/\Delta N) \right] + (\sqrt{2\epsilon_V}/M_p(\Delta N)^2) \\ + (1/4M_p\sqrt{\epsilon_V}(\Delta N)^3), \end{aligned} \quad (4.12)$$

$$\begin{aligned} \Delta\sigma_V^3/\Delta\phi \propto (\sigma_V^3/M_p\sqrt{\epsilon_V}\Delta N) + (8\epsilon_V\sqrt{\epsilon_V}/M_p\Delta N) \left[1 + \epsilon_V + (\sqrt{2}/\Delta N) \right] \\ + 8\epsilon_V^2 \left[(\sqrt{\epsilon_V}/M_p\Delta N) + (1/M_p\sqrt{2\epsilon_V}(\Delta N)^2) \right] \\ + (\sqrt{\epsilon_V}/M_p\sqrt{2}(\Delta N)^2) \left[\sqrt{2} + (1/2\epsilon_V\Delta N)^2 \right] \\ + (1/2M_p(2\epsilon_V)^{3/2}(\Delta N)^4) + (6\sqrt{\epsilon_V}/4M_p(\Delta N)^3), \end{aligned} \quad (4.13)$$

and

$$|\Delta\epsilon_V/\Delta N| \propto (4\epsilon_V/\Delta N), \quad (4.14)$$

$$|\Delta\eta_V/\Delta N| \propto (8\epsilon_V/\Delta N) + (1/\sqrt{2}(\Delta N)^2), \quad (4.15)$$

$$\begin{aligned} |\Delta\xi_V^2/\Delta N| \propto (8\epsilon_V/\Delta N) \left[1 + 2\epsilon_V + (\sqrt{2}/\Delta N) \right] + 2\epsilon_V \left[(8\epsilon_V/\Delta N) + (\sqrt{2}/(\Delta N)^2) \right] \\ + (1/\Delta N)^3, \end{aligned} \quad (4.16)$$

$$\begin{aligned} |\Delta\sigma_V^3/\Delta N| \propto (2\sigma_V^3/\Delta N) + (32\epsilon_V^2/\Delta N) \left[1 + \epsilon_V + (\sqrt{2}/\Delta N) \right] \\ + 8\epsilon_V^2 \left[(4\epsilon_V/\Delta N) + (\sqrt{2}/(\Delta N)^2) \right] \\ + (\sqrt{2\epsilon_V}/(\Delta N)^2) \left[\sqrt{2} + (1/2\epsilon_V\Delta N)^2 \right] \\ + (\sqrt{2}/(\Delta N)^4) + (6\sqrt{2}\epsilon_V/(\Delta N)^3). \end{aligned} \quad (4.17)$$

- Just before the end of inflation ϵ_V and the other slow-roll parameters must eventually increase again.
- The change in ϵ_V and other slow-roll parameters must also not be too sharp in order not to violate slow-roll condition within the prescribed setup.
- In case of usual monotonic case the end of inflation (ϕ_e) is fixed by the condition:

$$\max_{\phi=\phi_e} [\epsilon_V, |\eta_V|, |\xi_V^2|, |\sigma_V^3|] \equiv 1. \quad (4.18)$$

But in the present case the non-monotonicity of the slow-roll parameters cannot be able to push the maximum field value upto unity at the end of inflation. In this case fig (1) suggest that

$$\max_{\phi=\phi_e} [|\eta_V|] > \max_{\phi=\phi_e} [\epsilon_V] = \max_{\phi=\phi_e} [|\sigma_V^3|] > \max_{\phi=\phi_e} [|\xi_V^2|] \ll 1 \quad (4.19)$$

and this also implies that from the maximization of $|\eta_V|$ one can compute the field value corresponding to the end of inflation. Eq (4.19) can also be represented in the form of the following constraint conditions:

$$|V''(\phi_e)| \ll \left| \frac{V(\phi_e)}{M_p^2} \right|, \quad (4.20)$$

$$V'(\phi_e) \ll \frac{\sqrt{2}V(\phi_e)}{M_p}, \quad (4.21)$$

$$|V'(\phi_e)| \ll \sqrt{2|V(\phi_e)V'''(\phi_e)|}, \quad (4.22)$$

$$V(\phi_e) = 2M_p^4 V''''(\phi_e), \quad (4.23)$$

$$|V''''(\phi_e)| \gg \left| \frac{\sqrt{V'(\phi_e)V''''(\phi_e)}}{2M_p^2} \right|, \quad (4.24)$$

$$|V'(\phi_e)| \gg 2M_p^2 |V''''(\phi_e)|, \quad (4.25)$$

$$|V(\phi_e)| \gg M_p^2 |V''''(\phi_e)|. \quad (4.26)$$

Further substituting Eq (1.6) in Eq (4.23) finally one can find the field value $(\phi_e - \phi_0)$.

The most demanding aspect of the conditions is that the single scalar potential in a non-trivial fashion reduces $\epsilon_V, \eta_V, \xi_V^2, \sigma_V^3$ after observable scales leaving the horizon at $k > aH$ and subsequently in a non-standard way increases $\epsilon_V, \eta_V, \xi_V^2, \sigma_V^3$ just before the end of inflation. If inflation is, instead, brought to an end by another non-trivial mechanism, such as a hybrid transition [22], then one can relax the fifth condition in the present context. This makes the task of reconstructing the inflationary potential simpler. However, in this work I have utilized almost all of the conditions to reconstruct the structure of inflationary potential.

Most importantly, the condition that ϵ_V first increases and then decreases is not very uncommon in the context of inflationary model building and can easily be achieved by simply adding a constant vacuum energy correction term to a potential that already supports inflation and has increased ϵ_V as well. Before the constant vacuum energy correction term becomes completely dominant, ϵ_V and the slow-roll parameters will continue to increase as before. Then, when the constant term does come to completely dominate, ϵ_V as well as the other slow-roll parameters approach towards zero. If the contribution from such vacuum energy dominated correction term is sufficiently large enough, this transition will occur before the end of inflation. This also suggests that to successfully evade the Lyth bound in the present context, the occurrence of this special feature must coincide with the end of the observational window and occur with the right magnitude, which is not guaranteed. However, the non-monotonic variation of ϵ_V as well as the other slow-roll parameters are the examples of this physical mechanism, which will take care of all these issues successfully.

Additionally it is important to note that with non-monotonic evolution of ϵ_V will modify the power-law feature in the primordial density perturbations. Apart from an observable tensor-to-scalar ratio, such non-monotonicity criteria of the slow-roll parameters generically exhibit the following unconventional features in the present context:

- Existence of a non-negligible, scale-dependent running (α_S) and running of the running (κ_S), of the scalar spectral index (n_S).
- Appearance of a significant increase in the primordial power spectrum on very small momentum scales.

The non-negligible running and running of the running arises because there must be significant evolution of ϵ_V as well as the other slow-roll parameters while observable momentum scales are crossing the horizon at $k = aH$. This is possible in principle for all the evolution of ϵ_V to occur only after the observable scales have crossed the horizon, it requires sharp features in ϵ_V and after that the decrement in ϵ_V and other slow-roll parameters begin, the greater the decrement must be in order to get sufficient e -folds to achieve inflation. If this decrement is huge and very faster, then the perturbative approach of the scalar fluctuations, and consequently the consistency of inflation, breaks down in the context of inflationary reconstruction of potential. This problem can only be addressed by a concurrent sharp fall in the energy scale associated with inflation. For details see ref. [35] where such a sharp change would be described as an inflationary model with multiple periods of inflation, rather than one single period with an evolving ϵ_V . Also to explain the non-monotonicity of slow-roll parameters the reconstruction technique is implemented in order to impose a sufficient running and running of the running at the pivot scale. The necessary evolution of ϵ_V required for consistency of inflation pointing towards the fact that the running and running of the running will be scale-dependent. This implies that the description of the scalar primordial power spectrum using the simple power-law parameterization in momentum scale is not sufficient enough to explain non-monotonic evolution of ϵ_V and as well as other slow-roll parameters to evade the Lyth bound. Finally, the increase in the primordial power spectrum at very small momentum scales is an outcome of the necessary decrement of ϵ_V and other slow-roll parameters outside the observational window. If the amplitude of the primordial power spectrum on these scales is sufficiently large enough then primordial black holes (PBHs) will be formed ¹³.

¹³Present cosmological constraints on PBH's restrict $P_S \lesssim 10^{-2}$. See refs. [36–38] for details.

5 Reconstruction technique of the structure of inflationary effective potential

Let us now mention the crucial steps followed during the reconstruction of inflationary potential:-

- **STEP I:**

First of all I need the required data for inflationary observables from an observational probe at CMB scale. In our case I use Planck (2013)+WMAP-9+high-L, **Planck (2014)+WMAP-9+high L+BICEP2 (dust)**, Planck (2015) +WMAP-9+high-L (TT) and Planck (2015)+BICEP2/Keck Array data sets for the numerical estimations. Most importantly, I need to implement the reconstruction technique in such a way that I can check the validity and convergence of the proposed methodology using any observational probe.

- **STEP II:**

Next I assume the slow-roll paradigm within our prescription. Also I demand from the field theoretic requirement that the reconstructed potential is renormalizable and for this reason the Taylor series expansion of the potential is truncated at the fourth order derivative term.

- **STEP III:**

Further I construct the scale and the Taylor series expansion co-efficients of inflationary potential from the derivatives upto fourth order at the CMB scale.

- **STEP IV:**

Hence I use matrix inversion technique to determine the Taylor series expansion co-efficients of the potential around the VEV ϕ_0 of the inflationary potential. This is only possible when the system (square) matrix computed from the difference in the field value of the potential at the CMB scale and at VEV is non-singular.

- **STEP V:**

Finally, to determine the various cosmological parameters and to check the validity of the reconstruction technique I fit the reconstructed potential with the observed CMB angular power spectra from TT, TE, EE and BB mode obtained from WMAP9, Planck (2013, 2014, 2015) along with BICEP2/Keck Array joint data.

Let us now discuss observational constraints on the Taylor expansion coefficients $(V(\phi_0), V'(\phi_0), \dots)$ as appearing in Eq (1.6).

Let us first write down $V(\phi_\star), V'(\phi_\star), V''(\phi_\star), \dots$ in terms of the inflationary observables (see Appendix, Eqs. (10.4, 10.6, 10.8)):

$$\begin{aligned}
V(\phi_\star) &= \frac{3}{2} P_S(k_\star) r(k_\star) \pi^2 M_p^4, \\
V'(\phi_\star) &= \frac{3}{2} P_S(k_\star) r(k_\star) \pi^2 \sqrt{\frac{r(k_\star)}{8}} M_p^3, \\
V''(\phi_\star) &= \frac{3}{4} P_S(k_\star) r(k_\star) \pi^2 \left(n_S(k_\star) - 1 + \frac{3r(k_\star)}{8} \right) M_p^2, \\
V'''(\phi_\star) &= \frac{3}{2} P_S(k_\star) r(k_\star) \pi^2 \left[\sqrt{2r(k_\star)} \left(n_S(k_\star) - 1 + \frac{3r(k_\star)}{8} \right) \right. \\
&\quad \left. - \frac{1}{2} \left(\frac{r(k_\star)}{8} \right)^{\frac{3}{2}} - \alpha_S(k_\star) \sqrt{\frac{2}{r(k_\star)}} \right] M_p, \\
V''''(\phi_\star) &= 12 P_S(k_\star) \pi^2 \left\{ \frac{\kappa_S(k_\star)}{2} - \frac{1}{2} \left(\frac{r(k_\star)}{8} \right)^2 \left(n_S(k_\star) - 1 + \frac{3r(k_\star)}{8} \right) \right. \\
&\quad \left. + 12 \left(\frac{r(k_\star)}{8} \right)^3 + r(k_\star) \left(n_S(k_\star) - 1 + \frac{3r(k_\star)}{8} \right)^2 \right. \\
&\quad \left. + \left[\sqrt{2r(k_\star)} \left(n_S(k_\star) - 1 + \frac{3r(k_\star)}{8} \right) \right. \right. \\
&\quad \left. \left. - \frac{1}{2} \left(\frac{r(k_\star)}{8} \right)^{\frac{3}{2}} - \alpha_S(k_\star) \sqrt{\frac{2}{r(k_\star)}} \right] \right. \\
&\quad \left. \times \left[\sqrt{\frac{r(k_\star)}{8}} \left(n_S(k_\star) - 1 + \frac{3r(k_\star)}{8} \right) - 6 \left(\frac{r(k_\star)}{8} \right)^{\frac{3}{2}} \right] \right\} \quad (5.1)
\end{aligned}$$

Therefore, for any chosen sub-Planckian VEV of ϕ_\star , I can obtain a matrix equation characterizing the coefficients: $V(\phi_0), V'(\phi_0), V''(\phi_0), \dots$:

$$\underbrace{\begin{pmatrix} 1 & \vartheta_\star & \frac{\vartheta_\star^2}{2} & \frac{\vartheta_\star^3}{6} & \frac{\vartheta_\star^4}{24} \\ 0 & 1 & \vartheta_\star & \frac{\vartheta_\star^2}{2} & \frac{\vartheta_\star^3}{6} \\ 0 & 0 & 1 & \vartheta_\star & \frac{\vartheta_\star^2}{2} \\ 0 & 0 & 0 & 1 & \vartheta_\star \\ 0 & 0 & 0 & 0 & 1 \end{pmatrix}} \begin{pmatrix} V(\phi_0) \\ V'(\phi_0) \\ V''(\phi_0) \\ V'''(\phi_0) \\ V''''(\phi_0) \end{pmatrix} = \begin{pmatrix} V(\phi_\star) \\ V'(\phi_\star) \\ V''(\phi_\star) \\ V'''(\phi_\star) \\ V''''(\phi_\star) \end{pmatrix}, \quad (5.2)$$

where I have define

$$\vartheta_\star := (\phi_\star - \phi_0) < M_p.$$

The square matrix marked by the symbol $\underbrace{\dots}$ is nonsingular, since its determinant is nonzero, for which the matrix inversion technique is applicable in the present context. Finally, I get the following physical solution to the problem:

$$\begin{pmatrix} V(\phi_0) \\ V'(\phi_0) \\ V''(\phi_0) \\ V'''(\phi_0) \\ V''''(\phi_0) \end{pmatrix} = \begin{pmatrix} 1 & -\vartheta_\star & \frac{\vartheta_\star^2}{2} & -\frac{\vartheta_\star^3}{6} & \frac{\vartheta_\star^4}{24} \\ 0 & 1 & -\vartheta_\star & \frac{\vartheta_\star^2}{2} & -\frac{\vartheta_\star^3}{6} \\ 0 & 0 & 1 & -\vartheta_\star & \frac{\vartheta_\star^2}{2} \\ 0 & 0 & 0 & 1 & -\vartheta_\star \\ 0 & 0 & 0 & 0 & 1 \end{pmatrix} \begin{pmatrix} V(\phi_\star) \\ V'(\phi_\star) \\ V''(\phi_\star) \\ V'''(\phi_\star) \\ V''''(\phi_\star) \end{pmatrix}. \quad (5.3)$$

For a model independent constraint on the shape of the potential, the parameter,

$$\vartheta_\star \sim \mathcal{O}(10^{-1}M_p), \quad (5.4)$$

as

$$\Delta\phi \sim \mathcal{O}(10^{-1}M_p), \quad (5.5)$$

which is applicable to a large class of sub-Planckian inflationary models to generate sufficient amount of inflation within $50 < N_{total} < 70$. This criteria holds good for high scale inflation, but within the regime of sub-Planckian cut-off.

In order to satisfy the preferred bounds, see Eq. (1.17)-Eq. (1.36), the following model independent theoretical constraints on $V(\phi_\star), V'(\phi_\star), \dots$ have to be imposed:

Planck (2013)+WMAP-9+high L:

$$V(\phi_\star) \leq \mathcal{O}(3.79 - 3.99) \times 10^{-9}M_p^4, \quad (5.6)$$

$$V'(\phi_\star) \leq \mathcal{O}(4.65 - 4.89) \times 10^{-10}M_p^3, \quad (5.7)$$

$$V''(\phi_\star) \leq \mathcal{O}((-0.41) - 2.42) \times 10^{-11}M_p^2, \quad (5.8)$$

$$V'''(\phi_\star) \leq \mathcal{O}(8.52 - 35.1) \times 10^{-11}M_p, \quad (5.9)$$

$$V''''(\phi_\star) \leq \mathcal{O}(0.39 - 4.76) \times 10^{-9}, \quad (5.10)$$

Planck (2014)+WMAP-9+high L+BICEP2 (dust):

$$5.27 \times 10^{-9}M_p^4 \leq V(\phi_\star) \leq 9.52 \times 10^{-9}M_p^4, \quad (5.11)$$

$$2.45 \times 10^{-10}M_p^3 \leq V'(\phi_\star) \leq 1.75 \times 10^{-9}M_p^3, \quad (5.12)$$

$$2.41 \times 10^{-11}M_p^2 \leq V''(\phi_\star) \leq 3.25 \times 10^{-10}M_p^2, \quad (5.13)$$

$$6.35 \times 10^{-10}M_p \leq V'''(\phi_\star) \leq 7.56 \times 10^{-10}M_p, \quad (5.14)$$

$$5.56 \times 10^{-10} \leq V''''(\phi_\star) \leq 4.82 \times 10^{-9}, \quad (5.15)$$

Planck (2015)+WMAP-9+high L(TT):

$$V(\phi_*) \leq \mathcal{O}(3.45 - 3.71) \times 10^{-9} M_p^4, \quad (5.16)$$

$$V'(\phi_*) \leq \mathcal{O}(4.04 - 4.35) \times 10^{-10} M_p^3, \quad (5.17)$$

$$V''(\phi_*) \leq \mathcal{O}((-2.93) - 1.08) \times 10^{-11} M_p^2, \quad (5.18)$$

$$V'''(\phi_*) \leq \mathcal{O}((-0.48) - (-3.88)) \times 10^{-10} M_p, \quad (5.19)$$

$$V''''(\phi_*) \leq \mathcal{O}(5.52 - 5.76) \times 10^{-9}, \quad (5.20)$$

Planck (2015)+BICEP2/Keck Array:

$$V(\phi_*) \leq \mathcal{O}(3.80 - 3.99) \times 10^{-9} M_p^4, \quad (5.21)$$

$$V'(\phi_*) \leq \mathcal{O}(4.65 - 4.89) \times 10^{-10} M_p^3, \quad (5.22)$$

$$V''(\phi_*) \leq \mathcal{O}((-0.41) - 2.42) \times 10^{-11} M_p^2, \quad (5.23)$$

$$V'''(\phi_*) \leq \mathcal{O}(8.52 - 35.1) \times 10^{-10} M_p, \quad (5.24)$$

$$V''''(\phi_*) \leq \mathcal{O}(0.39 - 4.76) \times 10^{-9}, \quad (5.25)$$

Now, substituting the above expressions in Eq (5.3), I obtain model independent constraints on the Taylor expansion co-efficients at $\phi = \phi_0$ i.e. $V(\phi_0), V'(\phi_0), \dots$ as:

Planck (2013)+WMAP-9+high L:

$$V(\phi_0) \leq \mathcal{O}(3.79 - 3.94) \times 10^{-9} M_p^4, \quad (5.26)$$

$$V'(\phi_0) \leq \mathcal{O}(4.66 - 4.88) \times 10^{-10} M_p^3, \quad (5.27)$$

$$V''(\phi_0) \leq \mathcal{O}((-1.07) - 1.29) \times 10^{-11} M_p^2, \quad (5.28)$$

$$V'''(\phi_0) \leq \mathcal{O}(8.13 - (-1.25)) \times 10^{-10} M_p, \quad (5.29)$$

$$V''''(\phi_0) \leq \mathcal{O}(0.39 - 4.76) \times 10^{-9}, \quad (5.30)$$

Planck (2014)+WMAP-9+high L+BICEP2 (dust):

$$5.26 \times 10^{-9} M_p^4 \leq V(\phi_0) \leq 9.50 \times 10^{-9} M_p^4, \quad (5.31)$$

$$2.44 \times 10^{-10} M_p^3 \leq V'(\phi_0) \leq 1.74 \times 10^{-9} M_p^3, \quad (5.32)$$

$$2.10 \times 10^{-11} M_p^2 \leq V''(\phi_0) \leq 3.22 \times 10^{-10} M_p^2, \quad (5.33)$$

$$6.29 \times 10^{-10} M_p \leq V'''(\phi_0) \leq 7.08 \times 10^{-10} M_p, \quad (5.34)$$

$$5.56 \times 10^{-10} \leq V''''(\phi_0) \leq 4.82 \times 10^{-9}, \quad (5.35)$$

Planck (2015)+WMAP-9+high L(TT):

$$V(\phi_0) \leq \mathcal{O}(3.41 - 3.67) \times 10^{-9} M_p^4, \quad (5.36)$$

$$V'(\phi_0) \leq \mathcal{O}(4.06 - 4.31) \times 10^{-10} M_p^3, \quad (5.37)$$

$$V''(\phi_0) \leq \mathcal{O}(0.31 - 7.84) \times 10^{-11} M_p^2, \quad (5.38)$$

$$V'''(\phi_0) \leq \mathcal{O}((-6.00) - (-9.64)) \times 10^{-10} M_p, \quad (5.39)$$

$$V''''(\phi_0) \leq \mathcal{O}(5.52 - 5.76) \times 10^{-9}, \quad (5.40)$$

Planck (2015)+BICEP2/Keck Array:

$$V(\phi_0) \leq \mathcal{O}(3.75 - 3.95) \times 10^{-9} M_p^4, \quad (5.41)$$

$$V'(\phi_0) \leq \mathcal{O}(4.70 - 5.03) \times 10^{-10} M_p^3, \quad (5.42)$$

$$V''(\phi_0) \leq \mathcal{O}((-8.74) - 30.30) \times 10^{-11} M_p^2, \quad (5.43)$$

$$V'''(\phi_0) \leq \mathcal{O}(8.13 - 30.34) \times 10^{-10} M_p, \quad (5.44)$$

$$V''''(\phi_0) \leq \mathcal{O}(0.39 - 4.76) \times 10^{-9}, \quad (5.45)$$

Consequently, the slow-roll parameters $(\epsilon_V, \eta_V, \xi_V^2, \sigma_V^3)$ are constrained by:

Planck (2013)+WMAP-9+high L:

$$\epsilon_V \lesssim \mathcal{O}(7.66 - 7.72) \times 10^{-3}, \quad (5.46)$$

$$|\eta_V| \lesssim \mathcal{O}(6.14 \times 10^{-3} - 0.019), \quad (5.47)$$

$$|\xi_V^2| \lesssim \mathcal{O}(2.34 \times 10^{-6} - 0.027), \quad (5.48)$$

$$|\sigma_V^3| \lesssim \mathcal{O}(1.58 \times 10^{-3} - 0.019). \quad (5.49)$$

Planck (2014)+WMAP-9+high L+BICEP2 (dust):

$$\epsilon_V \sim \mathcal{O}(0.10 - 1.69) \times 10^{-2}, \quad (5.50)$$

$$|\eta_V| \sim \mathcal{O}(4.57 \times 10^{-3} - 0.030), \quad (5.51)$$

$$|\xi_V^2| \sim \mathcal{O}(5.60 \times 10^{-3} - 0.014), \quad (5.52)$$

$$|\sigma_V^3| \sim \mathcal{O}(2.28 \times 10^{-4} - 0.017). \quad (5.53)$$

Planck (2015)+WMAP-9+high L(TT):

$$\epsilon_V \lesssim \mathcal{O}(7.02 - 7.03) \times 10^{-3}, \quad (5.54)$$

$$|\eta_V| \lesssim \mathcal{O}(2.94 - 8.59) \times 10^{-3}, \quad (5.55)$$

$$|\xi_V^2| \lesssim \mathcal{O}(1.52 \times 10^{-3} - 0.012), \quad (5.56)$$

$$|\sigma_V^3| \lesssim \mathcal{O}(0.022 - 0.023). \quad (5.57)$$

Planck (2015)+BICEP2/Keck Array:

$$\epsilon_V \lesssim \mathcal{O}(7.70 - 9.67) \times 10^{-3}, \quad (5.58)$$

$$|\eta_V| \lesssim \mathcal{O}(5.20 \times 10^{-4} - 0.160), \quad (5.59)$$

$$|\xi_V^2| \lesssim \mathcal{O}(5.60 \times 10^{-3} - 0.123), \quad (5.60)$$

$$|\sigma_V^3| \lesssim \mathcal{O}(1.60 \times 10^{-3} - 0.023). \quad (5.61)$$

Further, by applying the joint constraints from Planck (2013)+WMAP-9+high L, **Planck (2014)+WMAP-9+high L+BICEP2 (dust)**, Planck (2015)+WMAP-9+high L(TT) and Planck (2015)+BICEP2/Keck Array I obtain the following model independent

bound on field excursion $|\Delta\phi|/M_p$ by using Eq (3.16) or Eq (3.31):

Planck (2013)+WMAP-9+high L:

$$\frac{|\Delta\phi|}{M_p} \leq \mathcal{O}(0.239 - 0.241) \quad \text{for} \quad r_\star \leq 0.12. \quad (5.62)$$

Planck (2014)+WMAP-9+high L+BICEP2 (dust):

$$0.242 \leq \frac{|\Delta\phi|}{M_p} \leq 0.354 \quad \text{for} \quad 0.15 \leq r_\star \leq 0.27. \quad (5.63)$$

Planck (2015)+WMAP-9+high L(TT):

$$\frac{|\Delta\phi|}{M_p} \leq \mathcal{O}(0.230 - 0.231) \quad \text{for} \quad r_\star \leq 0.11. \quad (5.64)$$

Planck (2015)+BICEP2/Keck Array:

$$\frac{|\Delta\phi|}{M_p} \leq \mathcal{O}(0.223 - 0.242) \quad \text{for} \quad r_\star \leq 0.12. \quad (5.65)$$

Finally following the present analysis I get the following constraints on the tensor spectral tilt, n_T , running of the tensor spectral tilt, α_T , the running of the tensor-to-scalar ratio n_r and running of the running of tensor spectral tilt κ_T and tensor-to-scalar ratio κ_r as:

Planck (2013)+WMAP-9+high L:

$$n_T < \mathcal{O}((-0.0151) - (-0.0154)), \quad (5.66)$$

$$\alpha_T < \mathcal{O}((-2.69) - (-4.815)) \times 10^{-4}, \quad (5.67)$$

$$|n_r| < \mathcal{O}(3.00 - 3.23) \times 10^{-4}, \quad (5.68)$$

$$\kappa_T < \mathcal{O}((-5.92) - (-32.20)) \times 10^{-5}, \quad (5.69)$$

$$\kappa_r < \mathcal{O}((-6.86) - 14.53) \times 10^{-4}, \quad (5.70)$$

Planck (2014)+WMAP-9+high L+BICEP2 (dust):

$$-0.019 < n_T < -0.033, \quad (5.71)$$

$$-2.97 \times 10^{-4} < \alpha_T < 2.86 \times 10^{-5}, \quad (5.72)$$

$$2.28 \times 10^{-4} < |n_r| < 0.010, \quad (5.73)$$

$$-0.11 \times 10^{-4} < \kappa_T < -3.58 \times 10^{-4}, \quad (5.74)$$

$$-5.25 \times 10^{-3} < \kappa_r < -6.27 \times 10^{-3}, \quad (5.75)$$

Planck (2015)+WMAP-9+high L(TT):

$$n_T < \mathcal{O}((-0.0140) - (-0.0142)), \quad (5.76)$$

$$\alpha_T < \mathcal{O}((-2.98) - (-5.09)) \times 10^{-4}, \quad (5.77)$$

$$|n_r| < \mathcal{O}(2.47 \times 10^{-3}), \quad (5.78)$$

$$\kappa_T < \mathcal{O}((-0.07) - 3.46) \times 10^{-4}, \quad (5.79)$$

$$\kappa_r < \mathcal{O}((-0.14) - 2.89) \times 10^{-3}, \quad (5.80)$$

Planck (2015)+BICEP2/Keck Array:

$$n_T < \mathcal{O}((-0.0153) - (-0.0154)), \quad (5.81)$$

$$\alpha_T < \mathcal{O}((-2.69) - (-4.82)) \times 10^{-4}, \quad (5.82)$$

$$|n_r| < \mathcal{O}(2.11 - 3.75) \times 10^{-3}, \quad (5.83)$$

$$\kappa_T < \mathcal{O}((-1.79) - (-4.72)) \times 10^{-4}, \quad (5.84)$$

$$\kappa_r < \mathcal{O}((-0.20) - (-4.49)) \times 10^{-3}, \quad (5.85)$$

Further, if I had set ϑ to a slightly larger value, $\vartheta \sim \mathcal{O}(10^{-1} M_p)$ as $\Delta\phi \sim \mathcal{O}(10^{-1} M_p)$, then the order of magnitude of the numerics would not change, but the numerical pre-factors would slightly change.

6 Higher order consistency relationships in effective theory

Let us now provide the new set of consistency relationships *between slow roll parameters* for sub-Planckian models of inflation:

$$n_T = -\frac{r}{8} \left(2 - \frac{r}{8} - n_S \right) + \dots, \quad (6.1)$$

$$\alpha_T = \frac{dn_T}{d \ln k} = \frac{r}{8} \left(\frac{r}{8} + n_S - 1 \right) + \dots, \quad (6.2)$$

$$n_r = \frac{dr}{d \ln k} = \frac{16}{9} \left(n_S - 1 + \frac{3r}{4} \right) \left(2n_S - 2 + \frac{3r}{8} \right) + \dots, \quad (6.3)$$

$$\kappa_T = \frac{d^2 n_T}{d \ln k^2} = \frac{2}{9} \left(n_S - 1 + \frac{3r}{4} \right) \left(2n_S - 2 + \frac{3r}{8} \right) \left(\frac{r}{8} + n_S - 1 \right) \quad (6.4)$$

$$+ \frac{r}{8} \left[\alpha_S + \frac{2}{9} \left(n_S - 1 + \frac{3r}{4} \right) \left(2n_S - 2 + \frac{3r}{8} \right) \right] + \dots, \quad (6.5)$$

$$\begin{aligned} \kappa_r &= \frac{d^2 r}{d \ln k^2} \\ &= \frac{16}{9} \left(2n_S - 2 + \frac{3r}{8} \right) \left\{ \alpha_S + \frac{4}{3} \left(n_S - 1 + \frac{3r}{4} \right) \left(2n_S - 2 + \frac{3r}{8} \right) \right\} \\ &\quad + \frac{16}{9} \left(n_S - 1 + \frac{3r}{4} \right) \left\{ 2\alpha_S + \frac{2}{3} \left(n_S - 1 + \frac{3r}{4} \right) \left(2n_S - 2 + \frac{3r}{8} \right) \right\} + \dots \end{aligned} \quad (6.6)$$

One can compare these relationships with respect to super-Planckian models of inflation where the slow roll parameters vary monotonically, see Re. [39]. Observationally, now one can differentiate sub versus super Planckian excursion models of inflation with the help of the above consistency relationships. In particular, the slope of the tensor modes, see Eq. (6.1), will play a crucial role in deciding the fate of the sub-primordial inflation in the early universe.

In Fig. (1) and Fig. (2), I have shown the evolution of ϵ_V , $|\eta_V|$, $|\xi_V^2|$, $|\sigma_V^3|$ (see Eqs. (10.3)) with respect to $|\phi - \phi_0|$ and number of e-foldings N respectively, where the upper and lower bounds are given by Eqs. (5.26-5.45). In particular, note that the evolution of ϵ_V is non-monotonic for sub-Planckian inflation, which is in stark contrast with the Lyth-bound for the super-Planckian models of inflation, where ϵ_V can evolve monotonically for polynomial potentials [39]. In future the data would be sufficiently good to compare the running of the gravitational tensor perturbations, n_T , for sub-vs-super-Planckian excursions of the inflaton.

In Fig. (3), Fig. (4(a)-7(c)) and Fig. (8(a)-11(d)), I have shown the variation of $\ln N(k)$, $P_S(k)$, $n_S(k)$, $\alpha_S(k)$, $P_T(k)$ and $r(k)$ (applying all the previously mentioned joint constraints), at any arbitrary momentum scale k . Here the **black** dotted line corresponds to

$$k_{max} = 0.3 \text{ Mpc}^{-1} \quad \text{for} \quad l_{max} = 2500, \quad (6.7)$$

the **blue** dotted line corresponds to

$$k_{min} = 4.488 \times 10^{-5} \text{ Mpc}^{-1} \quad \text{for} \quad l_{min} = 2, \quad (6.8)$$

and in all the plots **violet** dashed dotted line represents the pivot scale of momentum at

$$k_\star = 0.002 \text{ Mpc}^{-1} \quad \text{for} \quad l_\star \sim 80 \quad (6.9)$$

at which

$$P_S(k_\star) = 2.2 \times 10^{-9}, \quad (6.10)$$

$$n_S = 0.96, \quad (6.11)$$

$$\alpha_S = -0.02, \quad (6.12)$$

$$N(k_\star) = 63.26. \quad (6.13)$$

Within $2 < l < 2500$ the value of the required momentum scale is determined by the relation [31],

$$k_{reqd} \sim \frac{l_{reqd}}{\eta_0 \pi}, \quad (6.14)$$

where the conformal time at the present epoch is given by:

$$\eta_0 \sim 14000 \text{ Mpc}. \quad (6.15)$$

In Fig. (12(a)) and Fig. (12(b)), I have shown the total number of e-foldings N , with respect to the field $(\phi - \phi_0)$ and the field evolution $\Delta\phi$ with respect to ΔN respectively. In Fig. (12(a)) the allowed 2σ region is shown as obtained from Planck (2013)+WMAP-9+high L, Planck+WMAP-9+high L+BICEP2 (dust), Planck (2015)+WMAP-9+high L(TT) and Planck (2015) +BICEP2/Keck Array joint constraints. This also shows that the observational scanning region, $\Delta N \sim 17$ is consistent with the bound on the sub-Planckian value of the field excursion as obtained in earlier section of the paper. Fig. (12(b)) depicts that at $\Delta N \sim 8$ and $\Delta N \sim 17$ the numerical value of the field evolution turn out to be $\Delta\phi \sim 0.14 M_p$ and $\Delta\phi \sim 0.34 M_p$ respectively.

In Fig. (13(a)) and Fig. (13(b)), I have shown the variation of P_S , n_S and $r_{0.002}$, at the pivot scale $k_* = 0.002 Mpc^{-1}$. The overlapping *red* patch shows the allowed region by Planck (2013)+WMAP-9+high L, Planck+WMAP-9+high L+BICEP2 (dust), Planck (2015)+WMAP-9+high L(TT) and Planck (2015)+BICEP2/Keck Array joint constraints. The upper *green* and lower *yellow* bounds are set by Eqs. (5.26-5.45).

In Fig (14), I have shown r vs n_S at the pivot scale: $k_* \sim 0.002 Mpc^{-1}$. The allowed region is shown by the shaded violet colour, for $0.15 < r_* < 0.27$ and $0.952 < n_S < 0.967$. The green and yellow lines are drawn for lower and upper bound of the constraints derived in Eq (5.46-5.61). We have used the relation between n_S and r_* as mentioned in Eq (10.6, 10.8) in the appendix.

In Fig. (15(a)-15(c)), I have depicted running of the tensor-to-scalar ratio: $n_r = dr/d\ln k$, running of the running of the tensor-to-scalar ratio: $\kappa_r = d^2r/d\ln k$, running of the tensor spectral tilt: $\alpha_T = dn_T/d\ln k$, running of the running of tensor spectral tilt: $\kappa_T = d^2n_T/d\ln k$ vs scalar spectral tilt n_S . Shaded violet colour region is the allowed overlapping region for Planck (2013)+WMAP-9+high L, Planck+WMAP-9+high L+BICEP2 (dust), Planck (2015)+WMAP-9+high L(TT) and Planck (2015) +BICEP2/Keck Array joint constraints which further constrain n_r , κ_r , α_T and κ_T within the specified range mentioned in Eq (5.67) and Eq (5.70). The green and yellow lines are drawn for lower and upper bound on the constraints derived in Eq (5.46-5.51), We have used the relation between α_T , κ_T and n_S as mentioned in Eq (6.2) and Eq (6.4).

7 Example of Inflection point inflation within effective theory

Now I impose,

$$V''(\phi_0) = 0, \tag{7.1}$$

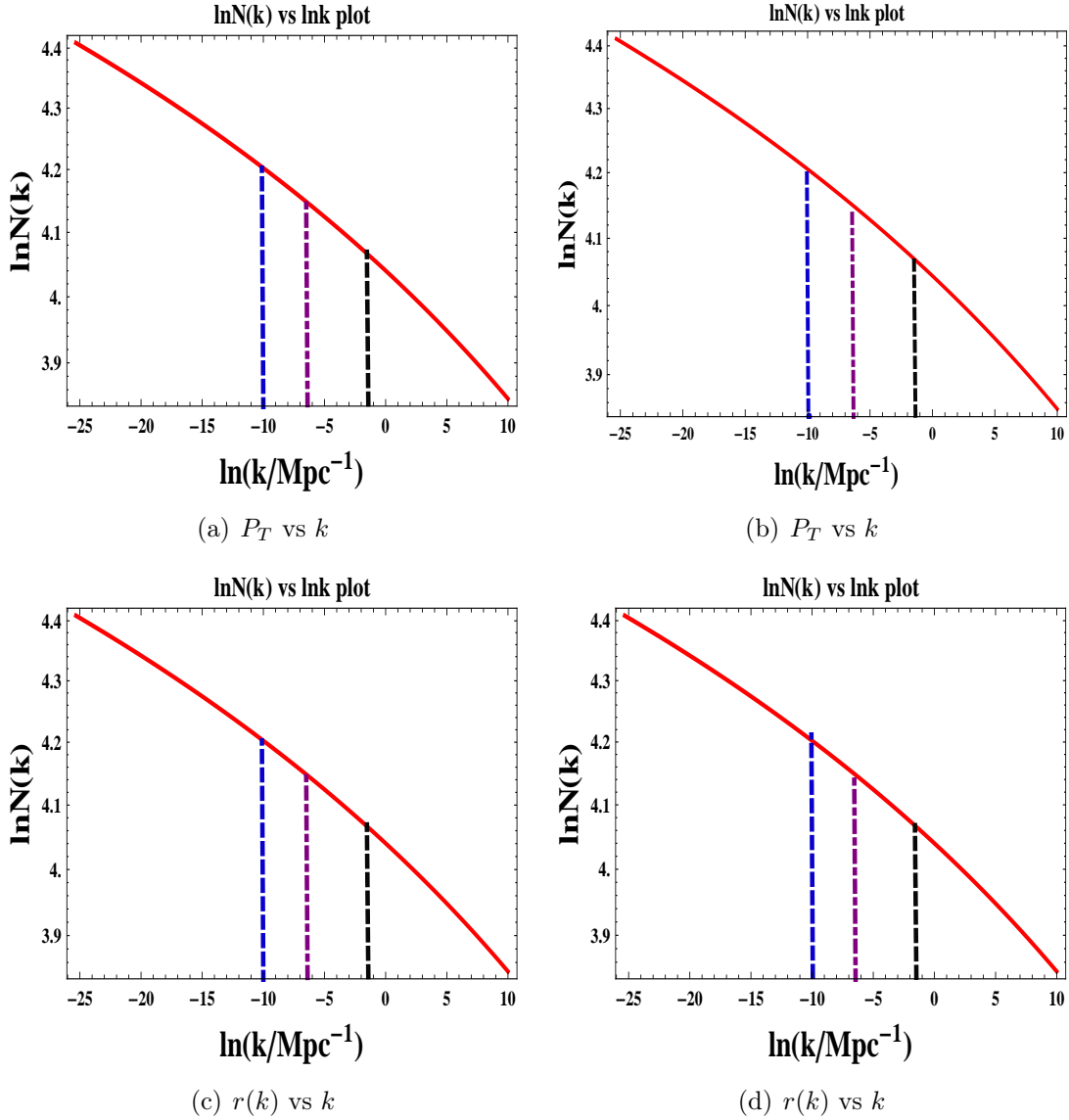


Figure 3. Here I show the variation of the total number of e-foldings $N(k)$, with respect to the momentum scale k . The **black** dotted line corresponds to $k_{max} = 0.3 \text{ Mpc}^{-1}$ for $l_{max} = 2500$, the **blue** dotted line corresponds to $k_{min} = 4.488 \times 10^{-5} \text{ Mpc}^{-1}$ for $l_{min} = 2$, and in all the plots **violet** dashed dotted line represents the pivot scale of momentum at $k_{\star} = 0.002 \text{ Mpc}^{-1}$ for $l_{\star} \sim 80$, at which for **3(a)** $P_S(k_{\star}) = 2.2 \times 10^{-9}$, $n_S = 0.9600$, $\alpha_S = -0.013$ and $N(k_{\star}) = 63.26$ (Planck (2013)+WMAP-9+high-L), **3(b)** $P_S(k_{\star}) = 2.2 \times 10^{-9}$, $n_S = 0.9600$, $\alpha_S = -0.022$ and $N(k_{\star}) = 63.26$ (Planck (2014)+WMAP-9+high-L+BICEP2 (dust)), **3(c)** $P_S(k_{\star}) = 2.2 \times 10^{-9}$, $n_S = 0.9569$, $\alpha_S = 0.011$ and $N(k_{\star}) = 63.26$ (Planck (2015)+WMAP-9+high-L(TT)), **3(d)** $P_S(k_{\star}) = 2.2 \times 10^{-9}$, $n_S = 0.9600$, $\alpha_S = -0.022$ and $N(k_{\star}) = 63.26$ (Planck (2015)+BICEP2/Keck Array). Within $2 < l < 2500$ the value of the required momentum scale is determined by the relation, $k_{reqd} \sim \frac{l_{reqd}}{\eta_0 \pi}$ [31], where the conformal time at the present epoch is $\eta_0 \sim 14000 \text{ Mpc}$.

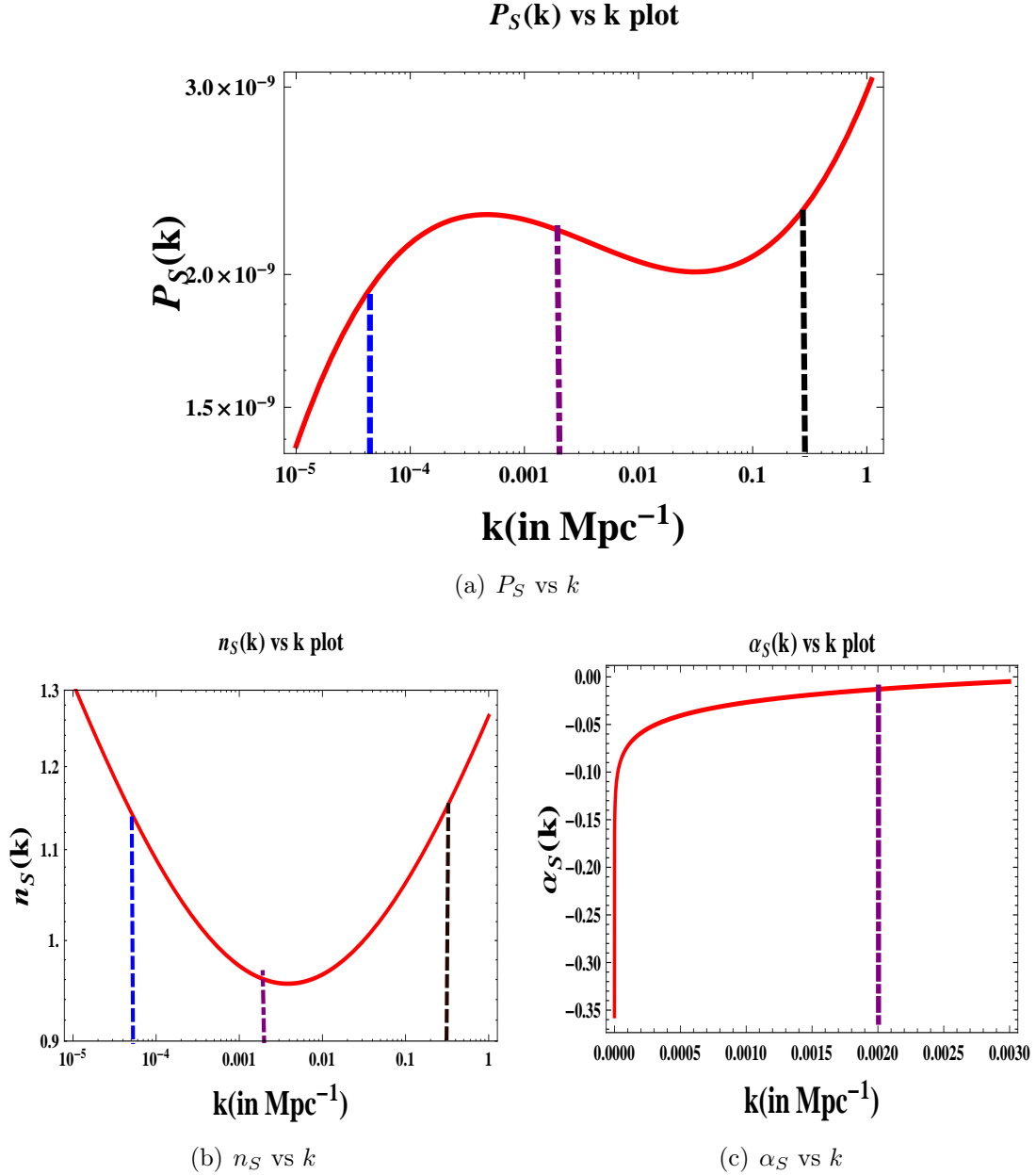


Figure 4. In 4(a), I show the scalar Power spectrum $P_s(k)$ 4(b), I show the scalar spectral index $n_s(k)$, and in 4(c), I show the running of the scalar spectral index $\alpha_s(k)$, with respect to the momentum scale k . The **black** dotted line corresponds to $k_{max} = 0.3 \text{ Mpc}^{-1}$ for $l_{max} = 2500$, the **blue** dotted line corresponds to $k_{min} = 4.488 \times 10^{-5} \text{ Mpc}^{-1}$ for $l_{min} = 2$, and in all the plots **violet** dashed dotted line represents the pivot scale of momentum at $k_* = 0.002 \text{ Mpc}^{-1}$ for $l_* \sim 80$ at which Planck (2013)+WMAP-9+high L constraints $P_S(k_*) = 2.2 \times 10^{-9}$, $n_S = 0.9600$, $\alpha_S = -0.02$ and $N(k_*) = 63.26$ are satisfied. Within $2 < l < 2500$ the value of the required momentum scale is determined by the relation, $k_{reqd} \sim \frac{l_{reqd}}{\eta_0 \pi}$ [31], where the conformal time at the present epoch is $\eta_0 \sim 14000 \text{ Mpc}$.

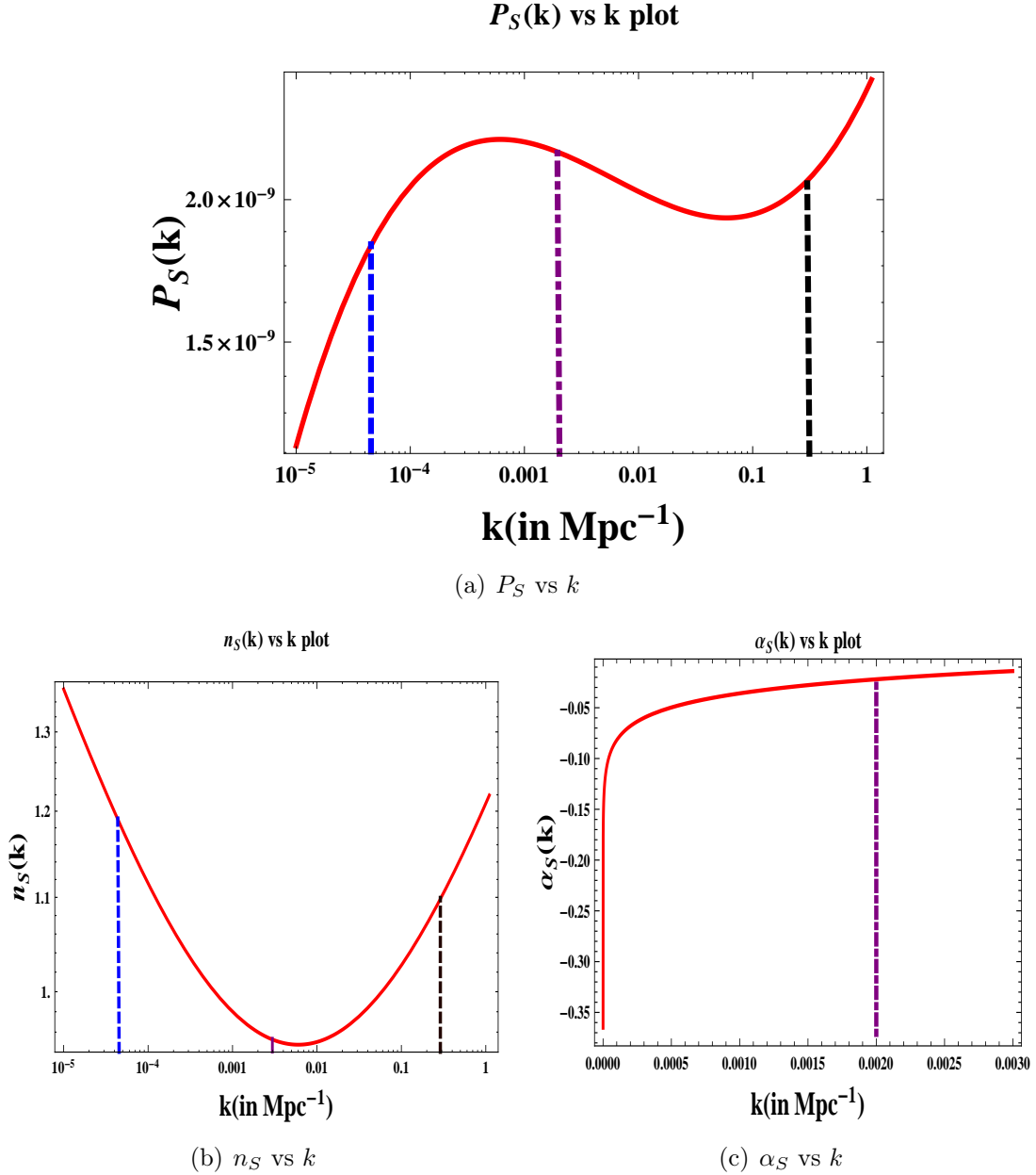
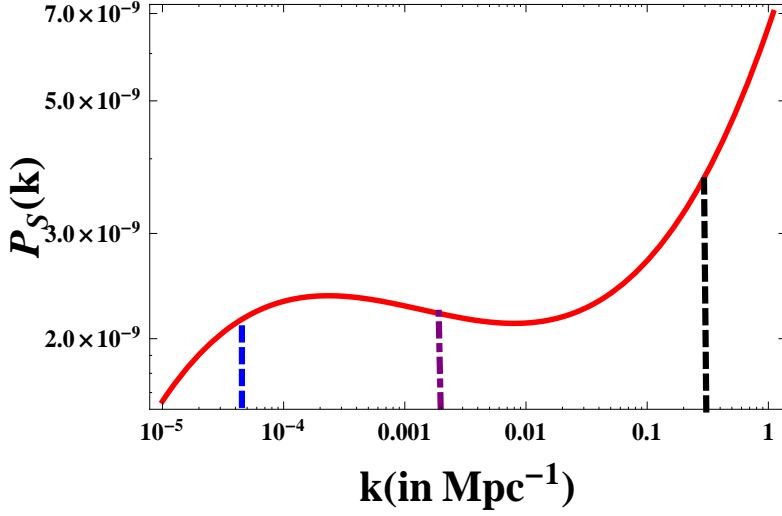


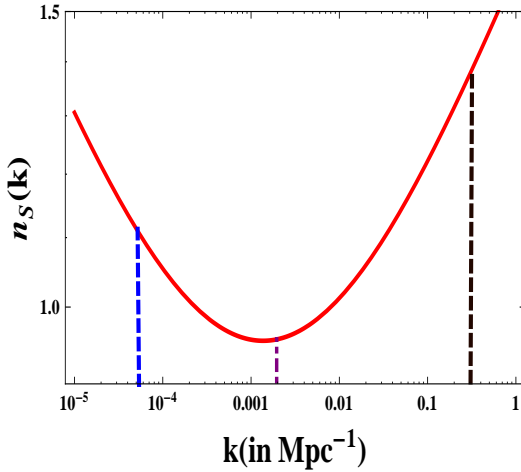
Figure 5. In 5(a), I show the scalar Power spectrum $P_s(k)$ 5(b), I show the scalar spectral index $n_s(k)$, and in 5(c), I show the running of the scalar spectral index $\alpha_s(k)$, with respect to the momentum scale k . The **black** dotted line corresponds to $k_{max} = 0.3 \text{ Mpc}^{-1}$ for $l_{max} = 2500$, the **blue** dotted line corresponds to $k_{min} = 4.488 \times 10^{-5} \text{ Mpc}^{-1}$ for $l_{min} = 2$, and in all the plots **violet** dashed dotted line represents the pivot scale of momentum at $k_* = 0.002 \text{ Mpc}^{-1}$ for $l_* \sim 80$ at which Planck (2014)+WMAP-9+high-L+BICEP2 (dust) $P_S(k_*) = 2.2 \times 10^{-9}$, $n_S = 0.9600$, $\alpha_S = -0.02$ and $N(k_*) = 63.26$ are satisfied. Within $2 < l < 2500$ the value of the required momentum scale is determined by the relation, $k_{reqd} \sim \frac{l_{reqd}}{\eta_0 \pi}$ [31], where the conformal time at the present epoch is $\eta_0 \sim 14000 \text{ Mpc}$.

$P_S(k)$ vs k plot



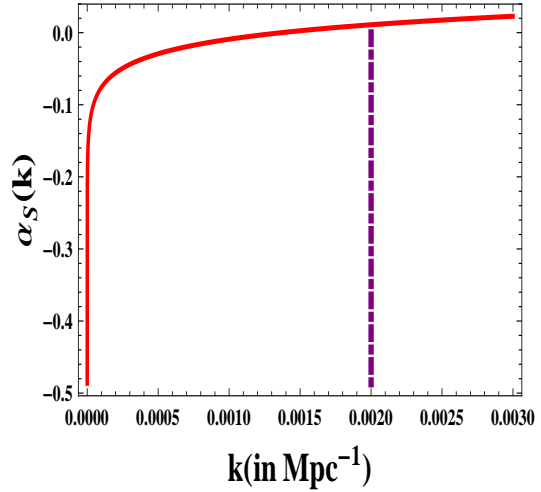
(a) P_S vs k

$n_S(k)$ vs k plot



(b) n_S vs k

$\alpha_S(k)$ vs k plot



(c) α_S vs k

Figure 6. In 6(a), I show the scalar Power spectrum $P_S(k)$ 6(b), I show the scalar spectral index $n_s(k)$, and in 6(c), I show the running of the scalar spectral index $\alpha_s(k)$, with respect to the momentum scale k . The **black** dotted line corresponds to $k_{max} = 0.3 \text{ Mpc}^{-1}$ for $l_{max} = 2500$, the **blue** dotted line corresponds to $k_{min} = 4.488 \times 10^{-5} \text{ Mpc}^{-1}$ for $l_{min} = 2$, and in all the plots **violet** dashed dotted line represents the pivot scale of momentum at $k_* = 0.002 \text{ Mpc}^{-1}$ for $l_* \sim 80$ at which Planck (2015)+WMAP-9+high-L(TT) constraints $P_S(k_*) = 2.2 \times 10^{-9}$, $n_S = 0.9569$, $\alpha_S = 0.011$ and $N(k_*) = 63.26$ are satisfied. Within $2 < l < 2500$ the value of the required momentum scale is determined by the relation, $k_{reqd} \sim \frac{l_{reqd}}{\eta_0 \pi}$ [31], where the conformal time at the present epoch is $\eta_0 \sim 14000 \text{ Mpc}$.

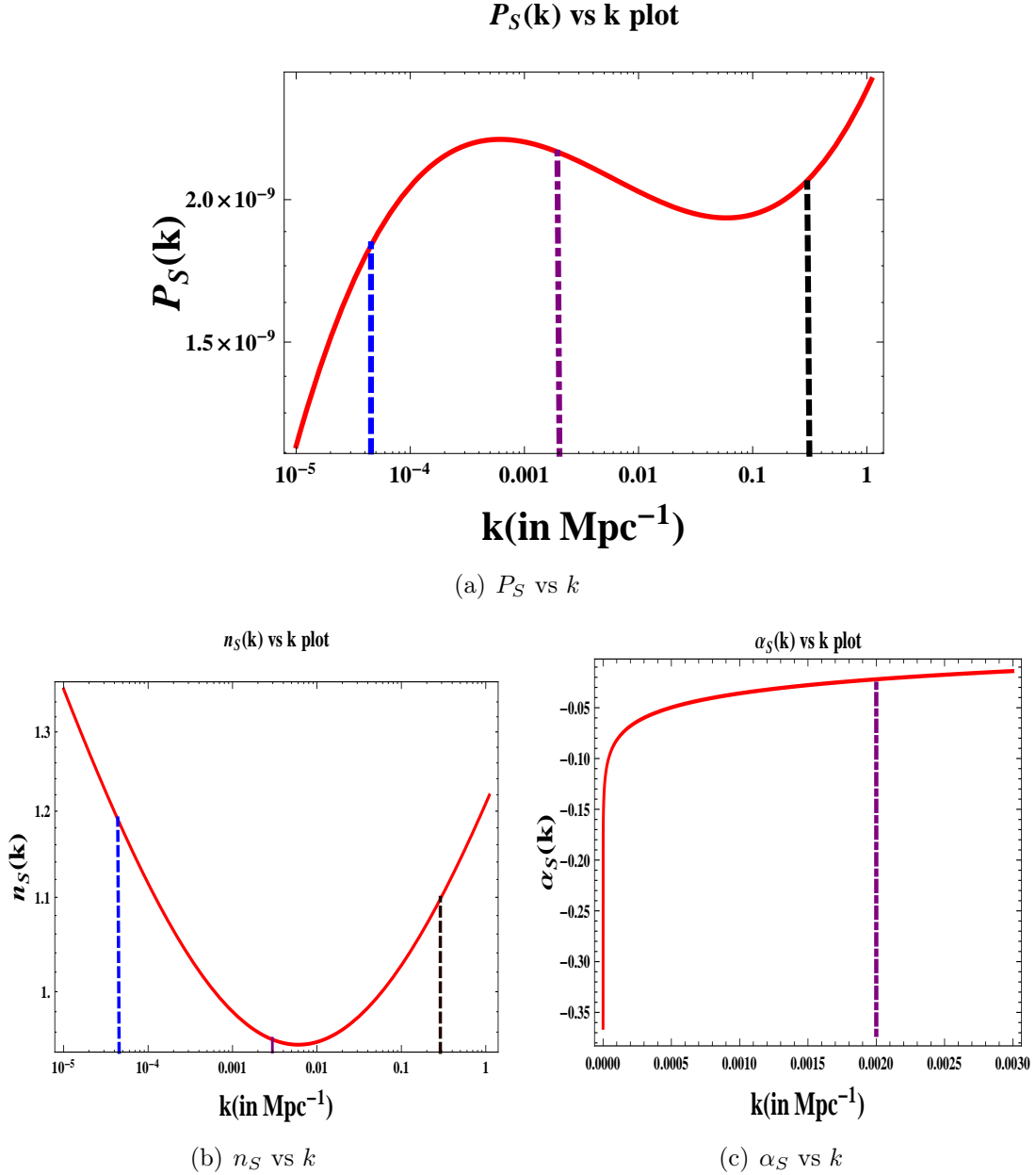


Figure 7. In 7(a), I show the scalar Power spectrum $P_S(k)$ 7(b), I show the scalar spectral index $n_s(k)$, and in 7(c), I show the running of the scalar spectral index $\alpha_s(k)$, with respect to the momentum scale k . The **black** dotted line corresponds to $k_{max} = 0.3 \text{ Mpc}^{-1}$ for $l_{max} = 2500$, the **blue** dotted line corresponds to $k_{min} = 4.488 \times 10^{-5} \text{ Mpc}^{-1}$ for $l_{min} = 2$, and in all the plots **violet** dashed dotted line represents the pivot scale of momentum at $k_* = 0.002 \text{ Mpc}^{-1}$ for $l_* \sim 80$ at which Planck (2015)+BICEP2/Keck Array joint constraint $P_S(k_*) = 2.2 \times 10^{-9}$, $n_S = 0.96$, $\alpha_S = -0.02$ and $N(k_*) = 63.26$ are satisfied. Within $2 < l < 2500$ the value of the required momentum scale is determined by the relation, $k_{reqd} \sim \frac{l_{reqd}}{\eta_0 \pi}$ [31], where the conformal time at the present epoch is $\eta_0 \sim 14000 \text{ Mpc}$.

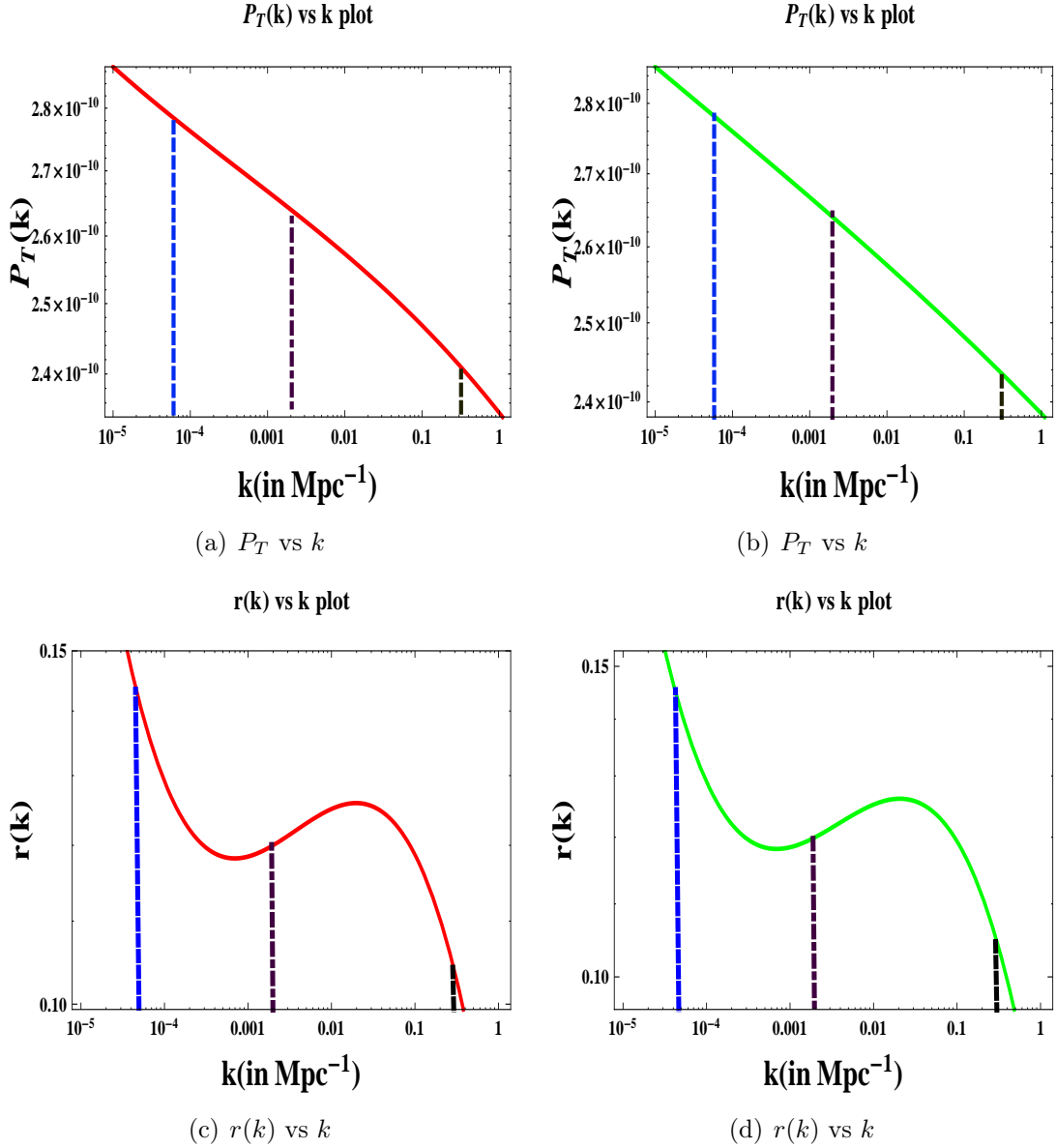


Figure 8. In 8(a), I show the Tensor spectrum $P_T(k)$ by assuming $r_{0.002} \sim 0.12$ 8(b), I show the Tensor spectrum $P_T(k)$ by assuming $r_{0.002} \sim 0.12$, 8(c), I show the scale dependence of tensor-to scalar ratio $r(k)$ with k by assuming $r_{0.002} \sim 0.12$, and in 8(d), I show the scale dependence of tensor-to scalar ratio $r(k)$ with k by assuming $r_{0.002} \sim 0.12$. The **black** dotted line corresponds to $k_{max} = 0.3 \text{ Mpc}^{-1}$ for $l_{max} = 2500$, the **blue** dotted line corresponds to $k_{min} = 4.488 \times 10^{-5} \text{ Mpc}^{-1}$ for $l_{min} = 2$, and in all the plots **violet** dashed dotted line represents the pivot scale of momentum at $k_* = 0.002 \text{ Mpc}^{-1}$ for $l_* \sim 80$ at which Planck (2013)+WMAP-9+high L constraints $P_S(k_*) = 2.2 \times 10^{-9}$, $n_S = 0.9600$, $\alpha_S = -0.013$ and $N(k_*) = 63.26$ are satisfied. Within $2 < l < 2500$ the value of the required momentum scale is determined by the relation, $k_{reqd} \sim \frac{l_{reqd}}{\eta_0 \pi}$ [31], where the conformal time at the present epoch is $\eta_0 \sim 14000 \text{ Mpc}$.

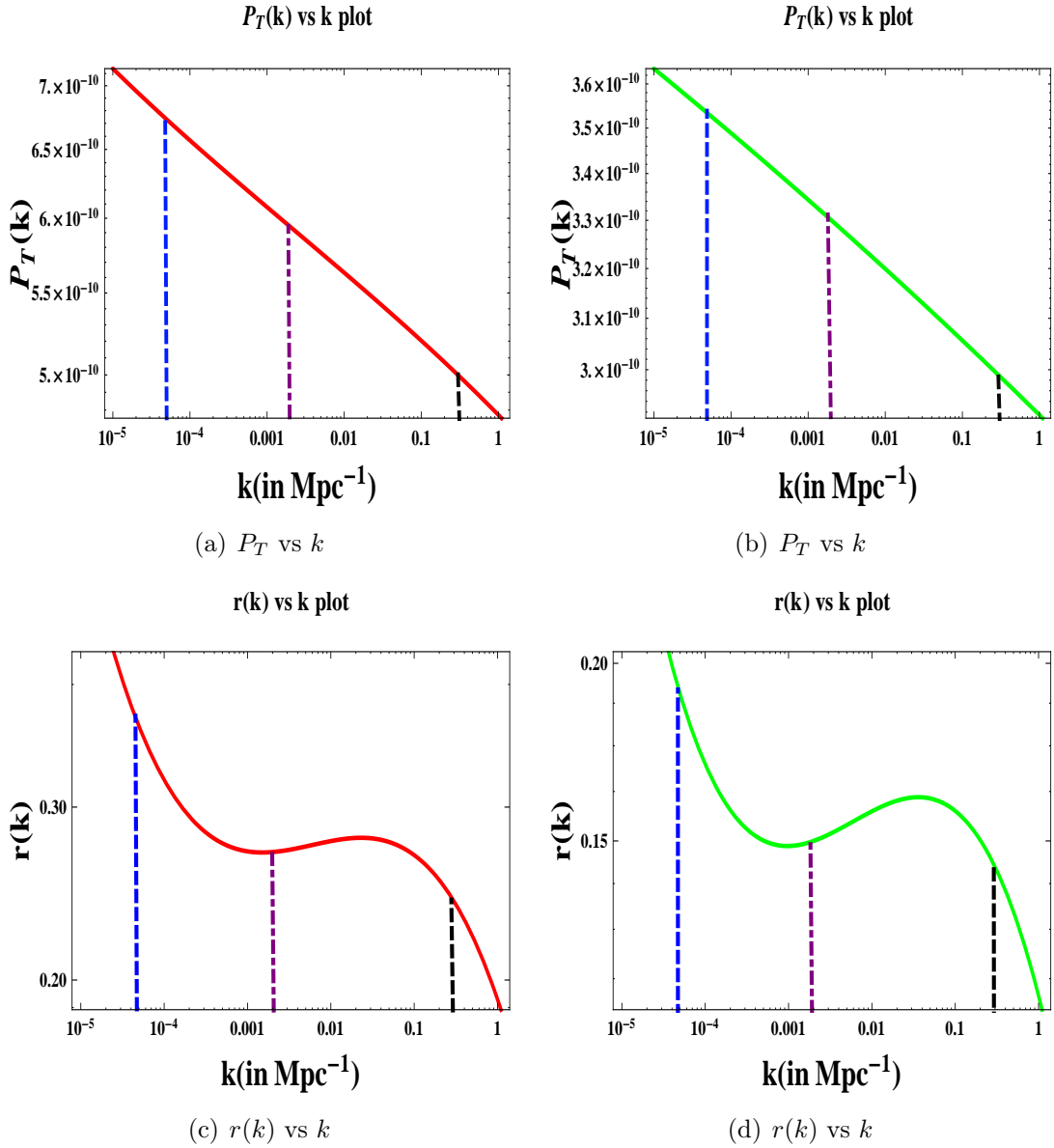


Figure 9. In 9(a), I show the Tensor spectrum $P_T(k)$ by assuming $r_{0.002} \sim 0.27$ 9(b), I show the Tensor spectrum $P_T(k)$ by assuming $r_{0.002} \sim 0.15$, 9(c), I show the scale dependence of tensor-to-scalar ratio $r(k)$ with k by assuming $r_{0.002} \sim 0.27$, and in 9(d), I show the scale dependence of tensor-to-scalar ratio $r(k)$ with k by assuming $r_{0.002} \sim 0.15$. The **black** dotted line corresponds to $k_{max} = 0.3 \text{ Mpc}^{-1}$ for $l_{max} = 2500$, the **blue** dotted line corresponds to $k_{min} = 4.488 \times 10^{-5} \text{ Mpc}^{-1}$ for $l_{min} = 2$, and in all the plots **violet** dashed dotted line represents the pivot scale of momentum at $k_* = 0.002 \text{ Mpc}^{-1}$ for $l_* \sim 80$ at which Planck (2014)+WMAP-9+high L+BICEP2 (dust) constraints $P_S(k_*) = 2.2 \times 10^{-9}$, $n_S = 0.96$, $\alpha_S = -0.022$ and $N(k_*) = 63.26$ are satisfied. Within $2 < l < 2500$ the value of the required momentum scale is determined by the relation, $k_{reqd} \sim \frac{l_{reqd}}{\eta_0 \pi}$ [31], where the conformal time at the present epoch is $\eta_0 \sim 14000 \text{ Mpc}$.

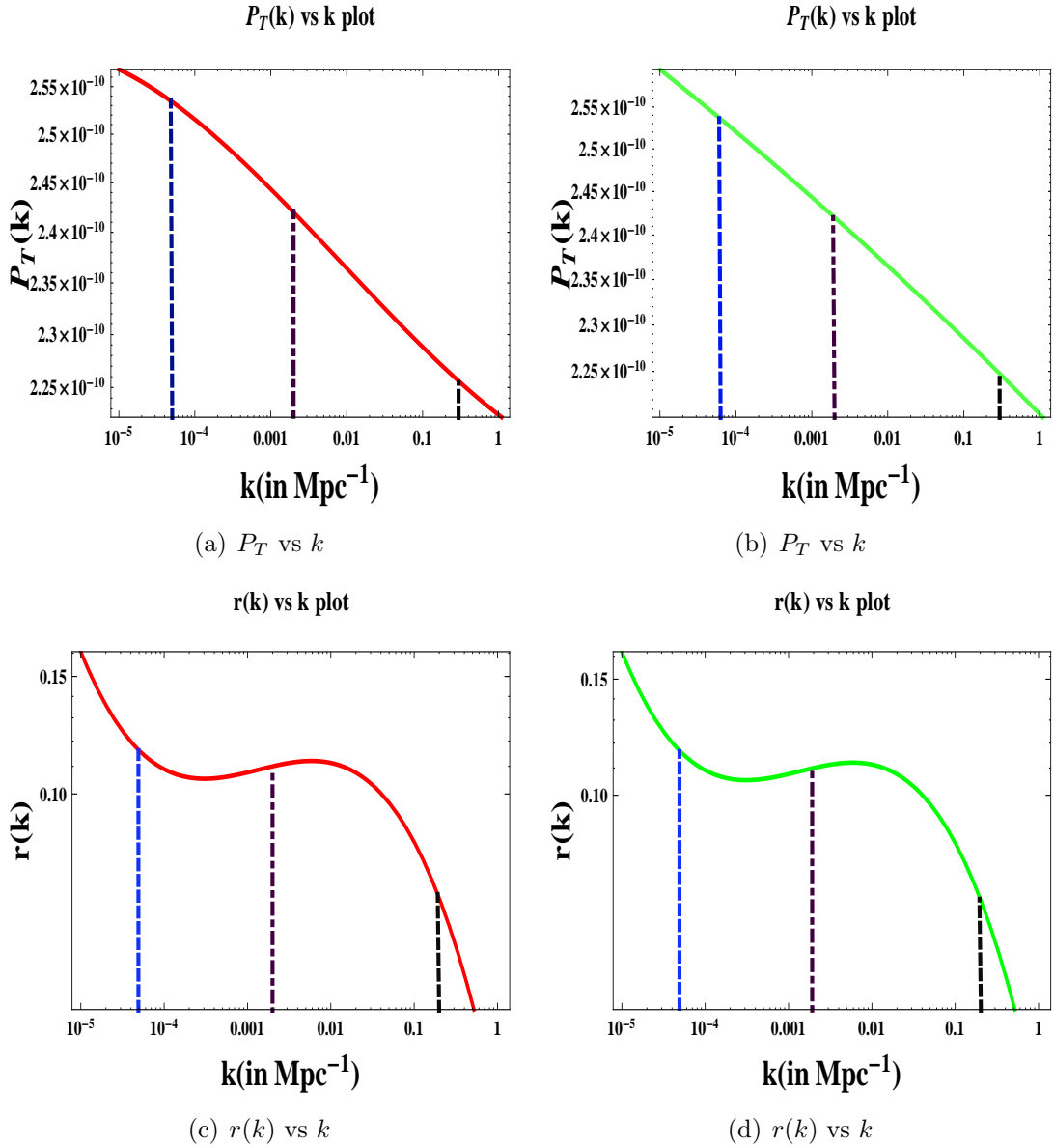
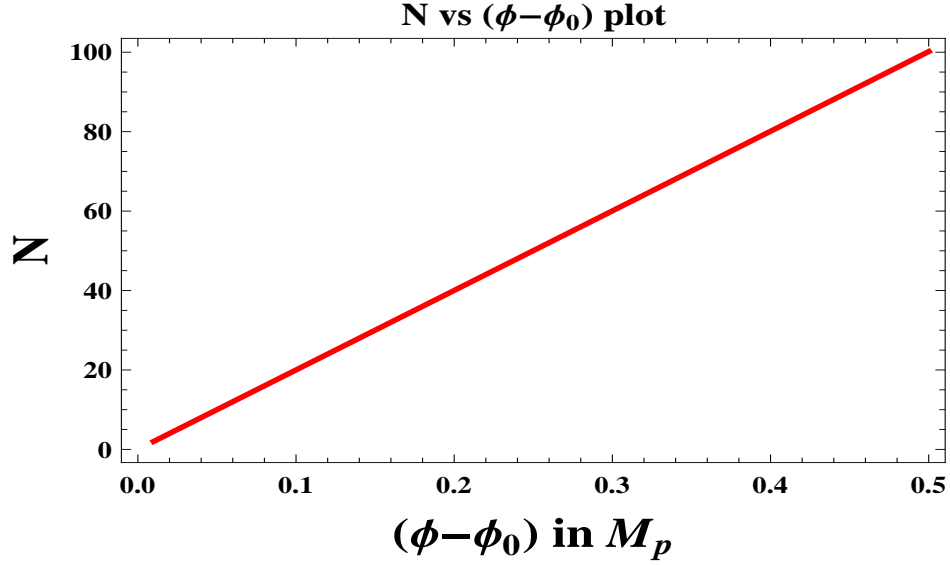
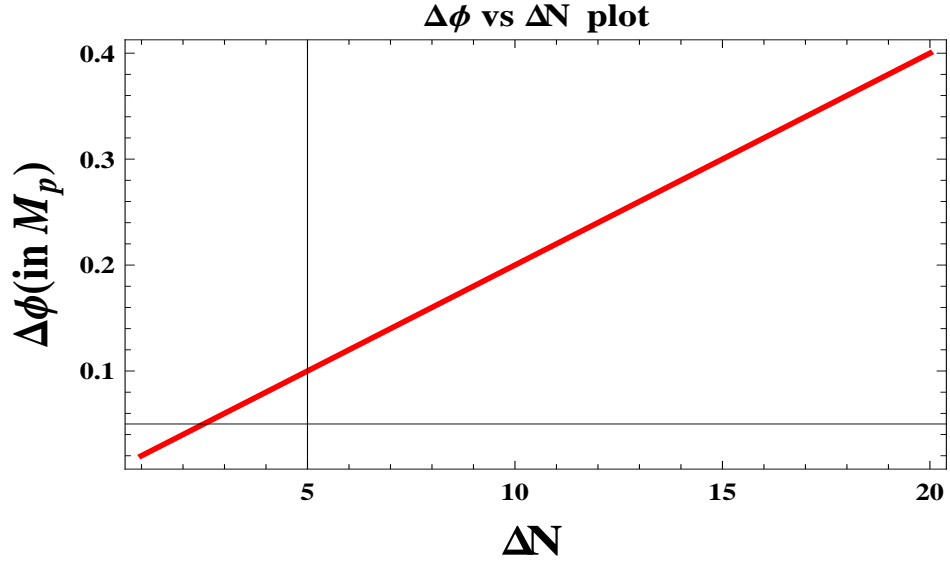


Figure 10. In 10(a), I show the Tensor spectrum $P_T(k)$ by assuming $r_{0.002} \sim 0.11$ 10(b), I show the Tensor spectrum $P_T(k)$ by assuming $r_{0.002} \sim 0.11$, 10(c), I show the scale dependence of tensor-to scalar ratio $r(k)$ with k by assuming $r_{0.002} \sim 0.11$, and in 10(d), I show the scale dependence of tensor-to scalar ratio $r(k)$ with k by assuming $r_{0.002} \sim 0.11$. The **black** dotted line corresponds to $k_{max} = 0.3 \text{ Mpc}^{-1}$ for $l_{max} = 2500$, the **blue** dotted line corresponds to $k_{min} = 4.488 \times 10^{-5} \text{ Mpc}^{-1}$ for $l_{min} = 2$, and in all the plots **violet** dashed dotted line represents the pivot scale of momentum at $k_* = 0.002 \text{ Mpc}^{-1}$ for $l_* \sim 80$ at which Planck (2015)+WMAP-9+high L constraints $P_S(k_*) = 2.2 \times 10^{-9}$, $n_S = 0.96$, $\alpha_S = 0.011$ and $N(k_*) = 63.26$ are satisfied. Within $2 < l < 2500$ the value of the required momentum scale is determined by the relation, $k_{reqd} \sim \frac{l_{reqd}}{\eta_0 \pi}$ [31], where the conformal time at the present epoch is $\eta_0 \sim 14000 \text{ Mpc}$.

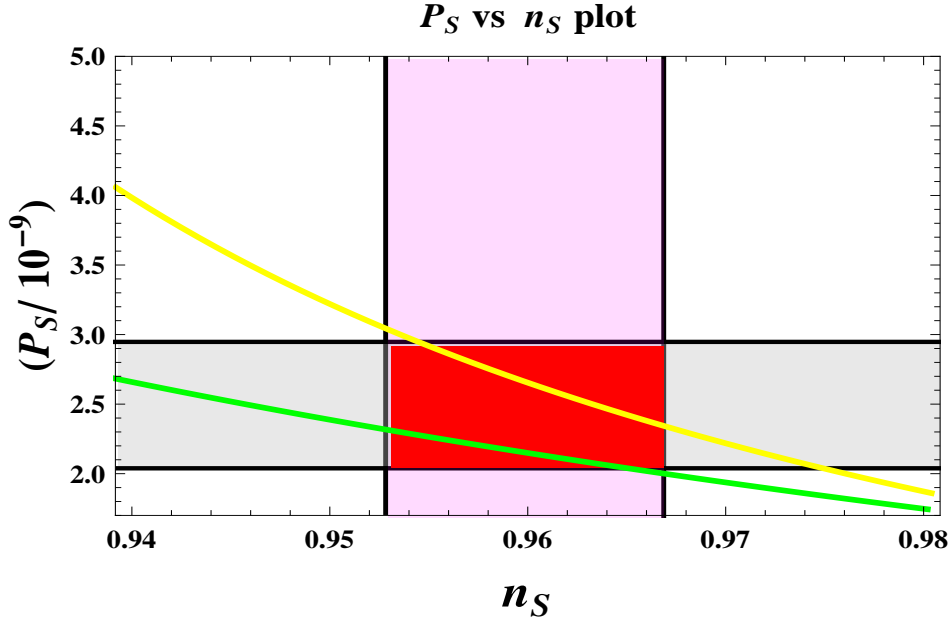


(a) N vs $(\phi - \phi_0)$

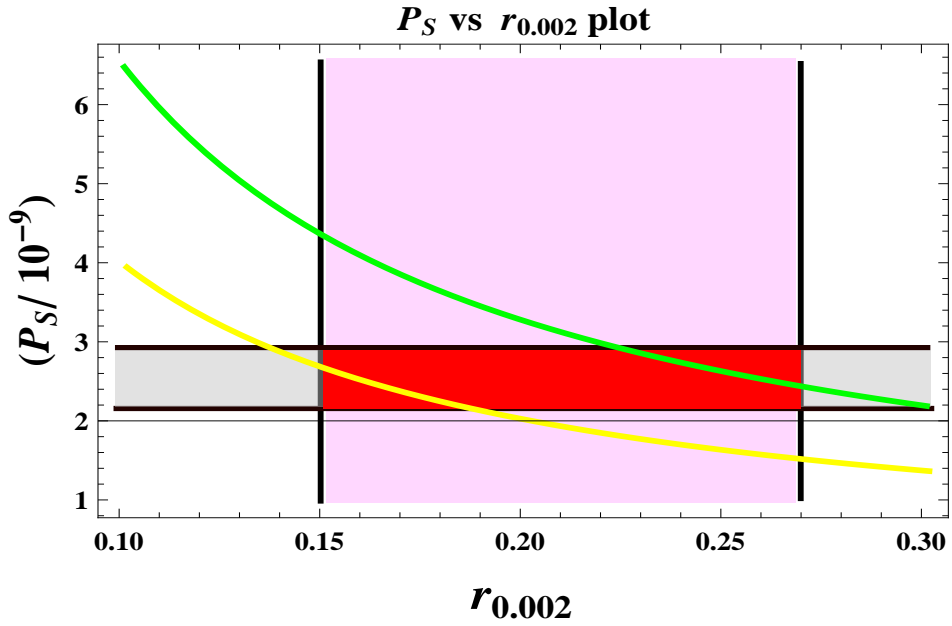


(b) $\Delta\phi$ vs ΔN

Figure 12. We show in 12(a) the total number of e-foldings N , with respect to the field $(\phi - \phi_0)$ and 12(b) the field evolution $\Delta\phi$, with respect to ΔN . Within the depicted parameter space 2σ constraints are allowed as obtained from Planck (2013)+WMAP-9+high-L, Planck (2014)+WMAP-9+high L+BICEP2 (dust), Planck (2015)+WMAP-9+high-L(TT) and Planck (2015)+BICEP2/Keck Array data. This also shows that the observational scanning region, $\Delta N \sim 17$ [23, 28, 29] obtained from CMB distortions is consistent with the sub-Planckian value of the field excursion. Here $|\Delta\phi| = |(\phi_{cmb} - \phi_0) - (\phi_e - \phi_0)| = |\phi_{cmb} - \phi_e| \approx |\phi_\star - \phi_e|$.



(a) P_S vs n_S



(b) P_S vs $r_{0.002}$

Figure 13. We have shown the variation of (a) P_S vs n_S , and (b) P_S vs $r_{0.002}$, for the pivot scale $k_* = 0.002 \text{ Mpc}^{-1}$. The overlapping *red* patch shows the 2σ allowed region by the joint constraints obtained from Planck (2013)+WMAP-9+high-L, Planck (2014)+WMAP-9+high L+BICEP2 (dust), Planck (2015)+WMAP-9+high-L(TT) and Planck (2015)+BICEP2/Keck Array data. The upper (*green*) and lower (*yellow*) bounds are set by Eqs. (5.26-5.45).

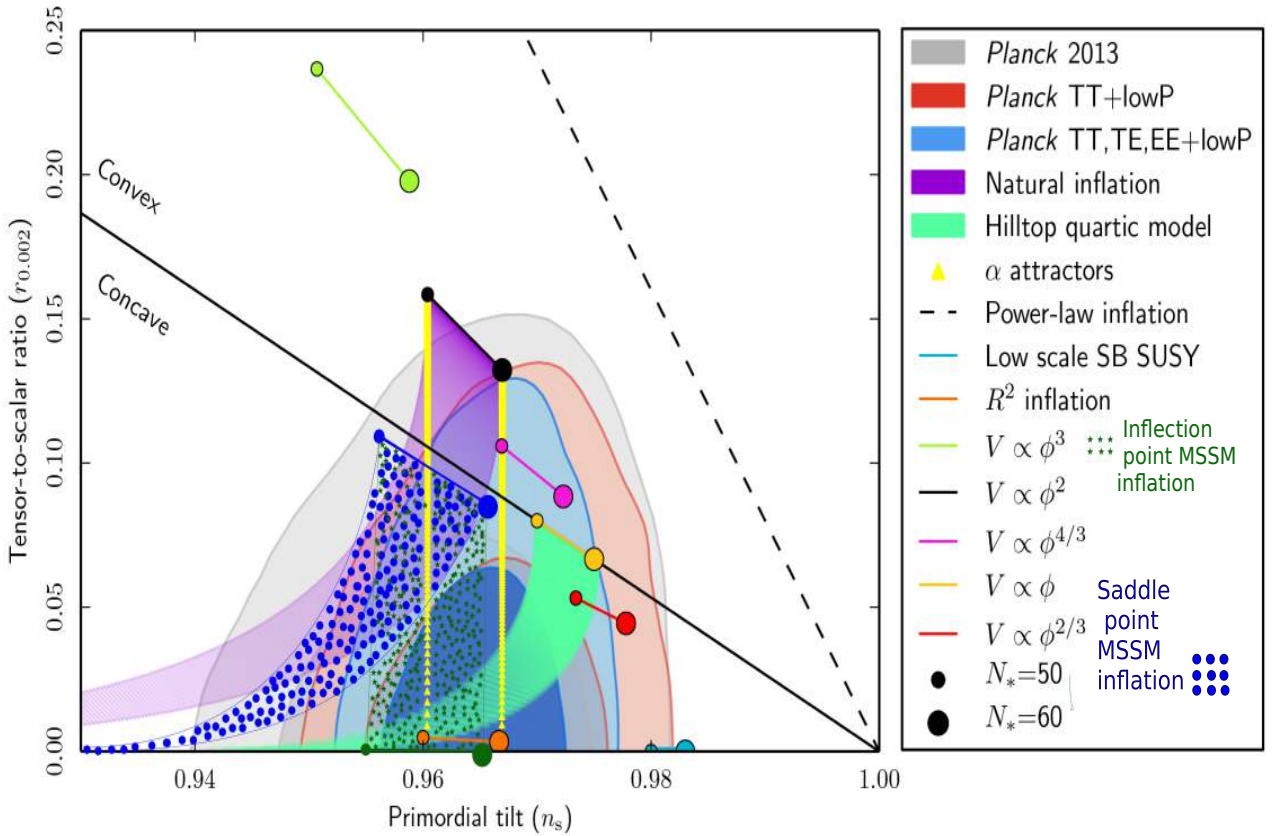


Figure 14. We show the joint 1σ and 2σ CL. contours using Planck 2013, Planck 2015 +TT+low P and Planck 2015 +TT+TE+EE+low P data for r vs n_S plot at the momentum pivot $k_\star \sim 0.002 \text{ Mpc}^{-1}$. The small circle on the left corresponds to $N = 50$, while the right big circle corresponds to $N = 60$. The allowed regions are shown by the shaded violet colour for $r_\star < 0.12$ and $0.952 < n_S < 0.967$. The blue and green bubbles and stars are drawn for saddle point MSSM inflation and inflection point MSSM inflation which are compatible with the constraints derived in Eq (5.46-5.49) and Eq (5.54-5.61). For Eq (5.50-5.54) the range of r_\star is outside the present upper bound from Planck 2015 and BICEP2/Keck Array joint data sets. The vertical black coloured lines are drawn to show the bounded regions of the sub-Planckian inflationary model, along which the number of e-foldings are fixed.

in order to study the *inflection point* scenario. The potential is given by ¹⁴:

$$V(\phi) = V(\phi_0) + V'(\phi_0)(\phi - \phi_0) + \frac{V'''(\phi_0)}{6}(\phi - \phi_0)^3 + \frac{V''''(\phi_0)}{24}(\phi - \phi_0)^4 + \dots, \quad (7.2)$$

¹⁴The inflection point inflation has been studied in Refs. [40], with a constant potential energy density $V(\phi_0)$.

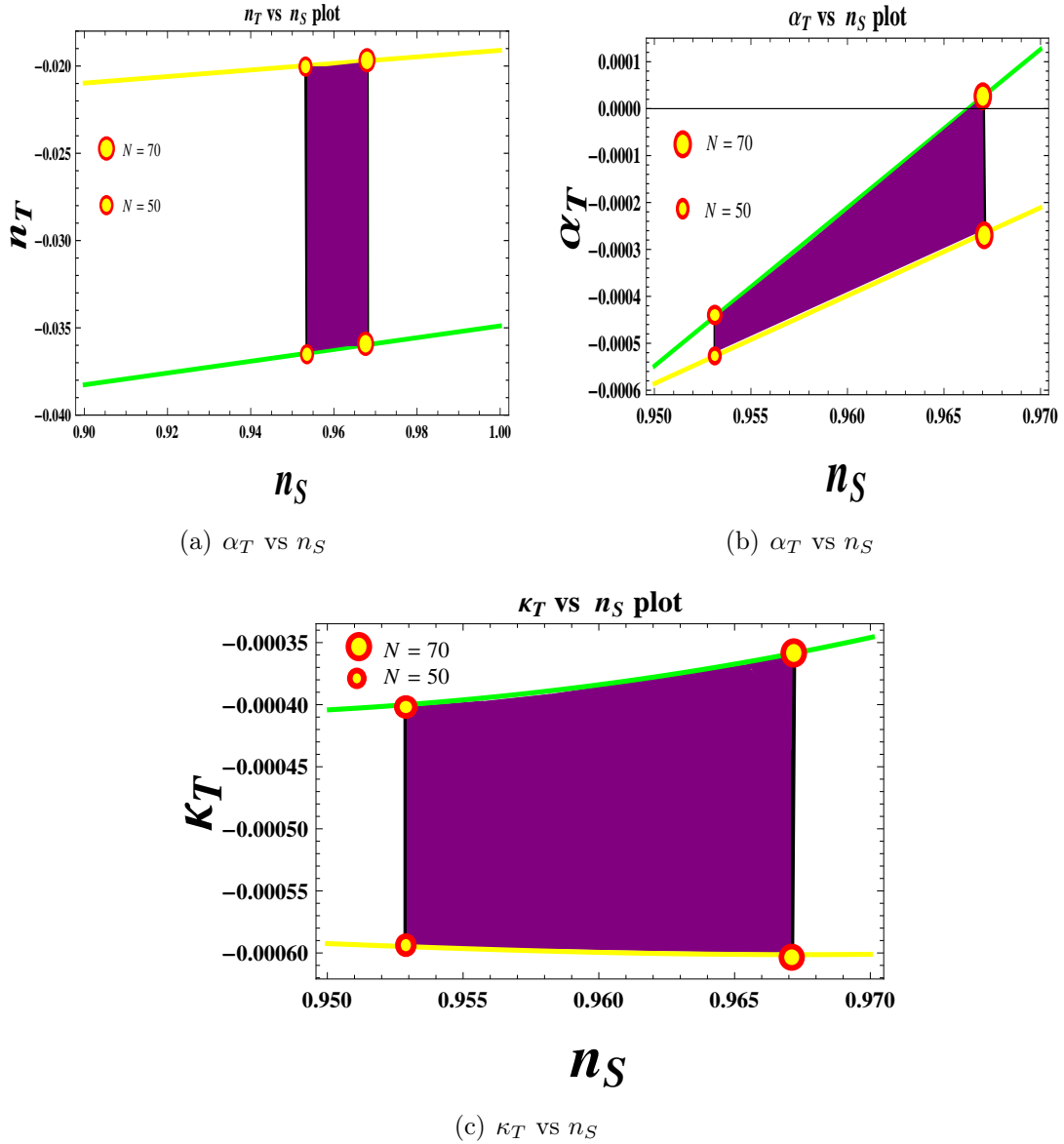


Figure 15. We show the (a) tensor spectral tilt n_T , (b) running of the tensor spectral tilt $\alpha_T = dn_T/d \ln k$, (c) running of the running of tensor spectral tilt $\kappa_T = d^2 n_T/d \ln k$ vs scalar spectral tilt n_S plot. The small circle on the left corresponds to $N = 50$, while the right big circle corresponds to $N = 70$. Shaded violet coloured regions are the allowed regions for Planck (2013)+WMAP-9+high L, Planck+WMAP-9+high L+BICEP2 (dust), Planck (2015)+WMAP-9+high L(TT) and Planck (2015) +BICEP2/Keck Array joint data sets which will further constrain α_T and κ_T within the specified ranges mentioned in Eq (5.67) and Eq (5.70). The green and yellow lines are drawn for lower and upper bounds on the constraints derived in Eq (5.46-5.61), The vertical black coloured lines are drawn to show the bounded regions of the sub-Planckian inflationary model, along which the number of e-foldings are fixed.

We can express $V(\phi_\star), V'(\phi_\star), \dots$ in terms of ϕ_0 for a sub-Planckian regime as:

$$\begin{aligned}
V(\phi_\star) &= V(\phi_0) + \vartheta_\star V'(\phi_0) + \frac{\vartheta_\star^3}{6} V'''(\phi_0) + \frac{\vartheta_\star^4}{24} V''''(\phi_0), \\
V'(\phi_\star) &= V'(\phi_0) + \frac{\vartheta_\star^2}{2} V'''(\phi_0) + \frac{\vartheta_\star^3}{6} V''''(\phi_0), \\
V''(\phi_\star) &= \vartheta_\star V'''(\phi_0) + \frac{\vartheta_\star^2}{2} V''''(\phi_0), \\
V'''(\phi_\star) &= V'''(\phi_0) + \vartheta_\star V''''(\phi_0), \\
V''''(\phi_\star) &= V''''(\phi_0).
\end{aligned} \tag{7.3}$$

Using Eq (7.3), I obtain a *particular* solution for the coefficients: $V(\phi_0), V'(\phi_0), \dots$, which can be written as ¹⁵:

$$\begin{aligned}
V(\phi_0) &= V(\phi_\star) - \vartheta_\star V'(\phi_\star) + \frac{\vartheta_\star^3}{3} V'''(\phi_\star) - \frac{5\vartheta_\star^4}{24} V''''(\phi_\star), \\
V'(\phi_0) &= V'(\phi_\star) - \frac{\vartheta_\star^2}{2} V'''(\phi_\star) + \frac{\vartheta_\star^3}{3} V''''(\phi_\star), \\
V'''(\phi_0) &= V'''(\phi_\star) - \vartheta_\star V''''(\phi_\star), \\
V''''(\phi_0) &= V''''(\phi_\star).
\end{aligned} \tag{7.4}$$

Now using the bound on $V(\phi_\star), V'(\phi_\star), \dots$ as mentioned in Eqs. (5.26-5.45), I can obtain the following constraints on the coefficients of $V(\phi_0), V'(\phi_0), \dots$:

Planck (2013)+WMAP-9+high L:

$$V(\phi_0) \leq \mathcal{O}(3.79 - 3.94) \times 10^{-9} M_p^4, \tag{7.5}$$

$$V'(\phi_0) \leq \mathcal{O}(4.66 - 4.88) \times 10^{-10} M_p^3, \tag{7.6}$$

$$V'''(\phi_0) \leq \mathcal{O}(8.13 - (-1.25)) \times 10^{-10} M_p, \tag{7.7}$$

$$V''''(\phi_0) \leq \mathcal{O}(0.39 - 4.76) \times 10^{-9}, \tag{7.8}$$

Planck (2014)+WMAP-9+high L+BICEP2 (dust):

$$5.26 \times 10^{-9} M_p^4 \leq V(\phi_0) \leq 9.50 \times 10^{-9} M_p^4, \tag{7.9}$$

$$2.44 \times 10^{-10} M_p^3 \leq V'(\phi_0) \leq 1.74 \times 10^{-9} M_p^3, \tag{7.10}$$

$$6.29 \times 10^{-10} M_p \leq V'''(\phi_0) \leq 7.08 \times 10^{-10} M_p, \tag{7.11}$$

$$5.56 \times 10^{-10} \leq V''''(\phi_0) \leq 4.82 \times 10^{-9}, \tag{7.12}$$

Planck (2015)+WMAP-9+high L(TT):

$$V(\phi_0) \leq \mathcal{O}(3.41 - 3.67) \times 10^{-9} M_p^4, \tag{7.13}$$

$$V'(\phi_0) \leq \mathcal{O}(4.06 - 4.31) \times 10^{-10} M_p^3, \tag{7.14}$$

$$V'''(\phi_0) \leq \mathcal{O}((-6.00) - (-9.64)) \times 10^{-10} M_p, \tag{7.15}$$

$$V''''(\phi_0) \leq \mathcal{O}(5.52 - 5.76) \times 10^{-9}, \tag{7.16}$$

¹⁵There will be in general 2 solutions around an inflection point, here I will provide one of the two solutions which is the most interesting one for the general case of study.

Planck (2015)+BICEP2/Keck Array:

$$V(\phi_0) \leq \mathcal{O}(3.75 - 3.95) \times 10^{-9} M_p^4, \quad (7.17)$$

$$V'(\phi_0) \leq \mathcal{O}(4.70 - 5.03) \times 10^{-10} M_p^3, \quad (7.18)$$

$$V'''(\phi_0) \leq \mathcal{O}(8.13 - 30.34) \times 10^{-10} M_p, \quad (7.19)$$

$$V''''(\phi_0) \leq \mathcal{O}(0.39 - 4.76) \times 10^{-9}, \quad (7.20)$$

We can compare these results with that of the constraints mentioned in Eq (5.46-5.61) for a generic sub-Planckian inflationary setup for $\vartheta_\star = \phi_\star - \phi_0 \sim 10^{-1} M_p$ for a sub-Planckian VEV model of inflation. We find a very nice agreement which testifies the power of a model independent reconstruction of the potential.

Let us give an example of Hubble induced supergravity motivated MSSM inflation which is guided by inflection point prescription. For the potential under consideration, I have

$$V_0 = 3H^2 M_p^2 \sim M_s^4 \gg m_\phi^2 |\phi|^2, \quad (7.21)$$

where $m_\phi \sim \mathcal{O}(\text{TeV})$ is the soft mass. In this case the contributions from the Hubble-induced terms are important compared to the soft SUSY breaking mass, m_ϕ . The potential, after stabilizing the angular direction of the complex scalar field $\phi = |\phi| \exp[i\theta]$, see [31, 41, 42], reduces to a simple form along the real direction, which is dominated by a single scale, i.e. $H \sim H_\star$:

$$V(\phi) = V_0 + c_H H^2 |\phi|^2 - \frac{a_H H \phi^n}{n M_p^{n-3}} + \frac{\lambda^2 |\phi|^{2(n-1)}}{M_p^{2(n-3)}}, \quad (7.22)$$

where I take $\lambda = 1$, and, the Hubble-induced mass parameter is c_H and the trilinear A term is a_H . Fortunately for this class of potential given by Eq (7.22), inflection point inflation can be accommodated, when

$$a_H^2 \approx 8(n-1)c_H. \quad (7.23)$$

This can be characterized by a fine-tuning parameter, δ , which is defined as:

$$\frac{a_H^2}{8(n-1)c_H} = 1 - \left(\frac{n-2}{2}\right)^2 \delta^2. \quad (7.24)$$

When $|\delta|$ is small ¹⁶, a point of inflection ϕ_0 exists, such that

$$V''(\phi_0) = 0, \quad (7.25)$$

with

$$\phi_0 = \left(\sqrt{\frac{c_H}{(n-1)}} H M_p^{n-3} \right)^{1/n-2} + \mathcal{O}(\delta^2). \quad (7.26)$$

¹⁶We will consider a moderate tuning of order $\delta \sim 10^{-4}$ between c_H and a_H .

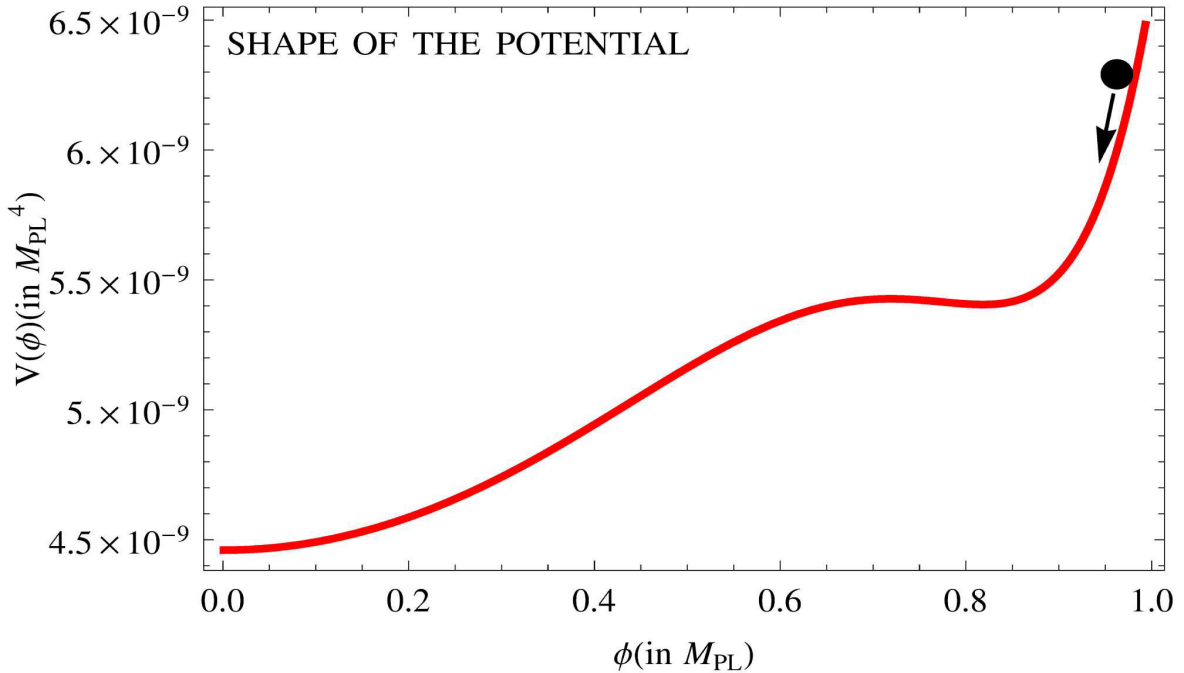


Figure 16. We show the variation of the $n=6$ MSSM inflationary potential with respect to the field ϕ , which satisfies all the obtained constraints from recent Planck 2015 data and Planck 2015 +BICEP2/Keck Array joint constraints.

For $\delta < 1$, I can Taylor-expand the inflaton potential around an inflection point, $\phi = \phi_0$, as [31, 41, 42]:

$$V(\phi) = \alpha + \beta(\phi - \phi_0) + \gamma(\phi - \phi_0)^3 + \kappa(\phi - \phi_0)^4 + \dots, \quad (7.27)$$

where the expansion coefficients are now given by:

$$\alpha = V(\phi_0) = V_0 + \left(\frac{(n-2)^2}{n(n-1)} + \frac{(n-2)^2}{n} \delta^2 \right) c_H H^2 \phi_0^2 + \mathcal{O}(\delta^4), \quad (7.28)$$

$$\beta = V'(\phi_0) = 2 \left(\frac{n-2}{2} \right)^2 \delta^2 c_H H^2 \phi_0 + \mathcal{O}(\delta^4), \quad (7.29)$$

$$\gamma = \frac{V'''(\phi_0)}{3!} = \frac{c_H H^2}{\phi_0} \left(4(n-2)^2 - \frac{(n-1)(n-2)^3}{2} \delta^2 \right) + \mathcal{O}(\delta^4), \quad (7.30)$$

$$\begin{aligned} \kappa &= \frac{V''''(\phi_0)}{4!} \\ &= \frac{c_H H^2}{\phi_0^2} \left(12(n-2)^3 - \frac{(n-1)(n-2)(n-3)(7n^2 - 27n + 26)}{2} \delta^2 \right) + \mathcal{O}(\delta^4). \end{aligned} \quad (7.31)$$

Note that once I specify c_H and H_* , all the terms in the potential are determined. In this regard the potential indeed simplifies a lot to study the cosmological observables.

As an concrete example, I considered $n = 6$ case, where the flatness of the superfield Φ is lifted by the non-renormalizable operator. This is appropriate for both $\tilde{u}\tilde{d}\tilde{d}$ and $\tilde{L}\tilde{L}\tilde{e}$ flat directions.

We fix $\lambda = \mathcal{O}(1)$ and $\delta \sim 10^{-4}$. In order to satisfy the Planck observational constraints on the amplitude of the power spectrum, $2.092 \times 10^{-9} < P_S < 2.297 \times 10^{-9}$ (within 2σ), spectral tilt $0.958 < n_S < 0.963$ (within 2σ), sound speed $c_S = 1$ (within 2σ), and tensor-to-scalar ratio $r_* \leq 0.12$, I obtain the following constraints on our parameters for $H_{inf} \geq m_\phi \sim \mathcal{O}(\text{TeV})$, where successful inflation can occur via *inflection point*:

$$\begin{aligned} c_H &\sim \mathcal{O}(10 - 10^{-6}), & \mathbf{for} & & 10^{-22} < r_* < 0.12 \\ a_H &\sim \mathcal{O}(30 - 10^{-3}), & \mathbf{for} & & 10^{-22} < r_* < 0.12 \\ M_s &\sim \mathcal{O}(9.50 \times 10^{10} - 1.77 \times 10^{16}) \text{ GeV}, & \mathbf{for} & & 10^{-22} < r_* < 0.12. \end{aligned} \quad (7.32)$$

This analysis justifies that the Hubble correction induced MSSM inflation is one of the examples of inflection point inflation where the present reconstruction technique holds good perfectly.

8 Example of Saddle point inflation within effective theory

Now I impose,

$$V'(\phi_0) = 0, \quad (8.1)$$

$$V''(\phi_0) = 0, \quad (8.2)$$

$$V'''(\phi_0) = 0, \quad (8.3)$$

in order to study the *saddle point* scenario. The potential is given by ¹⁷:

$$V(\phi) = V(\phi_0) + \frac{V''''(\phi_0)}{24}(\phi - \phi_0)^4 + \dots, \quad (8.4)$$

We can express $V(\phi_*)$, $V'(\phi_*)$, \dots in terms of ϕ_0 for a sub-Planckian regime as:

$$\begin{aligned} V(\phi_*) &= V(\phi_0) + \frac{\vartheta_*^4}{24} V''''(\phi_0), \\ V'(\phi_*) &= \frac{\vartheta_*^3}{6} V''''(\phi_0), \\ V''(\phi_*) &= \frac{\vartheta_*^2}{2} V''''(\phi_0), \\ V'''(\phi_*) &= \vartheta_* V''''(\phi_0), \\ V''''(\phi_*) &= V''''(\phi_0). \end{aligned} \quad (8.5)$$

¹⁷The saddle point inflation has been studied in Refs. [43].

Using Eq (8.5), I obtain a *particular* solution for the coefficients: $V(\phi_0)$, $V'(\phi_0)$, \dots , which can be written as ¹⁸:

$$\begin{aligned} V(\phi_0) &= V(\phi_\star) - \vartheta_\star V'(\phi_\star) + \frac{\vartheta_\star^3}{3} V'''(\phi_\star) - \frac{5\vartheta_\star^4}{24} V''''(\phi_\star), \\ V''''(\phi_0) &= V''''(\phi_\star). \end{aligned} \quad (8.6)$$

Now using the bound on $V(\phi_\star)$, $V'(\phi_\star)$, \dots as mentioned in Eqs. (5.26-5.45), I can obtain the following constraints on the coefficients of $V(\phi_0)$, $V'(\phi_0)$, \dots :

Planck (2013)+WMAP-9+high L:

$$V(\phi_0) \leq \mathcal{O}(3.79 - 3.94) \times 10^{-9} M_p^4, \quad (8.7)$$

$$V''''(\phi_0) \leq \mathcal{O}(0.39 - 4.76) \times 10^{-9}, \quad (8.8)$$

Planck (2014)+WMAP-9+high L+BICEP2 (dust):

$$5.26 \times 10^{-9} M_p^4 \leq V(\phi_0) \leq 9.50 \times 10^{-9} M_p^4, \quad (8.9)$$

$$5.56 \times 10^{-10} \leq V''''(\phi_0) \leq 4.82 \times 10^{-9}, \quad (8.10)$$

Planck (2015)+WMAP-9+high L(TT):

$$V(\phi_0) \leq \mathcal{O}(3.41 - 3.67) \times 10^{-9} M_p^4, \quad (8.11)$$

$$V''''(\phi_0) \leq \mathcal{O}(5.52 - 5.76) \times 10^{-9}, \quad (8.12)$$

Planck (2015)+BICEP2/Keck Array:

$$V(\phi_0) \leq \mathcal{O}(3.75 - 3.95) \times 10^{-9} M_p^4, \quad (8.13)$$

$$V''''(\phi_0) \leq \mathcal{O}(0.39 - 4.76) \times 10^{-9}, \quad (8.14)$$

We can compare these results with that of the constraints mentioned in Eq (5.46-5.61) for a generic sub-Planckian inflationary setup for $\vartheta_\star = \phi_\star - \phi_0 \sim 10^{-1} M_p$ for a sub-Planckian VEV model of inflation. We find a very nice agreement which testifies the power of a model independent reconstruction of the potential.

Let us consider a concrete example of soft SUSY breaking induced MSSM inflation which is guided by the principle of saddle point inflation. Considering the contribution from $\tilde{Q}\tilde{Q}\tilde{Q}\tilde{L}$, $\tilde{Q}\tilde{u}\tilde{Q}\tilde{d}$, $\tilde{Q}\tilde{u}\tilde{L}\tilde{e}$ and $\tilde{u}\tilde{u}\tilde{d}\tilde{e}$, the $n = 4$ indexed SUSY flat directions the effective potential within the framework of MSSM can be written as [43]:

$$V(\phi, \theta) = V_0 + \frac{1}{2} m_\phi^2 |\phi|^2 + \frac{\lambda A}{4M_p} |\phi|^4 \cos(4\theta + \theta_A) + \frac{\lambda^2 |\phi|^6}{M_p^2}, \quad (8.15)$$

¹⁸There will be in general 2 solutions around an inflection point, here I will provide one of the two solutions which is the most interesting one for the general case of study.

where V_0 is the vacuum energy dominated term which mimics the role of cosmological constant, m_ϕ represents the soft SUSY breaking mass term, the inflaton $|\phi|$ is the radial coordinate of the complex scalar field $\Phi = |\phi|e^{i\theta}$ and the second term is the trilinear A-term which has a periodicity of 2π in 2D along with an extra phase θ_A . The radiative correction slightly affects the soft term and the position of the saddle point in potential valley. One can tune the vacuum energy term $V_0 \approx 0$. But for the generality I keep this term. Once this term is switched on in the effective potential, the scale of the potential goes up to the GUT scale. This will change the value of tensor-to-scalar ratio upto $r(k_*) \sim 0.12$. But the other inflationary observables computed from the model is insensitive to the addition of vacuum energy term V_0 . After minimizing with respect to the angular coordinate θ the effective potential takes the following form [43]:

$$V(\phi) = V_0 + \frac{1}{2}m_\phi^2|\phi|^2 - \frac{\lambda A}{4M_p}|\phi|^4 + \frac{\lambda^2|\phi|^6}{M_p^2} \quad (8.16)$$

using which the position for the saddle point is computed from the model as:

$$\phi_0 = \sqrt{\frac{M_p}{4\lambda(D_3+3)} \left[A \left(1 + \frac{D_2}{2}\right) \pm \sqrt{A^2 \left(1 + \frac{D_2}{2}\right)^2 - 8m_\phi^2(D_1+1)(D_3+3)} \right]} \quad (8.17)$$

where D_1, D_2, D_3 are the contribution from one loop radiative corrections appearing as:

$$\lambda = \lambda_0 \left[1 + 2D_3 \ln \left(\frac{\phi_0}{\mu_0} \right) \right], \quad (8.18)$$

$$A = A_0 \left[1 + 2D_2 \ln \left(\frac{\phi_0}{\mu_0} \right) \right] \left[1 + 2D_3 \ln \left(\frac{\phi_0}{\mu_0} \right) \right]^{-1}, \quad (8.19)$$

$$m_\phi^2 = m_0^2 \left[1 + 2D_1 \ln \left(\frac{\phi_0}{\mu_0} \right) \right]. \quad (8.20)$$

Also the trilinear A term and the radiative correction term D_3 satisfy the following constraints:

$$A = \sqrt{2(D_3+3)G_1G_2G_3}m_0, \quad (8.21)$$

$$D_3 = \frac{M_p A_0}{4\lambda_0\phi_0^2 \left(37 + 60 \ln \left(\frac{\phi_0}{\mu_0} \right) \right)} \left[D_2 \left(13 + 12 \ln \left(\frac{\phi_0}{\mu_0} \right) \right) - \frac{2m_0^2 D_1 M_p}{\lambda_0 m_0 \phi_0^2} + 6 \left(1 - \frac{20\lambda_0\phi_0^2}{M_p A_0} \right) \right]. \quad (8.22)$$

Here G_1, G_2 and G_3 is given by:

$$G_1 = \left[\frac{(D_1 + 1)}{(D_3 + 3)} (15 + 11D_3) - (3D_1 + 1) \right]^2, \quad (8.23)$$

$$G_2 = \left[(D_1 + 1) \left(\frac{7}{2} D_3 + 3 \right) - (3D_1 + 1) \left(1 + \frac{D_2}{2} \right) \right]^{-1}, \quad (8.24)$$

$$G_3 = \left[\frac{\left(1 + \frac{D_2}{2} \right)}{(D_3 + 3)} (11D_3 + 15) - \left(3 + \frac{7D_3}{2} \right) \right]^{-1}. \quad (8.25)$$

After applying the saddle point technique around ϕ_0 the effective potential can be recast as [43]:

$$V(\phi) = \Delta_1 + \Delta_2 (\phi - \phi_0)^4, \quad (8.26)$$

where Δ_1 and Δ_2 are the Taylor expansion co-efficients defined as:

$$\begin{aligned} \Delta_1 &= V(\phi_0) \\ &= V_0 + \frac{m_0^3 M_p}{6\sqrt{6}\lambda} \left[3 \left(1 + \frac{D_1}{2} - \frac{D_3}{6} \right) \left[1 + 2D_1 \ln \left(\frac{\phi_0}{\mu_0} \right) \right] \right. \\ &\quad \left. - 2 \left(1 + \frac{D_1}{2} - \frac{D_3}{6} \right)^2 \left[1 + 2D_2 \ln \left(\frac{\phi_0}{\mu_0} \right) \right] \right], \end{aligned} \quad (8.27)$$

$$\begin{aligned} \Delta_2 &= \frac{V''''(\phi_0)}{4!} \\ &= \frac{m_0^2}{24\sqrt{6}\phi_0^2} \left(1 + \frac{D_1}{2} - \frac{D_3}{6} \right)^2 \left[\left(\frac{360}{\sqrt{6}} - 12\sqrt{6} + 684D_3 - 50\sqrt{6}D_2 - \frac{2\sqrt{6}D_1}{\left(1 + \frac{D_1}{2} - \frac{D_3}{6} \right)^2} \right) \right. \\ &\quad \left. + 2 \left(\frac{360D_3}{\sqrt{6}} - 12\sqrt{6}D_2 \right) \ln \left(\frac{\phi_0}{\mu_0} \right) \right]. \end{aligned} \quad (8.28)$$

In order to satisfy the Planck observational constraints on the amplitude of the power spectrum, $2.092 \times 10^{-9} < P_S < 2.297 \times 10^{-9}$ (within 2σ), spectral tilt $0.958 < n_S < 0.963$ (within 2σ), sound speed $c_S = 1$ (within 2σ), and tensor-to-scalar ratio $r_\star \leq 0.12$, I obtain the following constraints on our parameters, where successful inflation can occur via *saddle point*:

$$\begin{aligned} \Delta_1 &\sim \mathcal{O}(10^{-36} - 10^{-9}) M_p^4, & \mathbf{for} & \quad 10^{-29} < r_\star < 0.12 \\ \Delta_2 &\sim \mathcal{O}(10^{-13} - 10^{-9}), & \mathbf{for} & \quad 10^{-29} < r_\star < 0.12. \end{aligned} \quad (8.29)$$

This analysis justifies that the soft SUSY breaking induced MSSM inflation is one of the examples of inflection point inflation where the present reconstruction technique holds good perfectly.

9 Multipole scanning of CMB spectra via reconstructed effective potential

In this section I study the CMB TT, TE, EE, BB-angular power spectrum ¹⁹. The angular power spectra are defined as:

$$C_\ell^{XY} \equiv \frac{1}{2\ell + 1} \sum_{m=-\ell}^{\ell} \langle a_{X,\ell m}^* a_{Y,\ell m} \rangle, \quad X, Y = T, E, B. \quad (9.1)$$

Further substituting the inflationary input spectra $P(k) \equiv \{P_S(k), P_T(k)\}$ and the angular power spectra of CMB temperature fluctuations and polarization

$$C_\ell^{XY} = \frac{2}{\pi} \int k^2 dk \underbrace{P(k)}_{\text{Inflation}} \underbrace{\Delta_{X\ell}(k)\Delta_{Y\ell}(k)}_{\text{Anisotropies}}, \quad (9.2)$$

where

$$\Delta_{X\ell}(k) = \int_0^{\eta_0} d\eta \underbrace{S_X(k, \eta)}_{\text{Sources}} \underbrace{P_{X\ell}(k[\eta_0 - \eta])}_{\text{Projection}}. \quad (9.3)$$

The integral (9.2) relates the inhomogeneities predicted by inflation, $P(k)$, to the anisotropies observed in the CMB, C_ℓ^{XY} . The correlations between the different X and Y modes are related by the transfer functions $\Delta_{X\ell}(k)$ and $\Delta_{Y\ell}(k)$. The transfer functions may be written as the line-of-sight integral Eq (9.3) which factorizes into physical source terms $S_X(k, \eta)$ and geometric projection factors $P_{X\ell}(k[\eta_0 - \eta])$ through combinations of Bessel functions.

¹⁹In this work I have not consider possibility of other cross correlators i.e. TB, EB as there is no observational evidence of such contributions in the CMB map. Also till date there is no observational evidence for inflationary origin of BB angular power spectrum except from CMB lensing. However, for the completeness in this paper I show the theoretical BB angular power spectra from the reconstructed potential.

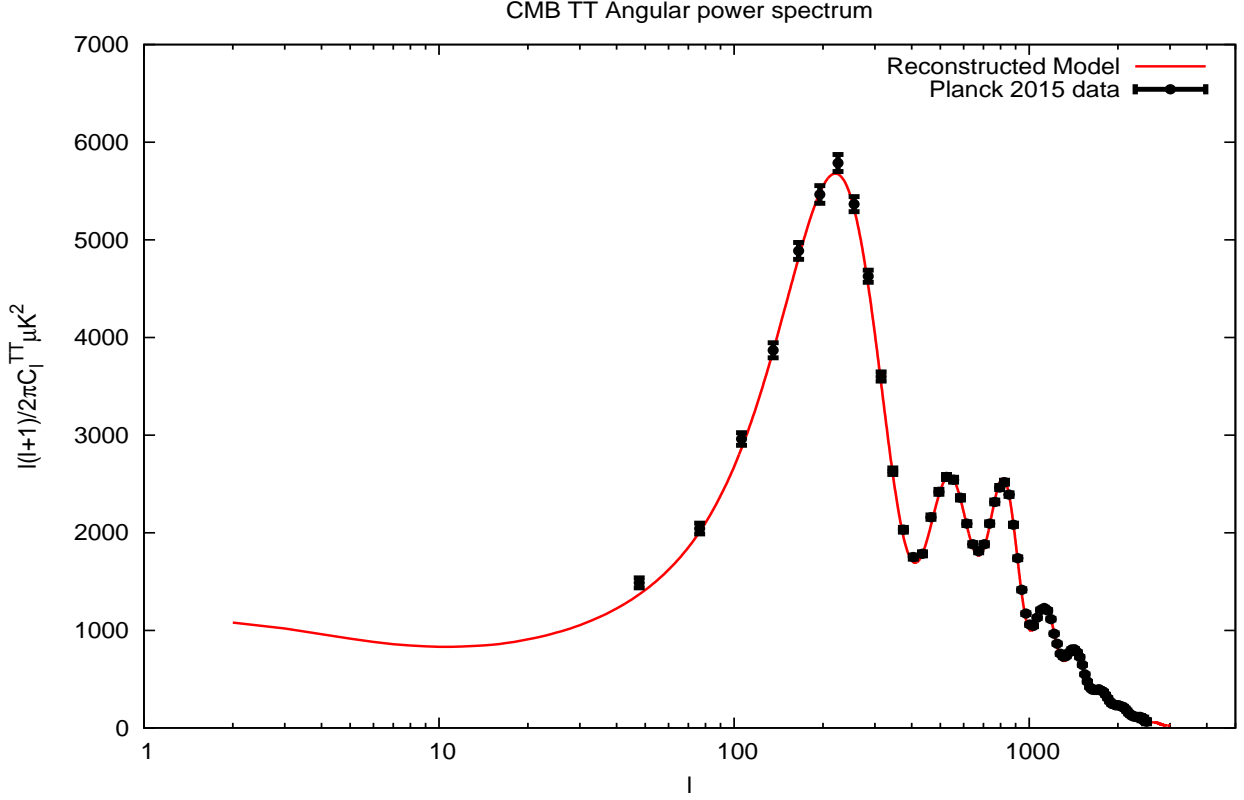


Figure 17. We show the variation of CMB TT Angular power spectrum with respect to the multipole, l for scalar modes with the choice of best fit reconstructed model parameters: $V(\phi_0) \sim \mathcal{O}(10^{-9} M_p^4)$, $V'(\phi_0) \sim \mathcal{O}(10^{-10} M_p^3)$, $V''(\phi_0) \sim \mathcal{O}(10^{-11} M_p^2)$, $V'''(\phi_0) \sim \mathcal{O}(10^{-10} M_p)$ and $V''''(\phi_0) \sim \mathcal{O}(10^{-9})$ obtained from Planck 2015 data, which is consistent with the bound on field excursion value. From this analysis finally I get: $P_S(k_*) \sim 2.215 \times 10^{-9}$, $n_S(k_*) \sim 0.962$, $r(k_*) \sim 0.2$, $\alpha_S(k_*) \sim -10^{-2}$ and $\kappa_S(k_*) \sim 5 \times 10^{-3}$.

Further expressing Eq (9.2) in terms of TT, TE, EE, BB correlation I get:

$$\text{For scalar : } C_\ell^{TT} = \frac{2}{\pi} \int k^2 dk P_S(k) \Delta_{T\ell}(k) \Delta_{T\ell}(k), \quad (9.4)$$

$$C_\ell^{TE} = (4\pi)^2 \int k^2 dk P_S(k) \Delta_{T\ell}(k) \Delta_{E\ell}(k), \quad (9.5)$$

$$C_\ell^{EE} = (4\pi)^2 \int k^2 dk P_S(k) \Delta_{E\ell}(k) \Delta_{T\ell}(k), \quad (9.6)$$

$$\text{For tensor : } C_\ell^{BB} = (4\pi)^2 \int k^2 dk P_T(k) \Delta_{E\ell}(k) \Delta_{T\ell}(k) \quad (9.7)$$

$$C_\ell^{TT} = \frac{2}{\pi} \int k^2 dk P_T(k) \Delta_{T\ell}(k) \Delta_{T\ell}(k), \quad (9.8)$$

$$C_\ell^{TE} = (4\pi)^2 \int k^2 dk P_T(k) \Delta_{T\ell}(k) \Delta_{E\ell}(k), \quad (9.9)$$

$$C_\ell^{EE} = (4\pi)^2 \int k^2 dk P_T(k) \Delta_{E\ell}(k) \Delta_{T\ell}(k). \quad (9.10)$$

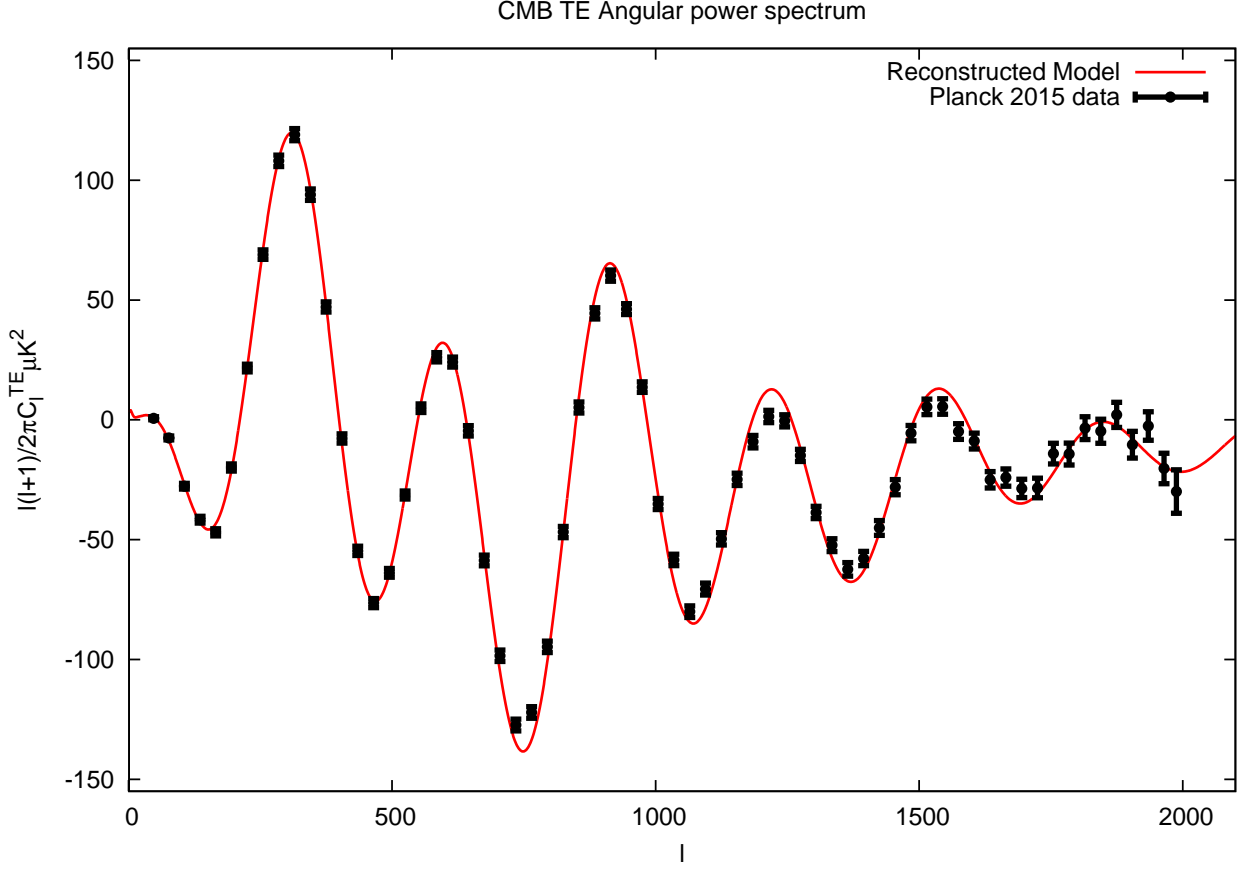


Figure 18. We show the variation of CMB TE Angular power spectrum with respect to the multipole, l for scalar modes with the choice of best fit reconstructed model parameters: $V(\phi_0) \sim \mathcal{O}(10^{-9} M_p^4)$, $V'(\phi_0) \sim \mathcal{O}(10^{-10} M_p^3)$, $V''(\phi_0) \sim \mathcal{O}(10^{-11} M_p^2)$, $V'''(\phi_0) \sim \mathcal{O}(10^{-10} M_p)$ and $V''''(\phi_0) \sim \mathcal{O}(10^{-9})$ obtained from Planck 2015 data, which is consistent with the bound on field excursion value. From this analysis finally I get: $P_S(k_*) \sim 2.215 \times 10^{-9}$, $n_S(k_*) \sim 0.962$, $r(k_*) \sim 0.2$, $\alpha_S(k_*) \sim -10^{-2}$ and $\kappa_S(k_*) \sim 5 \times 10^{-3}$.

where the inflationary power spectra $\{P_S(k), P_T(k)\}$ are parametrized at any arbitrary momentum scale as:

$$P_S(k) = P_S(k_*) \left(\frac{k}{k_*} \right)^{n_S - 1 + \frac{\alpha_S}{2} \ln\left(\frac{k}{k_*}\right) + \frac{\kappa_S}{6} \ln^2\left(\frac{k}{k_*}\right) + \dots}, \quad (9.11)$$

$$P_T(k) = r(k) P_S(k) = P_T(k_*) \left(\frac{k}{k_*} \right)^{n_T + \frac{\alpha_T}{2} \ln\left(\frac{k}{k_*}\right) + \frac{\kappa_T}{6} \ln^2\left(\frac{k}{k_*}\right) + \dots}. \quad (9.12)$$

It is important to note that the cosmological significance of the E and B decomposition of CMB polarization carries the following significant features:

- Scalar (density) perturbations create only E -modes.

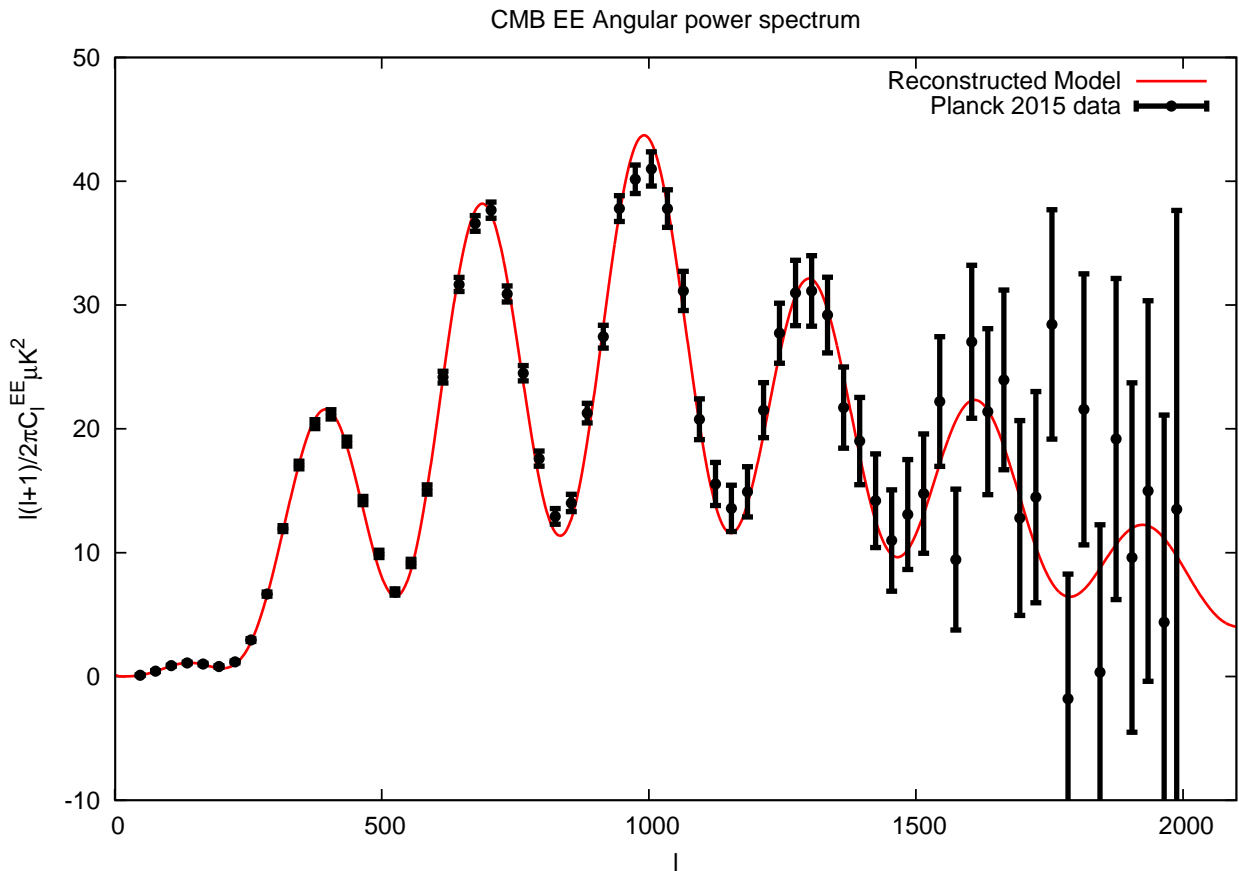
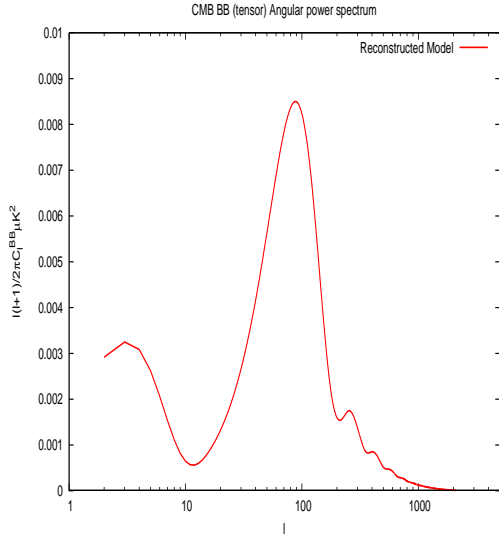


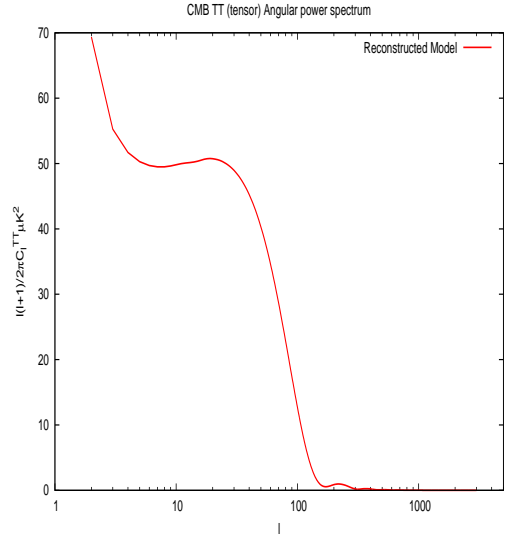
Figure 19. We show the variation of CMB EE Angular power spectrum with respect to the multipole, l for scalar modes with the choice of best fit reconstructed model parameters: $V(\phi_0) \sim \mathcal{O}(10^{-9} M_p^4)$, $V'(\phi_0) \sim \mathcal{O}(10^{-10} M_p^3)$, $V''(\phi_0) \sim \mathcal{O}(10^{-11} M_p^2)$, $V'''(\phi_0) \sim \mathcal{O}(10^{-10} M_p)$ and $V''''(\phi_0) \sim \mathcal{O}(10^{-9})$ obtained from Planck 2015 data, which is consistent with the bound on field excursion value. From this analysis finally I get: $P_S(k_*) \sim 2.215 \times 10^{-9}$, $n_S(k_*) \sim 0.962$, $r(k_*) \sim 0.2$, $\alpha_S(k_*) \sim -10^{-2}$ and $\kappa_S(k_*) \sim 5 \times 10^{-3}$.

- Vector (vorticity) perturbations create mainly B -modes. However, the contributions of vectors decay with the expansion of the universe and are therefore sub-dominant at the epoch of recombination. For this reason I have neglected such sub-dominant effects from our analysis.
- Tensor (gravitational wave) perturbations create both E -modes and B -modes.

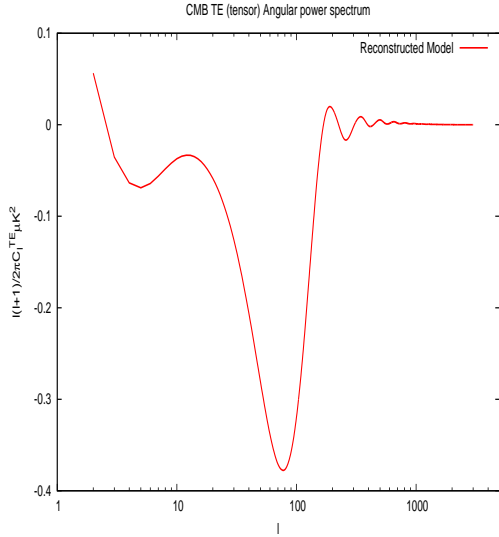
To compute the momentum integrals numerically and to analyze the various features of CMB angular power spectra from the prescribed reconstruction algorithm I use a numerical code “CAMB” [44]. For the numerical analysis I use here the best



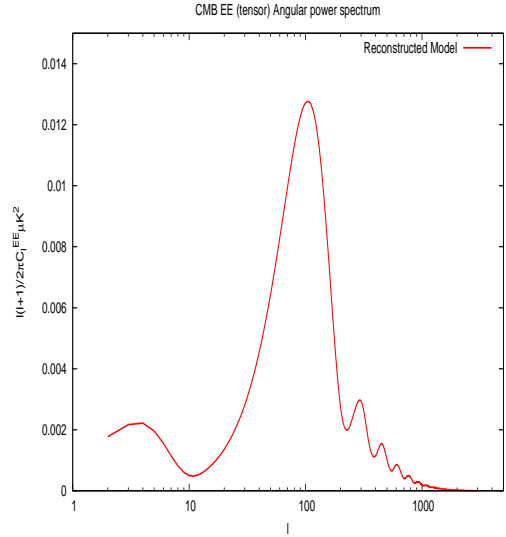
(a) $l(l+1)C_l^{BB}/2\pi$ vs l (tensor)



(b) $l(l+1)C_l^{TT}/2\pi$ vs l (tensor)



(c) $l(l+1)C_l^{TE}/2\pi$ vs l (tensor)



(d) $l(l+1)C_l^{EE}/2\pi$ vs l (tensor)

Figure 20. We show the variation of (a) CMB BB Angular power spectrum, (b) CMB TT Angular power spectrum, (c) CMB TE Angular power spectrum and (d) CMB EE Angular power spectrum with respect to the multipole, l for scalar modes with the choice of best fit reconstructed model parameters: $V(\phi_0) \sim \mathcal{O}(10^{-9} M_p^4)$, $V'(\phi_0) \sim \mathcal{O}(10^{-10} M_p^3)$, $V''(\phi_0) \sim \mathcal{O}(10^{-11} M_p^2)$, $V'''(\phi_0) \sim \mathcal{O}(10^{-10} M_p)$ and $V''''(\phi_0) \sim \mathcal{O}(10^{-9})$ obtained from Planck 2015 data, which is consistent with the bound on the field excursion value. From this analysis finally I get: $P_S(k_*) \sim 2.215 \times 10^{-9}$, $n_S(k_*) \sim 0.962$, $r(k_*) \sim 0.1$, $\alpha_S(k_*) \sim -10^{-2}$ and $\kappa_S(k_*) \sim 5 \times 10^{-3}$.

fit reconstructed model parameters:

$$V(\phi_0) \sim \mathcal{O}(10^{-9} M_p^4), \quad (9.13)$$

$$V'(\phi_0) \sim \mathcal{O}(10^{-10} M_p^3), \quad (9.14)$$

$$V''(\phi_0) \sim \mathcal{O}(10^{-11} M_p^2), \quad (9.15)$$

$$V'''(\phi_0) \sim \mathcal{O}(10^{-10} M_p), \quad (9.16)$$

$$V''''(\phi_0) \sim \mathcal{O}(10^{-9}) \quad (9.17)$$

which is compatible with Planck 2015 data. For this specific choice of multi parameter space finally the inflationary observables are estimated as:

$$P_S(k_*) \sim 2.215 \times 10^{-9}, \quad (9.18)$$

$$n_S(k_*) \sim 0.962, \quad (9.19)$$

$$r(k_*) \sim 0.1, \quad (9.20)$$

$$\alpha_S(k_*) \sim -10^{-2}, \quad (9.21)$$

$$\kappa_S(k_*) \sim 5 \times 10^{-3}. \quad (9.22)$$

Additionally I take Λ CDM background in which I fix:

$$\Omega_b h^2 = 0.022220, \quad (9.23)$$

$$\Omega_c h^2 = 0.119700, \quad (9.24)$$

$$\Omega_\nu h^2 = 0.000640, \quad (9.25)$$

$$\Omega_K \approx 0, \quad (9.26)$$

$$100 \theta = 1.040832, \quad (9.27)$$

$$N_{eff} = 3.046. \quad (9.28)$$

Further I put all these inputs to ‘‘CAMB’’ and modify the inbuilt parameterization of power spectrum for scalar and tensor modes accordingly. Finally from the analysis I

get:

$$\Omega_\Lambda = 0.685342, \quad (9.29)$$

$$\Omega_m (= 1 - \Omega_K - \Omega_\Lambda) = 0.314658, \quad (9.30)$$

$$z_{Reion} = 9.959, \quad (9.31)$$

$$z_{eq} = 3391.45, \quad (9.32)$$

$$t_0 = 13.814 \text{ Gyr}, \quad (9.33)$$

$$z_\star = 1089.87, \quad (9.34)$$

$$r_S(z_\star) = 144.64 \text{ Mpc}, \quad (9.35)$$

$$D_A(z_\star) = 13.89228 \text{ Mpc}, \quad (9.36)$$

$$z_{drag} = 1059.40, \quad (9.37)$$

$$r_S(z_{drag}) = 147.35 \text{ Mpc}, \quad (9.38)$$

$$k_D(z_\star) = 0.1407 \text{ Mpc}^{-1}, \quad (9.39)$$

$$100 \theta_D = 0.160737, \quad (9.40)$$

$$100 \theta_{eq} = 0.814740, \quad (9.41)$$

$$\eta_{recomb} = 280.75 \text{ Mpc}, \quad (9.42)$$

$$\eta_{now} = 14164.5 \text{ Mpc}, \quad (9.43)$$

$$\sigma_8(\text{all matter}) = 0.8234. \quad (9.44)$$

After performing all the numerical computations via ‘‘CAMB’’ finally from our analysis I have generated all the theoretical CMB angular power spectra from which I observed the following significant features:-

- In Fig. (17), at low ℓ region ($2 < l < 49$) the contributions from the running (α_S, α_T), and running of running (κ_S, κ_T) are very small. Their additional contribution to the CMB power spectrum for scalar and tensor modes becomes unity ($\mathcal{O}(1)$) within low- l region and the original power spectrum becomes unchanged. As a result the reconstructed model will be well fitted with the CMB TT spectrum at low- l region within high cosmic variance as observed by Planck except for a few outliers according to the Planck 2013 data release. But to update our analysis with the latest Planck 2015 data set I have not shown such high cosmic variance explicitly. In case of WMAP9 data for CMB TT spectrum the cosmic variance in the low- l region is not very large compared to the Planck low- l data. But our reconstructed model is also well fitted with WMAP9 low- l data also which I have not shown explicitly in the plot to update the analysis using Planck 2015 data. It is also important to mention that if I incorporate the uncertainties in the scanning multipole l for the measurement of CMB TT spectrum, then also our prescribed analysis is pretty consistent with the Planck 2015 data. Further if I move towards high ℓ regime ($47 <$

$l < 2500$) the contribution of running and running of running become stronger and this will enhance the power spectrum to a permissible value such that it will accurately fit high- l data within very small cosmic variance as observed by Planck. In this way one can easily scan over all the multipoles starting from low- l to high- l using the same momentum dependent parameterization of tensor-to-scalar ratio as prescribed in Eq (2.17).

- From Fig. (17), we see that the Sachs-Wolfe plateau obtained from our proposed reconstructed model is non flat, confirming the appearance of running, and running of the running in the spectrum observed for low l region ($l < 47$). For larger value of the multipole ($47 < l < 2500$), CMB anisotropy spectrum is dominated by the Baryon Acoustic Oscillations (BAO), giving rise to several ups and downs in the CMB TT spectrum. In the low l region due to the presence of very large cosmic variance there may be other pre-inflationary scenarios which might be able to describe the TT-power spectrum better. In my study I have considered only the possibility for which the behaviour of reconstructed model is analyzed for both low and high l regions.
- From Fig. (17), Fig. (18), Fig. (19), we observe that if I include the uncertainties in multipole l as well in the observed CMB angular power spectra then the proposed reconstructed model is pretty consistent with the CMB TT, TE, EE for scalar mode from Planck 2015 data.
- In Fig. (20(a)), Fig. (20(b)), Fig. (20(c)) and Fig. (20(d)) I have explicitly shown the theoretical CMB BB, TT, TE and EE angular power spectrum from tensor mode. Most importantly, if inflationary paradigm is responsible for the nearly de-Sitter expansion of the early universe then the CMB BB spectra for tensor modes is one of the prime components through which one can detect the contribution for primordial gravitational waves via tensor-to-scalar ratio. But till date only the contribution from the lesing B-modes are detected via South Pole Telescope [45] and Planck 2015 +BICEP2/Keck Array joint mission [14]. But confirming the sole inflationary origin from the detection of the de-lensed version of the signal is not sufficient enough to draw any final conclusion ²⁰. There are other possibilities as well through which it is possible to generate CMB B-modes, those components are:
 1. Primordial Magnetic Field [47–49],
 2. Gravitational Lensing [45, 50],
 3. CP asymmetry in the lepton sector of particle theory [48, 49] etc.

²⁰In this respect one may consider the alternative frameworks of inflationary paradigm as well [46].

10 Conclusion

In this paper I have obtained the following results:

- We derive the most generalized analytical expressions for the field excursion $|\Delta\phi|/M_p$ in terms of $r(k_*)$, $V(\phi_*)$, $H(k_*)$ for a generic sub-Planckian model of inflation by taking into account of higher order slow roll corrections and Buch-Davies initial condition. We derive the results for various parameterization of the primordial power spectrum by allowing:
 1. scale invariant feature,
 2. further modification in presence of spectral tilt,
 3. the modification in presence of spectral tilt and running of the tilt,
 4. the effect of spectral tilt, running of the tilt and running of the running of tilt,

through which it is possible to evade the well known *Lyth bound*. Using these relations one can easily rule out all classes of super Planckian or trans-Planckian inflationary models available in inflationary literature.

- For the completeness, I also extend the idea by deriving the most generalized analytical expressions for the field excursion $|\Delta\phi|/M_p$ in terms of $r(k_*)$, $V(\phi_*)$, $H(k_*)$ for a generic sub-Planckian model for the various limiting situations of non Buch-Davies vacuum.
- In order to satisfy the observational constraints from Planck 2015 and Planck 2015+BICEP2/Keck Array joint constraints, one requires a non-monotonic evolution of the first slow-roll parameter, ϵ_V , if one wants to build a model of inflation with a sub-Planckian field excursion and VEV, as pointed out in earlier Refs. [21, 23, 24, 26].
- Hence in this paper I have reconstructed the inflationary potential around the VEV ϕ_0 by computing the Taylor expansion co-efficients $V(\phi_0), V'(\phi_0), V''(\phi_0), V'''(\phi_0)$ and $V''''(\phi_0)$ in terms of the Taylor expansion co-efficients $V(\phi_*), V'(\phi_*), V''(\phi_*), V'''(\phi_*)$ and $V''''(\phi_*)$ at the CMB pivot scale ϕ_* using matrix inversion technique using Planck 2015 and Planck 2015+BICEP2/Keck Array joint data.
- In order to satisfy the current observational constraints from Planck 2015 and Planck 2015+BICEP2/Keck Array joint data, I have found that the upper bound of the scale of inflation to be within: $\sqrt[4]{V_*} \leq \mathcal{O}(1.856 - 1.926) \times 10^{16}$ GeV, for the upper bound on field excursion of inflaton varying within: $\frac{|\Delta\phi|}{M_p} \leq \mathcal{O}(0.223 - 0.242)$.

- We have also derived a new set of second order *consistency relationships* for any generic sub-Planckian model of inflation within slow-roll prescription. In particular, this can be treated as a discriminator to break the degeneracy between various cosmological models of inflation. Most importantly, using these relations one can break also various class of models of inflation as well.
- Furthermore, if the data could be refined to constrain tensor spectral tilt n_T , running α_T and running of the running κ_T , then this would play a very crucial role to break the degeneracy between various cosmological parameters estimated from different class of inflationary models and also rule out various models available in inflationary literature.
- Within our prescribed methodology I have also found that the choice of the field interval ϑ is sensitive to the number of e-foldings $\Delta N \sim \mathcal{O}(8-17)$, which is necessarily required to solve the horizon problem associated with standard big bang cosmology and to produce sufficient amount of inflation by constraining the Taylor expansion co-efficients of the generic potential using Planck 2015 and Planck 2015+BICEP2/Keck Array joint data.
- Finally, I have checked the validity of our prescribed reconstruction technique by fitting the theoretical CMB angular power spectra from TT, TE, EE for scalar mode and BB, TT, TE, EE correlation for tensor mode with the observed Planck 2015 data within multipole scanning region $2 < l < 2500$, in which I cover the momentum scale within the window, $4.488 \times 10^{-5} \text{ Mpc}^{-1} < k < 0.3 \text{ Mpc}^{-1}$.
- Typically, within the framework of particle physics, the nature and shape of the inflationary potential will not *just* be a single monomial. In principle the inflationary potential could contain quadratic, cubic and quartic renormalizable interactions for effective field theory, or even higher order non-renormalizable UV cut-off scale suppressed effective operators arising from integrating out the heavy degrees of freedom originated from string theory inspired hidden sector. In this respect our derived expressions and numerical results are important for reconstructing a particle physics motivated effective potential for inflation in a successful fashion. One can extend the prescribed methodology to various string theory motivated effective potentials, where the VEV of the inflaton field and field excursion both are sub-Planckian. Consequently, the reconstructed version of the inflationary potential allow only the *concave* feature, which is compatible with both particle physics and string theory framework.

The future prospects of the present work are appended below:

1. First of all, using the non Bunch-Davies initial conditions one can repeat the prescribed methodology presented in this paper. Then applying the ob-

servational constraints from Planck 2015 and Planck 2015+BICEP2/Keck Array data one can constrain the exact version of the non Bunch-Davies initial condition applicable for effective field theory description of inflationary paradigm.

2. Hence applying the observational constraints one can derive the first order and second order inflationary consistency relations from the exact version of the non Bunch-Davies initial condition.
3. Further, one can compare the results obtained from non Bunch-Davies and Bunch-Davies vacuum and check which initial condition is more compatible with the observed data. This will in turn fix the ambiguity of choosing the proper initial condition for inflationary paradigm. Also by doing this analysis one can further constrain the nature and shape of the inflationary potential.
4. Using various other parameterization of primordial power spectra one can also derive the most generic relationship between tensor-to-scalar ratio, scale of inflation, Hubble parameter and the field excursion and also repeat the rest of the reconstruction methodology presented in this paper.
5. As I have already mentioned at the end of last section that one of the prime source of generating CMB B-mode polarization is primordial magnetic field, by applying the observational constraint one can reconstruct an effective field theory of inflationary magnetogenesis for sub-Planckian inflation.
6. Finally using the results for non Bunch-Davies initial condition one can also check the compatibility of the theoretical CMB angular power spectra with the temperature anisotropy and polarization data obtained from Planck 2015.

Acknowledgments

SC would like to thank Department of Theoretical Physics, Tata Institute of Fundamental Research, Mumbai for providing me Visiting (Post-Doctoral) Research Fellowship. SC take this opportunity to thank sincerely to Prof. Sandip P. Trivedi, Prof. Shiraz Minwalla, Prof. Soumitra SenGupta, Prof. Subhabrata Majumdar, Prof. Sudhakar Panda, Prof. Sayan Kar and Dr. Supratik Pal for their constant support and inspiration. SC take this opportunity to thank all the active members and the regular participants of weekly student discussion meet “COSMOMEET” from Department of Theoretical Physics and Department of Astronomy and Astrophysics, Tata Institute of Fundamental Research for their strong support. SC additionally Indian Association for the Cultivation of Science (IACS), Kolkata and Physics and

Applied Mathematics Unit (PAMU), Indian Statistical Institute (ISI), Kolkata for extending hospitality during the work. Additionally SC take this opportunity to thank the organizers of STRINGS, 2015, International Centre for Theoretical Science, Tata Institute of Fundamental Research (ICTS,TIFR) and Indian Institute of Science (IISc) for providing the local hospitality during the work and give a chance to discuss with Prof. Nima Arkani-Hamed on related issues, which finally helped us to improve the qualitative and quantitative discussion in the paper. Last but not the least, I would all like to acknowledge our debt to the people of India for their generous and steady support for research in natural sciences, especially for various areas in theoretical high energy physics i.e. cosmology, string theory and particle physics.

Appendix

A. Slow-roll Integration from the reconstructed potential:

The expressions for the slow-roll parameters $(\epsilon_V, \eta_V, \xi_V^2, \sigma_V^3)$ can be expressed as:

$$\begin{aligned}
\epsilon_V(k) &= \epsilon_V - \frac{\alpha_T}{2} \ln\left(\frac{k}{k_\star}\right) + \frac{\kappa_T}{4} \ln^2\left(\frac{k}{k_\star}\right) + \dots, \\
\eta_V(k) &= \eta_V - \frac{(\alpha_S - 3\alpha_T)}{2} \ln\left(\frac{k}{k_\star}\right) + \frac{1}{2} \left(\kappa_S - 3\kappa_T + \{n_T^2 + \alpha_T\} \left[\frac{n_S - 3n_T - 1}{2} \right] \right. \\
&\quad \left. + \frac{\xi_V^2}{2} \{1 - n_S - 3n_T\} \right) \ln^2\left(\frac{k}{k_\star}\right) + \dots, \\
\xi_V^2(k) &= \xi_V^2 - \frac{1}{2} (\kappa_S - 4\kappa_T + 4n_T^2 \{n_S - n_T - 1\}) \ln\left(\frac{k}{k_\star}\right) \\
&\quad + \frac{1}{4} (\xi_V^2 \{16n_T^2 + 9n_T [n_S - 3n_T - 1] + [n_S - 3n_T - 1]^2 + 2\xi_V^2\}) \ln^2\left(\frac{k}{k_\star}\right) + \dots, \\
\sigma_V^3(k) &= \sigma_V^3 + \sigma_V^3 (1 - n_S) \ln\left(\frac{k}{k_\star}\right) \\
&\quad + \frac{\sigma_V^3}{4} (30n_T^2 + 20n_T [n_S - 3n_T - 1] + \xi_V^2 + 2 [n_S - 3n_T - 1]^2) \ln^2\left(\frac{k}{k_\star}\right) + \dots
\end{aligned} \tag{10.1}$$

where at the pivot scale $k = k_\star$ the slow roll parameters are defined as follows:

$$\epsilon_V = \frac{M_P^2}{2} \left(\frac{V'}{V}\right)^2, \eta_V = M_P^2 \left(\frac{V''}{V}\right), \xi_V^2 = M_P^4 \left(\frac{V'V'''}{V^2}\right), \sigma_V^3 = M_P^6 \left(\frac{V'^2V''''}{V^3}\right) \tag{10.2}$$

Further in terms of the reconstructed potential I get:

$$\begin{aligned}
\epsilon_V &\approx \frac{M_p^2}{2V(\phi_0)^2} \left[V'(\phi_0) + V''(\phi_0)(\phi - \phi_0) + \frac{V'''(\phi_0)}{2}(\phi - \phi_0)^2 + \frac{V''''(\phi_0)}{6}(\phi - \phi_0)^3 + \dots \right]^2, \\
\eta_V &\approx \frac{M_p^2}{V(\phi_0)} \left[V''(\phi_0) + V'''(\phi_0)(\phi - \phi_0) + \frac{V''''(\phi_0)}{2}(\phi - \phi_0)^2 + \dots \right], \\
\xi_V^2 &\approx \frac{M_p^4}{V(\phi_0)^2} \left[V'''(\phi_0)V'(\phi_0) + (V''''(\phi_0)V'(\phi_0) + V'''(\phi_0)V''(\phi_0))(\phi - \phi_0) \right. \\
&\quad \left. + \left(V''''(\phi_0)V''(\phi_0) + \frac{V''''(\phi_0)^2}{2} \right) (\phi - \phi_0)^2 + \dots \right], \\
\sigma_V^3 &\approx \frac{V''''(\phi_0)M_p^6}{V(\phi_0)^3} \left[V'(\phi_0) + V''(\phi_0)(\phi - \phi_0) + \frac{V'''(\phi_0)}{2}(\phi - \phi_0)^2 + \frac{V''''(\phi_0)}{6}(\phi - \phi_0)^3 + \dots \right]^2.
\end{aligned} \tag{10.3}$$

Furthermore, the inflationary observables, i.e. the amplitude of scalar and tensor power spectrum (P_S, P_T), spectral tilt (n_S, n_T), and tensor-to-scalar ratio (r_*) at the pivot scale k_* can be expressed as:

$$\begin{aligned}
P_S(k_*) &= [1 - (2\mathcal{C}_E + 1)\epsilon_V + \mathcal{C}_E\eta_V]^2 \frac{V}{24\pi^2 M_p^4 \epsilon_V} \\
&\approx \frac{V(\phi_0)^2}{12\pi^2 M_p^6 V'(\phi_0)^2} \left[V(\phi_0) + V'(\phi_0)(\phi_* - \phi_0) + \frac{V''(\phi_0)}{2}(\phi_* - \phi_0)^2 + \frac{V'''(\phi_0)}{6}(\phi_* - \phi_0)^3 \right. \\
&\quad \left. + \frac{V''''(\phi_0)}{24}(\phi_* - \phi_0)^4 + \dots \right] \left[1 - (2\mathcal{C}_E + 1) \frac{V'(\phi_0)^2 M_p^2}{2V(\phi_0)^2} + \mathcal{C}_E \frac{M_p^2 V''(\phi_0)}{V(\phi_0)} \right]^2,
\end{aligned} \tag{10.4}$$

$$\begin{aligned}
P_T(k_*) &= [1 - (\mathcal{C}_E + 1)\epsilon_V]^2 \frac{2V}{3\pi^2 M_p^4} \\
&\approx \frac{2}{3\pi^2 M_p^4} \left[V(\phi_0) + V'(\phi_0)(\phi_* - \phi_0) + \frac{V''(\phi_0)}{2}(\phi_* - \phi_0)^2 + \frac{V'''(\phi_0)}{6}(\phi_* - \phi_0)^3 \right. \\
&\quad \left. + \frac{V''''(\phi_0)}{24}(\phi_* - \phi_0)^4 + \dots \right] \left[1 - (\mathcal{C}_E + 1) \frac{V'(\phi_0)^2 M_p^2}{2V(\phi_0)^2} \right]^2,
\end{aligned} \tag{10.5}$$

$$n_S - 1 \approx (2\eta_V - 6\epsilon_V) + \dots$$

$$= M_p^2 \left[\left(\frac{2V''(\phi_0)}{V(\phi_0)} - \frac{V'(\phi_0)^2}{2V(\phi_0)^2} \right) + \left(\frac{2V'''(\phi_0)}{V(\phi_0)} - \frac{2V'(\phi_0)V''(\phi_0)}{V(\phi_0)^2} \right) (\phi_* - \phi_0) + \dots \right], \tag{10.6}$$

$$n_T \approx -2\epsilon_V + \dots = -\frac{M_p^2}{V(\phi_0)^2} \left[V'(\phi_0) + V''(\phi_0)(\phi_* - \phi_0) + \dots \right]^2, \tag{10.7}$$

$$\begin{aligned}
r(k_\star) &\approx 16\epsilon_V [1 + 2\mathcal{C}_E(\epsilon_V - \eta_V)] + \dots \\
&= \frac{8M_p^2}{V(\phi_0)^2} \left[V'(\phi_0) + V''(\phi_0)(\phi_\star - \phi_0) + \dots \right]^2 \left[1 + 2\mathcal{C}_E M_p^2 \left(\frac{V'(\phi_0)^2}{2V(\phi_0)^2} - \frac{V''(\phi_0)}{V(\phi_0)} \right) \right]
\end{aligned} \tag{10.8}$$

$$\begin{aligned}
\alpha_S(k_\star) &= \left(\frac{dn_S}{d \ln k} \right)_\star \approx (16\eta_V \epsilon_V - 24\epsilon_V^2 - 2\xi_V^2) + \dots, \\
&= \frac{8M_p^4}{V(\phi_0)^3} \left[V'(\phi_0) + V''(\phi_0)(\phi_\star - \phi_0) + \dots \right]^2 \left[V''(\phi_0) + V'''(\phi_0)(\phi_\star - \phi_0) + \dots \right] \\
&\quad - \frac{6M_p^4}{V(\phi_0)^4} \left[V'(\phi_0) + V''(\phi_0)(\phi_\star - \phi_0) + \dots \right]^2 \\
&\quad - \frac{2M_p^4}{V(\phi_0)^2} \left[V'''(\phi_0)V'(\phi_0) + \left(V''''(\phi_0)V'(\phi_0) + V'''(\phi_0)V''(\phi_0) \right) (\phi_\star - \phi_0) \right. \\
&\quad \quad \left. + \left(V''''(\phi_0)V''(\phi_0) + \frac{V'''(\phi_0)^2}{2} \right) (\phi_\star - \phi_0)^2 + \dots \right]
\end{aligned} \tag{10.9}$$

$$\begin{aligned}
\kappa_S(k_\star) &= \left(\frac{d^2 n_S}{d \ln k^2} \right)_\star \approx 192\epsilon_V^2 \eta_V - 192\epsilon_V^3 + 2\sigma_V^3 - 24\epsilon_V \xi_V^2 + 2\eta_V \xi_V^2 - 32\eta_V^2 \epsilon_V + \dots \\
&= \frac{48M_p^6 V'(\phi_0)^4 V''(\phi_0)}{V(\phi_0)^5} - \frac{24M_p^6 V'(\phi_0)^6}{V(\phi_0)^6} - \frac{12M_p^6 V'(\phi_0)^3 V'''(\phi_0)}{V(\phi_0)^4} \\
&\quad + \frac{2M_p^6 V'(\phi_0)V''(\phi_0)V'''(\phi_0)}{V(\phi_0)^3} - \frac{16M_p^6 V'(\phi_0)^2 V''(\phi_0)^2}{V(\phi_0)^4} \\
&\quad \quad + \frac{2M_p^6 V'(\phi_0)^2 V''''(\phi_0)}{V(\phi_0)^3} + \dots
\end{aligned} \tag{10.10}$$

$$\begin{aligned}
n_r(k_\star) &= \left(\frac{dr}{d \ln k} \right)_\star \approx 32\epsilon_V \eta_V - 64\epsilon_V^2 + \dots \\
&= 16M_p^4 \left(\frac{V'(\phi_0)^2 V''(\phi_0)}{V(\phi_0)^3} - \frac{V'(\phi_0)^4}{V(\phi_0)^4} \right) + \dots
\end{aligned} \tag{10.11}$$

The crucial integrals of the first and second slow-roll parameters (ϵ_V, η_V) appearing in the right hand side of Eq. (2.14), which can be written up to the leading order as:

$$\int_{\phi_e}^{\phi_\star} d\phi \epsilon_V \approx \frac{1}{2} \sum_{p=0}^{\infty} \frac{M_p^{p+2} \mathbf{C}_p}{(p+1)} \left(\frac{\phi_e - \phi_0}{M_p} \right)^{p+1} \left\{ \left(1 + \frac{\Delta\phi}{M_p} \left(\frac{\phi_e - \phi_0}{M_p} \right)^{-1} \right)^{p+1} - 1 \right\} + \dots \tag{10.12}$$

$$\int_{\phi_e}^{\phi_*} d\phi \eta_V \approx \sum_{q=0}^{\infty} \frac{M_p^{q+2} \mathbf{D}_q}{(q+1)} \left(\frac{\phi_e - \phi_0}{M_p} \right)^{q+1} \left\{ \left(1 + \frac{\Delta\phi}{M_p} \left(\frac{\phi_e - \phi_0}{M_p} \right)^{-1} \right)^{q+1} - 1 \right\} + \dots \quad (10.13)$$

where I have used the $(\phi - \phi_0) < M_p$ (including at $\phi = \phi_*$ and $\phi = \phi_e$) around ϕ_0 . The leading order dimensionful Planck scale suppressed expansion co-efficients (\mathbf{C}_p) and (\mathbf{D}_q) are given in terms of the model parameters $(V(\phi_0), V'(\phi_0), \dots)$, which determine the hight and shape of the potential in terms of the model parameters as:

$$\begin{aligned} \mathbf{C}_0 &= \frac{V'(\phi_0)^2}{V(\phi_0)^2}, \quad \mathbf{C}_1 = \frac{2V''(\phi_0)V'(\phi_0)}{V(\phi_0)^2} - \frac{2V'(\phi_0)^3}{V(\phi_0)^3}, \\ \mathbf{C}_2 &= \frac{V''(\phi_0)^2}{V(\phi_0)^2} - \frac{5V'(\phi_0)^2V''(\phi_0)}{V(\phi_0)^3} + \frac{V'(\phi_0)V'''(\phi_0)}{V(\phi_0)^2}, \\ \mathbf{C}_3 &= \frac{V'(\phi_0)V''''(\phi_0)}{3V(\phi_0)^2} - \frac{7V'(\phi_0)^2V'''(\phi_0)}{3V(\phi_0)^3} + \frac{V''(\phi_0)V'''(\phi_0)}{V(\phi_0)^2} \\ &\quad - \frac{4V'(\phi_0)V''(\phi_0)^2}{V(\phi_0)^3} + \frac{9V'(\phi_0)^3V''(\phi_0)}{V(\phi_0)^4}, \\ &\dots\dots\dots \\ \mathbf{D}_0 &= \frac{V''(\phi_0)}{V(\phi_0)}, \quad \mathbf{D}_1 = \frac{V'''(\phi_0)}{V(\phi_0)} - \frac{V'(\phi_0)V''(\phi_0)}{V(\phi_0)^2}, \\ \mathbf{D}_2 &= \frac{V''''(\phi_0)}{2V(\phi_0)} - \frac{V'(\phi_0)V'''(\phi_0)}{V(\phi_0)^2} - \frac{V''(\phi_0)}{V(\phi_0)^2} + \frac{V''(\phi_0)V'(\phi_0)^2}{V(\phi_0)^3}, \\ \mathbf{D}_3 &= \frac{4V'(\phi_0)\delta^2}{V(\phi_0)^3} - \frac{2V'(\phi_0)^3\delta}{V(\phi_0)^4} + \frac{V'(\phi_0)^2V'''(\phi_0)}{V(\phi_0)^3} - \frac{2V''(\phi_0)V'''(\phi_0)}{3V(\phi_0)^2} - \frac{V''''(\phi_0)V'(\phi_0)}{2V(\phi_0)^2}, \\ &\dots\dots\dots \end{aligned} \quad (10.14)$$

Here $V(\phi_0), V'(\phi_0), V'''(\phi_0), V''''(\phi_0) \neq 0, V''(\phi_0) = 0$ and $V(\phi_0), V''(\phi_0), V''''(\phi_0) \neq 0, V'(\phi_0), V'''(\phi_0) = 0$ are two limiting situations which signifies the *inflection point* and *saddle point* inflationary setup. For details, see Ref. [23].

B. Momentum Integration from various parameterization of tensor-to-scalar ratio:

In general, the tensor-to-scalar ratio can be parametrized at any arbitrary momentum scale as:

$$r(k) = \begin{cases} r(k_*) & \text{for Case I} \\ r(k_*) \left(\frac{k}{k_*}\right)^{n_T(k_*)-n_S(k_*)+1} & \text{for Case II} \\ r(k_*) \left(\frac{k}{k_*}\right)^{n_T(k_*)-n_S(k_*)+1+\frac{\alpha_T(k_*)-\alpha_S(k_*)}{2!} \ln\left(\frac{k}{k_*}\right)} & \text{for Case III} \\ r(k_*) \left(\frac{k}{k_*}\right)^{n_T(k_*)-n_S(k_*)+1+\frac{\alpha_T(k_*)-\alpha_S(k_*)}{2!} \ln\left(\frac{k}{k_*}\right)+\frac{\kappa_T(k_*)-\kappa_S(k_*)}{3!} \ln^2\left(\frac{k}{k_*}\right)} & \text{for Case IV}. \end{cases} \quad (10.15)$$

where k_* be the pivot scale of momentum. Here these four possibilities are:-

- **Case I** stands for a situation where the spectrum is scale invariant. This is the similar situation as considered in case of Lyth bound [39]. This possibility also surmounts to the Harrison & Zeldovich spectrum, which is completely ruled out by Planck+WMAP9 data within 5σ C.L.
- **Case II** stands for a situation where spectrum follows power law feature through the spectral tilt (n_S, n_T) . This possibility is also tightly constrained by the WMAP9 and Planck+WMAP9 data within 2σ C.L. Recently in Ref. [51] the authors have explicitly shown that power law feature in the primordial power spectrum is ruled out at more than 3σ C.L.,
- **Case III** signifies a situation where the spectrum shows deviation from power law in presence of running of the spectral tilt (α_S, α_T) along with logarithmic correction in the momentum scale as appearing in the exponent. This possibility is favoured by WMAP9 data and tightly constrained within 2σ window by Planck+WMAP9 data,
- **Case IV** characterizes a physical situation in which the spectrum is further modified compared to the **Case III**, by allowing running of the running of spectral tilt (κ_S, κ_T) along with square of the momentum dependent logarithmic correction. This case is satisfied by both WMAP9 and Planck+WMAP9 data within 2σ C.L. This is the only criteria which is always satisfied by a general class of inflationary potentials. In this article, I have only focused on this possibility, from which I have derived all the constraint conditions for a generic model of sub-Planckian inflationary potentials.

Let us start with the computation of momentum integration where I investigate the possibility of four physical situations as mentioned in Eq (10.15) finally leading to:

$$\begin{aligned}
& \int_{k_e}^{k_{cmb}} d \ln k \sqrt{r(k)} \\
& \left\{ \begin{aligned}
& \sqrt{r(k_*)} \ln \left(\frac{k_{cmb}}{k_e} \right) && \text{for Case I} \\
& \frac{2\sqrt{r(k_*)}}{n_T(k_*) - n_S(k_*) + 1} \left[\left(\frac{k_{cmb}}{k_*} \right)^{\frac{n_T(k_*) - n_S(k_*) + 1}{2}} - \left(\frac{k_e}{k_*} \right)^{\frac{n_T(k_*) - n_S(k_*) + 1}{2}} \right] && \text{for Case II} \\
& \sqrt{r(k_*)} e^{-\frac{(n_T(k_*) - n_S(k_*) + 1)^2}{2(\alpha_T(k_*) - \alpha_S(k_*))}} \sqrt{\frac{2\pi}{(\alpha_T(k_*) - \alpha_S(k_*))}} \\
& \left[\operatorname{erfi} \left(\frac{n_T(k_*) - n_S(k_*) + 1}{\sqrt{2(\alpha_T(k_*) - \alpha_S(k_*))}} + \sqrt{\frac{(\alpha_T(k_*) - \alpha_S(k_*))}{8}} \ln \left(\frac{k_{cmb}}{k_*} \right) \right) \right. \\
& \quad \left. - \operatorname{erfi} \left(\frac{n_T(k_*) - n_S(k_*) + 1}{\sqrt{2(\alpha_T(k_*) - \alpha_S(k_*))}} + \sqrt{\frac{(\alpha_T(k_*) - \alpha_S(k_*))}{8}} \ln \left(\frac{k_e}{k_*} \right) \right) \right] && \text{for Case III} \\
& \sqrt{r(k_*)} \left[\left(\frac{3}{2} - \frac{n_T(k_*) - n_S(k_*)}{2} + \frac{\alpha_T(k_*) - \alpha_S(k_*)}{8} \right. \right. \\
& \quad \left. \left. - \frac{\kappa_T(k_*) - \kappa_S(k_*)}{24} \right) \left\{ \frac{k_{cmb}}{k_*} - \frac{k_e}{k_*} \right\} - \left(\frac{1}{2} - \frac{n_T(k_*) - n_S(k_*)}{2} \right. \right. \\
& \quad \left. \left. + \frac{\alpha_T(k_*) - \alpha_S(k_*)}{8} - \frac{\kappa_T(k_*) - \kappa_S(k_*)}{24} \right) \left\{ \frac{k_{cmb}}{k_*} \ln \left(\frac{k_{cmb}}{k_*} \right) - \frac{k_e}{k_*} \ln \left(\frac{k_e}{k_*} \right) \right\} \right. \\
& \quad \left. + \left(\frac{\kappa_T(k_*) - \kappa_S(k_*)}{48} - \frac{\alpha_T(k_*) - \alpha_S(k_*)}{16} \right) \left\{ \frac{k_{cmb}}{k_*} \ln^2 \left(\frac{k_{cmb}}{k_*} \right) - \frac{k_e}{k_*} \ln^2 \left(\frac{k_e}{k_*} \right) \right\} \right. \\
& \quad \left. - \frac{\kappa_T(k_*) - \kappa_S(k_*)}{144} \left\{ \frac{k_{cmb}}{k_*} \ln^3 \left(\frac{k_{cmb}}{k_*} \right) - \frac{k_e}{k_*} \ln^3 \left(\frac{k_e}{k_*} \right) \right\} \right] && \text{for Case IV.}
\end{aligned} \right. \\
\end{aligned} \tag{10.16}$$

where in a realistic physical situation one assumes the pivot scale of momentum $k_* \approx k_{cmb}$. Now further substituting Eq (3.7) on Eq (10.16) I get:

$$\begin{aligned}
& \int_{k_e}^{k_{cmb}} d \ln k \sqrt{r(k)} \\
& = \left\{ \begin{array}{ll}
\sqrt{r(k_*)} \Delta N & \text{for Case I} \\
\frac{2\sqrt{r(k_*)}}{n_T(k_*) - n_S(k_*) + 1} \left[1 - e^{-\Delta N \left(\frac{n_T(k_*) - n_S(k_*) + 1}{2} \right)} \right] & \text{for Case II} \\
\sqrt{r(k_*)} e^{-\frac{(n_T(k_*) - n_S(k_*) + 1)^2}{2(\alpha_T(k_*) - \alpha_S(k_*))}} \sqrt{\frac{2\pi}{(\alpha_T(k_*) - \alpha_S(k_*))}} \\
\left[\operatorname{erfi} \left(\frac{n_T(k_*) - n_S(k_*) + 1}{\sqrt{2(\alpha_T(k_*) - \alpha_S(k_*))}} \right) \right. \\
\left. - \operatorname{erfi} \left(\frac{n_T(k_*) - n_S(k_*) + 1}{\sqrt{2(\alpha_T(k_*) - \alpha_S(k_*))}} - \sqrt{\frac{(\alpha_T(k_*) - \alpha_S(k_*))}{8}} \Delta N \right) \right] & \text{for Case III} \\
\sqrt{r(k_*)} \left[\left(\frac{3}{2} - \frac{n_T(k_*) - n_S(k_*)}{2} + \frac{\alpha_T(k_*) - \alpha_S(k_*)}{8} \right. \right. \\
\left. \left. - \frac{\kappa_T(k_*) - \kappa_S(k_*)}{24} \right) \{1 - e^{-\Delta N}\} - \left(\frac{1}{2} - \frac{n_T(k_*) - n_S(k_*)}{2} \right. \right. \\
\left. \left. + \frac{\alpha_T(k_*) - \alpha_S(k_*)}{8} - \frac{\kappa_T(k_*) - \kappa_S(k_*)}{24} \right) \Delta N e^{-\Delta N} \right. \\
\left. - \left(\frac{\kappa_T(k_*) - \kappa_S(k_*)}{48} - \frac{\alpha_T(k_*) - \alpha_S(k_*)}{16} \right) (\Delta N)^2 e^{-\Delta N} \right. \\
\left. - \frac{\kappa_T(k_*) - \kappa_S(k_*)}{144} (\Delta N)^3 e^{-\Delta N} \right] & \text{for Case IV.}
\end{array} \right. \tag{10.17}
\end{aligned}$$

C. Taylor expansion co-efficients of inflationary potential:

To write down all the Taylor expansion co-efficients in terms of the inflationary observables at the pivot scale k_* I start with the slow-roll parameters $\epsilon_V, \eta_V, \xi_V^2, \sigma_V^3$

which can be expressed as:

$$\epsilon_V(k_*) \approx \frac{M_p^2}{2} \left(\frac{V'(\phi_*)}{V(\phi_*)} \right)^2 = \frac{r(k_*)}{16} = \frac{V(\phi_*)}{24\pi^2 M_p^4 P_S(k_*)}, \quad (10.18)$$

$$\eta_V(k_*) = M_p^2 \left(\frac{V''(\phi_*)}{V(\phi_*)} \right) = \left(n_S(k_*) - 1 + \frac{3r(k_*)}{8} \right), \quad (10.19)$$

$$\begin{aligned} \xi_V^2(k_*) &= M_p^4 \left(\frac{V'(\phi_*)V'''(\phi_*)}{(V(\phi_*)^2)} \right), \\ &= \frac{1}{2} \left[\eta_V(k_*)r(k_*) - \left(\frac{r(k_*)}{8} \right)^2 - \alpha_S(k_*) \right], \end{aligned} \quad (10.20)$$

$$\sigma_V^3(k_*) = M_p^6 \left(\frac{(V'(\phi_*)^2)V''''(\phi_*)}{(V(\phi_*)^3)} \right), \quad (10.21)$$

$$= \frac{1}{2} \left[\kappa_S(k_*) - \left(\frac{r(k_*)}{8} \right)^2 \eta_V + 6 \left(\frac{r(k_*)}{8} \right)^3 \right] \quad (10.22)$$

$$+ \left(\frac{3r(k_*)}{8} - \eta_V(k_*) \right) \sqrt{\frac{r(k_*)}{8}} X_* + \eta_V^2 r(k_*) \quad (10.23)$$

where

$$V(\phi_*) = V(k_*) = V_* = \frac{3}{2} P_S(k_*) \pi^2 M_p^4, \quad (10.24)$$

$$X_* = \left[\eta_V \sqrt{2r(k_*)} - \frac{1}{2} \left(\frac{r(k_*)}{8} \right)^{\frac{3}{2}} - \alpha_S(k_*) \sqrt{\frac{2}{r(k_*)}} \right]. \quad (10.25)$$

Finally we are left with the following Taylor expansion co-efficients (derivatives of the potential) at the pivot scale in terms of the inflationary observables:

$$V'(\phi_*) = \frac{3}{2} P_S(k_*) r(k_*) \pi^2 \sqrt{\frac{r(k_*)}{8}} M_p^3, \quad (10.26)$$

$$V''(\phi_*) = \frac{3}{4} P_S(k_*) r(k_*) \pi^2 \left(n_S(k_*) - 1 + \frac{3r(k_*)}{8} \right) M_p^2, \quad (10.27)$$

$$V'''(\phi_*) = \frac{3}{2} P_S(k_*) r(k_*) \pi^2 X_* M_p, \quad (10.28)$$

$$\begin{aligned} V''''(\phi_*) &= 12 P_S(k_*) \pi^2 \left\{ \frac{\kappa_S(k_*)}{2} - \frac{1}{2} \left(\frac{r(k_*)}{8} \right)^2 \left(n_S(k_*) - 1 + \frac{3r(k_*)}{8} \right) \right. \\ &\quad + 12 \left(\frac{r(k_*)}{8} \right)^3 + r(k_*) \left(n_S(k_*) - 1 + \frac{3r(k_*)}{8} \right)^2 \\ &\quad \left. + \sqrt{\frac{r(k_*)}{8}} X_* \left(n_S(k_*) - 1 + \frac{3r(k_*)}{8} \right) - 6 X_* \left(\frac{r(k_*)}{8} \right)^{\frac{3}{2}} \right\}. \end{aligned} \quad (10.29)$$

D. Field excursion from various parameterization of tensor-to-scalar ratio:

Using the result of Eq (10.12), Eq (10.13), Eq (10.17) I get the following expression for the field excursion in terms of the tensor-to-scalar ratio and other inflationary observables as:

$$\left| \frac{\Delta\phi}{M_p} \right| = \left\{ \begin{array}{ll} \sqrt{\frac{r(k_*)}{8}} \Delta N & \text{for Case I} \\ \\ \frac{2\sqrt{\frac{r(k_*)}{8}}}{n_T(k_*) - n_S(k_*) + 1} \left[1 - e^{-\Delta N \left(\frac{n_T(k_*) - n_S(k_*) + 1}{2} \right)} \right] & \text{for Case II} \\ \\ \sqrt{\frac{r(k_*)}{8}} e^{-\frac{(n_T(k_*) - n_S(k_*) + 1)^2}{2(\alpha_T(k_*) - \alpha_S(k_*))}} \sqrt{\frac{2\pi}{(\alpha_T(k_*) - \alpha_S(k_*))}} \\ \left[\operatorname{erfi} \left(\frac{n_T(k_*) - n_S(k_*) + 1}{\sqrt{2(\alpha_T(k_*) - \alpha_S(k_*))}} \right) \right. \\ \left. - \operatorname{erfi} \left(\frac{n_T(k_*) - n_S(k_*) + 1}{\sqrt{2(\alpha_T(k_*) - \alpha_S(k_*))}} - \sqrt{\frac{(\alpha_T(k_*) - \alpha_S(k_*))}{8}} \Delta N \right) \right] & \text{for Case III} \\ \\ \sqrt{\frac{r(k_*)}{8}} \left[\left(\frac{3}{2} - \frac{n_T(k_*) - n_S(k_*)}{2} + \frac{\alpha_T(k_*) - \alpha_S(k_*)}{8} \right. \right. \\ \left. \left. - \frac{\kappa_T(k_*) - \kappa_S(k_*)}{24} \right) \{1 - e^{-\Delta N}\} - \left(\frac{1}{2} - \frac{n_T(k_*) - n_S(k_*)}{2} \right. \right. \\ \left. \left. + \frac{\alpha_T(k_*) - \alpha_S(k_*)}{8} - \frac{\kappa_T(k_*) - \kappa_S(k_*)}{24} \right) \Delta N e^{-\Delta N} \right. \\ \left. - \left(\frac{\kappa_T(k_*) - \kappa_S(k_*)}{48} - \frac{\alpha_T(k_*) - \alpha_S(k_*)}{16} \right) (\Delta N)^2 e^{-\Delta N} \right. \\ \left. - \frac{\kappa_T(k_*) - \kappa_S(k_*)}{144} (\Delta N)^3 e^{-\Delta N} \right] & \text{for Case IV.} \end{array} \right. \quad (10.30)$$

Substituting $\Delta N \sim \mathcal{O}(8-17)$ in Eq (10.17) for the previously mentioned four physical situations and further using Eq (2.14) the field excursion can be constrained as:

Planck (2013)+WMAP-9+high L:

$$\left| \frac{\Delta\phi}{M_p} \right| \leq \begin{cases} \mathcal{O}(0.98 - 2.08) & \text{for Case I} \\ \mathcal{O}(0.87 - 1.88) & \text{for Case II} \\ \mathcal{O}(0.51 - 0.96) & \text{for Case III} \\ \mathcal{O}(0.239 - 0.241) & \text{for Case IV}. \end{cases} \quad (10.31)$$

Planck (2014)+WMAP-9+high L+BICEP2 (dust):

$$\left| \frac{\Delta\phi}{M_p} \right| = \begin{cases} \mathcal{O}(2.32 - 3.12) & \text{for Case I} \\ \mathcal{O}(1.73 - 2.63) & \text{for Case II} \\ \mathcal{O}(0.62 - 0.94) & \text{for Case III} \\ \mathcal{O}(0.242 - 0.354) & \text{for Case IV}. \end{cases} \quad (10.32)$$

Planck (2015)+WMAP-9+high L(TT):

$$\left| \frac{\Delta\phi}{M_p} \right| \leq \begin{cases} \mathcal{O}(0.94 - 2) & \text{for Case I} \\ \mathcal{O}(0.82 - 1.42) & \text{for Case II} \\ \mathcal{O}(0.56 - 0.96) & \text{for Case III} \\ \mathcal{O}(0.230 - 0.231) & \text{for Case IV}. \end{cases} \quad (10.33)$$

Planck (2015)+BICEP2/Keck Array:

$$\left| \frac{\Delta\phi}{M_p} \right| \leq \begin{cases} \mathcal{O}(0.98 - 2.08) & \text{for Case I} \\ \mathcal{O}(0.84 - 1.49) & \text{for Case II} \\ \mathcal{O}(0.51 - 0.97) & \text{for Case III} \\ \mathcal{O}(0.223 - 0.242) & \text{for Case IV}. \end{cases} \quad (10.34)$$

In this paper I have only focused on the last possibility, from which I have derived all the constraint conditions for a generic model of sub-Planckian inflationary potentials. Also the last possibility is important because within this it is possible to generate large value of tensor-to-scalar ratio along with field excursion $\Delta\phi \lesssim M_p$. This also validates the effective field theory prescription within the regime of inflationary paradigm. There are other possibilities as well through which one can address this crucial issue in the context of inflation. Those possibilities are:-

- Multi-field inflationary prescription,
- Randall-Sundrum braneworld [20],
- Higher curvature gravity [52],
- Other ghost-free modifications in GR [53],
- Inflation from torsion [54] etc.

References

- [1] A. H. Guth, “*The Inflationary Universe: A Possible Solution to the Horizon and Flatness Problems,*” *Phys. Rev. D* **23**, 347 (1981).
A. A. Starobinsky, “*A New Type of Isotropic Cosmological Models Without Singularity,*” *Phys. Lett. B* **91**, 99 (1980).
- [2] A. D. Linde, “*A New Inflationary Universe Scenario: A Possible Solution of the Horizon, Flatness, Homogeneity, Isotropy and Primordial Monopole Problems,*” *Phys. Lett. B* **108**, 389 (1982).
- [3] A. Albrecht and P. J. Steinhardt, “*Cosmology for Grand Unified Theories with Radiatively Induced Symmetry Breaking,*” *Phys. Rev. Lett.* **48**, 1220 (1982).
- [4] V. F. Mukhanov and G. V. Chibisov, “*Quantum Fluctuation and Nonsingular Universe. (In Russian),*” *JETP Lett.* **33**, 532 (1981) [*Pisma Zh. Eksp. Teor. Fiz.* **33**, 549 (1981)].
A. A. Starobinsky, “*Relict Gravitation Radiation Spectrum and Initial State of the Universe. (In Russian),*” *JETP Lett.* **30**, 682 (1979) [*Pisma Zh. Eksp. Teor. Fiz.* **30**, 719 (1979)].
- [5] V. F. Mukhanov, H. A. Feldman and R. H. Brandenberger, “*Theory of cosmological perturbations. Part 1. Classical perturbations. Part 2. Quantum theory of perturbations. Part 3. Extensions,*” *Phys. Rept.* **215**, 203 (1992).
- [6] G. Hinshaw *et al.* [WMAP Collaboration], “*Nine-Year Wilkinson Microwave Anisotropy Probe (WMAP) Observations: Cosmological Parameter Results,*” *Astrophys. J. Suppl.* **208**, 19 (2013) [arXiv:1212.5226 [astro-ph.CO]].
- [7] P. A. R. Ade *et al.* [Planck Collaboration], “*Planck 2013 results. XVI. Cosmological parameters,*” arXiv:1303.5076 [astro-ph.CO].

- [8] P. A. R. Ade *et al.* [Planck Collaboration], “*Planck 2013 results. XXII. Constraints on inflation,*” [arXiv:1303.5082 \[astro-ph.CO\]](#).
- [9] P. A. R. Ade *et al.* [BICEP2 Collaboration], “*Detection of B-Mode Polarization at Degree Angular Scales by BICEP2,*” *Phys. Rev. Lett.* **112** (2014) 24, 241101 [[arXiv:1403.3985 \[astro-ph.CO\]](#)].
- [10] H. Liu, P. Mertsch and S. Sarkar, “*Fingerprints of Galactic Loop I on the Cosmic Microwave Background,*” *Astrophys. J.* **789** (2014) L29 [[arXiv:1404.1899 \[astro-ph.CO\]](#)].
- [11] M. J. Mortonson and U. Seljak, “*A joint analysis of Planck and BICEP2 B modes including dust polarization uncertainty,*” [arXiv:1405.5857 \[astro-ph.CO\]](#).
- [12] R. Flauger, J. C. Hill and D. N. Spergel, “*Toward an Understanding of Foreground Emission in the BICEP2 Region,*” *JCAP* **1408** (2014) 039 [[arXiv:1405.7351 \[astro-ph.CO\]](#)].
- [13] R. Adam *et al.* [Planck Collaboration], “*Planck intermediate results. XXXII. The relative orientation between the magnetic field and structures traced by interstellar dust,*” [arXiv:1409.6728 \[astro-ph.GA\]](#).
- [14] P. A. R. Ade *et al.* [BICEP2 and Planck Collaborations], “*A Joint Analysis of BICEP2/Keck Array and Planck Data,*” [arXiv:1502.00612 \[astro-ph.CO\]](#).
- [15] P. A. R. Ade *et al.* [Planck Collaboration], “*Planck 2015. XX. Constraints on inflation,*” [arXiv:1502.02114 \[astro-ph.CO\]](#).
- [16] N. D. Birrell and P. C. W. Davies, “*Quantum Fields in Curved Space,*” *Cambridge Monogr. Math. Phys.*.
- [17] R. Allahverdi, K. Enqvist, J. Garcia-Bellido and A. Mazumdar, “*Gauge invariant MSSM inflaton,*” *Phys. Rev. Lett.* **97**, 191304 (2006) [[hep-ph/0605035](#)].
R. Allahverdi, K. Enqvist, J. Garcia-Bellido, A. Jokinen and A. Mazumdar, “*MSSM flat direction inflation: Slow roll, stability, fine tuning and reheating,*” *JCAP* **0706**, 019 (2007) [[hep-ph/0610134](#)].
- [18] A. R. Liddle, A. Mazumdar and F. E. Schunck, “*Assisted inflation,*” *Phys. Rev. D* **58**, 061301 (1998) [[astro-ph/9804177](#)].
- [19] P. Kanti and K. A. Olive, “*Assisted chaotic inflation in higher dimensional theories,*” *Phys. Lett. B* **464**, 192 (1999) [[hep-ph/9906331](#)].
- [20] S. Choudhury, “*Can Effective Field Theory of inflation generate large tensor-to-scalar ratio within Randall Sundrum single braneworld?,*” *Nucl. Phys. B* **894** (2015) 29 [[arXiv:1406.7618 \[hep-th\]](#)].
- [21] I. Ben-Dayan and R. Brustein, “*Cosmic Microwave Background Observables of Small Field Models of Inflation,*” *JCAP* **1009** (2010) 007 [[arXiv:0907.2384 \[astro-ph.CO\]](#)].
- [22] M. U. Rehman, Q. Shafi and J. R. Wickman, “*Observable Gravity Waves from Supersymmetric Hybrid Inflation II,*” *Phys. Rev. D* **83** (2011) 067304 [[arXiv:1012.0309 \[astro-ph.CO\]](#)].

- Q. Shafi and J. R. Wickman, “*Observable Gravity Waves From Supersymmetric Hybrid Inflation*,” *Phys. Lett. B* **696** (2011) 438 [arXiv:1009.5340 [hep-ph]].
- N. Okada, M. U. Rehman and Q. Shafi, “*Non-Minimal B-L Inflation with Observable Gravity Waves*,” *Phys. Lett. B* **701** (2011) 520 [arXiv:1102.4747 [hep-ph]].
- M. Civiletti, M. U. Rehman, Q. Shafi and J. R. Wickman, “*Red Spectral Tilt and Observable Gravity Waves in Shifted Hybrid Inflation*,” *Phys. Rev. D* **84** (2011) 103505 [arXiv:1104.4143 [astro-ph.CO]].
- [23] S. Choudhury and A. Mazumdar, “*An accurate bound on tensor-to-scalar ratio and the scale of inflation*,” *Nucl. Phys. B* **882** (2014) 386 [arXiv:1306.4496 [hep-ph]].
- [24] S. Hotchkiss, A. Mazumdar and S. Nadathur, “*Observable gravitational waves from inflation with small field excursions*,” *JCAP* **1202** (2012) 008 [arXiv:1110.5389 [astro-ph.CO]].
- [25] D. H. Lyth, “*What would we learn by detecting a gravitational wave signal in the cosmic microwave background anisotropy?*,” *Phys. Rev. Lett.* **78** (1997) 1861 [hep-ph/9606387].
- A. Kehagias and A. Riotto, “*Remarks about the Tensor Mode Detection by the BICEP2 Collaboration and the Super-Planckian Excursions of the Inflaton Field*,” arXiv:1403.4811 [astro-ph.CO].
- [26] S. Choudhury and A. Mazumdar, “*Reconstructing inflationary potential from BICEP2 and running of tensor modes*,” arXiv:1403.5549 [hep-th].
- [27] S. Choudhury and A. Mazumdar, “*Sub-Planckian inflation & large tensor to scalar ratio with $r \geq 0.1$* ,” arXiv:1404.3398 [hep-th].
- [28] R. Khatri, “*Mixing of blackbodies: Increasing our view of inflation to 17 e-folds with spectral distortions from Silk damping*,” arXiv:1302.5633 [astro-ph.CO].
- [29] S. Clesse, B. Garbrecht and Y. Zhu, “*Testing Inflation and Curvaton Scenarios with CMB Distortions*,” arXiv:1402.2257 [astro-ph.CO].
- [30] R. Easther and H. Peiris, “*Implications of a Running Spectral Index for Slow Roll Inflation*,” *JCAP* **0609** (2006) 010 [astro-ph/0604214].
- [31] S. Choudhury, A. Mazumdar and S. Pal, “*Low & High scale MSSM inflation, gravitational waves and constraints from Planck*,” *JCAP* **1307** (2013) 041 [arXiv:1305.6398 [hep-ph]].
- [32] C. P. Burgess, et.al. “*Multiple inflation, cosmic string networks and the string landscape*,” *JHEP* **0505**, 067 (2005) [hep-th/0501125].
- [33] S. Choudhury and A. Mazumdar, “*Primordial blackholes and gravitational waves for an inflection-point model of inflation*,” *Phys. Lett. B* **733** (2014) 270 [arXiv:1307.5119 [astro-ph.CO]].
- [34] A. Mantz, S. W. Allen, D. Rapetti and H. Ebeling, “*The Observed Growth of Massive Galaxy Clusters I: Statistical Methods and Cosmological Constraints*,” *Mon. Not. Roy. Astron. Soc.* **406** (2010) 1759 [arXiv:0909.3098 [astro-ph.CO]].

- [35] J. A. Adams, G. G. Ross and S. Sarkar, “*Multiple inflation,*” *Nucl. Phys. B* **503** (1997) 405 [arXiv:hep-ph/9704286].
- [36] B. J. Carr, K. Kohri, Y. Sendouda and J. Yokoyama, “*New cosmological constraints on primordial black holes,*” *Phys. Rev. D* **81**, 104019 (2010) [arXiv:0912.5297 [astro-ph.CO]].
- [37] L. Alabidi and K. Kohri, “*Generating Primordial Black Holes Via Hilltop-Type Inflation Models,*” *Phys. Rev. D* **80**, 063511 (2009) [arXiv:0906.1398 [astro-ph.CO]].
- [38] M. Drees, E. Erfani, “*Running-Mass Inflation Model and Primordial Black Holes,*” *JCAP* **1104** (2011) 005 [arXiv:1102.2340 [hep-ph]].
- [39] Y. -Z. Ma and Y. Wang, “*Local Reconstruction of the Inflationary Potential with BICEP2 data,*” arXiv:1403.4585 [astro-ph.CO].
X. Calmet and V. Sanz, “*Excursion into Quantum Gravity via Inflation,*” arXiv:1403.5100 [hep-ph].
- [40] K. Enqvist, A. Mazumdar and P. Stephens, “*Inflection point inflation within supersymmetry,*” *JCAP* **1006**, 020 (2010) [arXiv:1004.3724 [hep-ph]].
- [41] S. Choudhury, A. Mazumdar and E. Pukartas, “*Constraining $\mathcal{N} = 1$ supergravity inflationary framework with non-minimal Kahler operators,*” *JHEP* **1404** (2014) 077 [arXiv:1402.1227 [hep-th]].
- [42] S. Choudhury, “*Constraining $N = 1$ supergravity inflation with non-minimal Kaehler operators using δN formalism,*” *JHEP* **1404** (2014) 105 [arXiv:1402.1251 [hep-th]].
- [43] S. Choudhury and S. Pal, “*Fourth level MSSM inflation from new flat directions,*” *JCAP* **1204** (2012) 018 [arXiv:1111.3441 [hep-ph]].
- [44] CAMB, *Online link: <http://camb.info/>.*
- [45] D. Hanson *et al.* [SPTpol Collaboration], “*Detection of B-mode Polarization in the Cosmic Microwave Background with Data from the South Pole Telescope,*” *Phys. Rev. Lett.* **111** (2013) 14, 141301 [arXiv:1307.5830 [astro-ph.CO]].
- [46] S. Choudhury and S. Banerjee, “*Hysteresis in the Sky,*” arXiv:1506.02260 [hep-th].
- [47] C. Bonvin, R. Durrer and R. Maartens, “*Can primordial magnetic fields be the origin of the BICEP2 data?,*” *Phys. Rev. Lett.* **112** (2014) 191303 [arXiv:1403.6768 [astro-ph.CO]].
- [48] S. Choudhury, “*Inflamagnetogenesis redux: Unzipping sub-Planckian inflation via various cosmoparticle probes,*” *Phys. Lett. B* **735** (2014) 138 [arXiv:1403.0676 [hep-th]].
- [49] S. Choudhury, “*Braneflamagnetogenesis from Cosmoparticle Physics after Planck,*” arXiv:1504.08206 [astro-ph.CO].
- [50] M. Zaldarriaga and U. Seljak, “*Gravitational lensing effect on cosmic microwave background polarization,*” *Phys. Rev. D* **58** (1998) 023003 [astro-ph/9803150].
- [51] D. K. Hazra, A. Shafieloo, G. F. Smoot and A. A. Starobinsky, “*Ruling out the*

- power-law form of the scalar primordial spectrum,*” JCAP **1406** (2014) 061 [arXiv:1403.7786 [astro-ph.CO]].
- [52] S. Choudhury, J. Mitra and S. SenGupta, “*Fermion localization and flavour hierarchy in higher curvature spacetime,*” arXiv:1503.07287 [hep-th].
 S. Choudhury, J. Mitra and S. SenGupta, “*Modulus stabilization in higher curvature dilaton gravity,*” JHEP **1408** (2014) 004 [arXiv:1405.6826 [hep-th]];
 S. Choudhury and S. SenGupta, “*A step toward exploring the features of Gravidilaton sector in Randall-Sundrum scenario via lightest Kaluza-Klein graviton mass,*” Eur. Phys. J. C **74** (2014) 11, 3159 [arXiv:1311.0730 [hep-ph]];
 S. Choudhury, S. Sadhukhan and S. SenGupta, “*Collider constraints on Gauss-Bonnet coupling in warped geometry model,*” arXiv:1308.1477 [hep-ph];
 S. Choudhury and S. SenGupta, “*Thermodynamics of Charged Kalb Ramond AdS black hole in presence of Gauss-Bonnet coupling,*” arXiv:1306.0492 [hep-th].
 S. Choudhury and S. Sengupta, “*Features of warped geometry in presence of Gauss-Bonnet coupling,*” JHEP **1302** (2013) 136 [arXiv:1301.0918 [hep-th]].
 S. Choudhury and S. Pal, “*Primordial non-Gaussian features from DBI Galileon inflation,*” Eur. Phys. J. C **75** (2015) 6, 241 [arXiv:1210.4478 [hep-th]].
 S. Choudhury and S. Pal, “*DBI Galileon inflation in background SUGRA,*” Nucl. Phys. B **874** (2013) 85 [arXiv:1208.4433 [hep-th]].
- [53] T. Biswas, E. Gerwick, T. Koivisto and A. Mazumdar, “*Towards singularity and ghost free theories of gravity,*” Phys. Rev. Lett. **108** (2012) 031101 [arXiv:1110.5249 [gr-qc]].
- [54] S. Choudhury, B. K. Pal, B. Basu and P. Bandyopadhyay, “*Measuring CP violation within Effective Field Theory of inflation from CMB,*” arXiv:1409.6036 [hep-th].